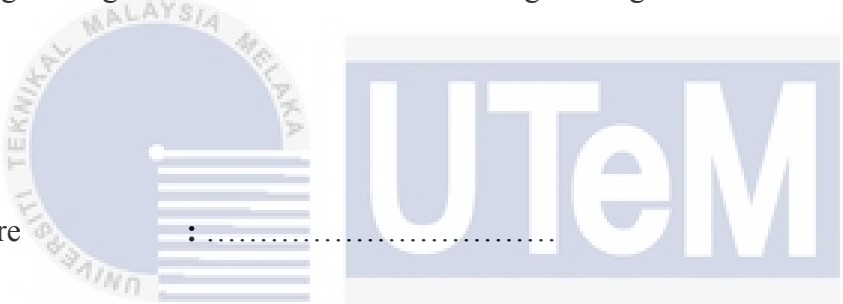


**DEVELOPMENT OF SINGLE PHASE TRANSFORMERLESS
INVERTER**



**BACHELOR OF ELECTRICAL ENGINEERING
UNIVERSITI TEKNIKAL MALAYSIA MELAKA**

“I hereby declare that I have read through this report entitle “*Development of Single-Phase Transformerless Inverter*” and found that it has comply the partial fulfilment for awarding the degree of Bachelor of Electrical Engineering”

Signature : 

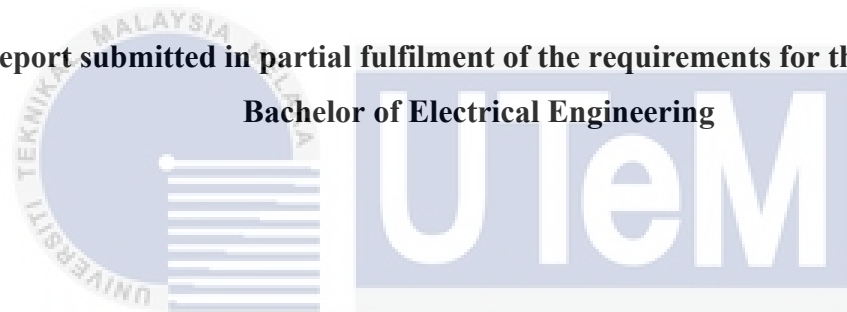
Supervisor's Name : DR. Maaspaliza Binti Azri 
UNIVERSITI TEKNIKAL MALAYSIA MELAKA

Date :

DEVELOPMENT OF SINGLE-PHASE TRANSFORMERLESS INVERTER

NUR SYAMIMI BINTI AHMAD FAUZI

**A report submitted in partial fulfilment of the requirements for the degree of
Bachelor of Electrical Engineering**



اونيورسيتي تيكنيكل مليسيا ملاك

UNIVERSITI TEKNIKAL MALAYSIA MELAKA

Faculty of Electrical Engineering

UNIVERSITI TEKNIKAL MALAYSIA MELAKA

JUNE 2018

I declare that this report entitles “*Single-Phase Transformerless Inverter*” is the result of my own research except as cited in the reference. The report has not been accepted for any degree and is not concurrently submitted in candidate of any other degree.

Signature

:



Name

: Nur Syamimi Binti Ahmad Fauzi

اونيور سيتي تیکنیکل ملیسیا ملاک

Date

:

UNIVERSITI TEKNIKAL MALAYSIA MELAKA

DEDICATION

This word is dedicated to my beloved parents and family for their supporting and for their helper no matter in what sense. Not forget to my beloved supervisor DR. Maaspaliza Binti Azri, which is the important person in helping and guide me to do this project with successful. Even though there are some problems that I faced in doing this project. Besides, thanks to all friends and lecturer that willing to give their hands to help me, without them I can't complete this project successful. Thank you everyone.

UNIVERSITI TEKNIKAL MALAYSIA MELAKA

ACKNOWLEDGEMENT

First of all, I would like to thank God with all His kindness to letting me finish this final year project. I can't achieve anything without His permission. Every project whether it big or small is successful largely due to the effort of a number of wonderful people who have always given their valuable advice or lend a helping hand.

I would like to express my deepest appreciation to my parents and all my family that always supports me till the end of this final year project. This project requires me to gain so many strength, patience and support to finish my final year project. My family is my strength and they were my everything.

At this junction I feel deeply honored in expressing my sincere thanks to my final year project's supervisor, Dr. Maaspaliza Binti Azri, whose have invested his full effort in guiding me in achieving the goal. She teaches me, guide me and give much information to complete this project. With all her advice and tips I had been used for this project came with expected output result. Without her, I will not solve the project's entire problem hence completing this final year project due to the date.

Last but not least, I want to give a special gratitude to Universiti Teknikal Malaysia Melaka (UTeM), Faculty of Electrical Engineering (FKE) and to all my friends for their critical advice and guidance without them, this project would not have been possible.

ABSTRACT

The efficiency of the inverter can be improved when there is no transformer used in photovoltaic (PV) single-phase inverter system. One of the main problems in single-phase photovoltaic (PV) inverter is to control leakage current appearing between parasitic capacitor and ground. The main problem of ground leakage current is, it poses an electrical hazard to anyone touching the photovoltaic (PV) array's surface. As required in VDE-0126-1-1 German standard, the ground leakage current must be below $300\text{mA}_{\text{rms}}$ for safety issues. To reduce the ground leakage current, the single-phase transformerless inverter is analyzed, verified and compared in this report. There are four factors that affect the ground leakage current which are the switching technique, parasitic capacitance, filter design and topology used. The effective way to control the ground leakage current is by keeping the common-mode voltage constant. H-bridge inverter topology was used to investigate the suitable switching technique, which is bipolar SPWM and unipolar SPWM is used. In order to analyze the effect of filter design to the bipolar H-bridge transformerless inverter, the LC filter using one inductor and LC filter split inductor with same value is investigated. Filter design using LC filter split inductor with same value having a low leakage current. Therefore, the effect of filter impedance matching was analyzed. In addition, the effect of the parasitic capacitance on the bipolar H-bridge transformerless inverter is studied. After the three factors have been analyzed, a switching frequency of single-phase transformerless inverter using bipolar SPWM is analyzed in terms of ground leakage current. Appearing leakage current causes the safety problem and increased system losses.

ABSTRAK

Kecekapan boleh ditingkatkan apabila tiada pengubah yang digunakan dalam sistem penyongsang fasa tunggal fotovoltaik (PV). Salah satu masalah utama dalam penyongsang photovoltaic (PV) fasa tunggal adalah untuk mengawal arus kebocoran ke bumi yang muncul di antara kapasitor parasit dan bumi. Masalah utama kebocoran arus bumi adalah, ia menimbulkan bahaya elektrik kepada sesiapa yang menyentuh permukaan array photovoltaic (PV). Seperti yang dikehendaki dalam standard Jerman VDE-0126-1-1, arus kebocoran tanah mestilah di bawah $300m_{rms}$ untuk isu keselamatan. Untuk mengurangkan arus kebocoran tanah, pengubah penyongsang fasa tunggal dianalisis, disahkan dan dibandingkan dalam laporan ini. Terdapat empat faktor yang mempengaruhi arus kebocoran ke bumi iaitu teknik pensuisan, kapasitans parasit, reka bentuk penapis dan topologi yang digunakan. Cara yang berkesan untuk mengawal arus kebocoran ke bumi adalah dengan mengekalkan pemalar voltan biasa mod. Topologi penyongsang H-bridge digunakan untuk menyiasat teknik penukaran yang sesuai, iaitu *bipolar SPWM* dan *unipolar SPWM* digunakan. Untuk menganalisis kesan reka bentuk penapis kepada penyongsang penukar *H-bridge bipolar*, penapis LC menggunakan satu penunjuk induktor dan LC penukar berpecah induktor dengan nilai yang sama disiasat. Reka bentuk penapis menggunakan LC penapis pemisah pecah dengan nilai yang sama mempunyai arus kebocoran yang rendah. Oleh itu, pepadanan impak penapis kesan telah dianalisis. Di samping itu, kesan kapasitans parasit pada penyongsang penukar *H-bipolar* dipelajari. Selepas tiga faktor telah dianalisis, satu penukar penyongsang fasa yang dicadangkan dan dianalisis dari segi kebocoran ke bumi. Kebocoran arus ke bumi menyebabkan masalah keselamatan dan peningkatan kehilangan sistem.

TABLE OF CONTENT

CHAPTER	TITLE	PAGE
	ACKNOWLEDGEMENT	ii
	ABSTRACT	iii
	ABSTRAK	iv
	TABLE OF CONTENT	v
	LIST OF FIGURE	ix
	LIST OF TABLE	xiv
	LIST OF APPENDICES	xv
1	INTRODUCTION	1
	1.1 Background	1
	1.2 Problem Statement	2
	1.3 Objective	3
	1.4 Scope	3
	1.5 Report Outline	4
2	LITERATURE REVIEW	5
	2.1 Introduction	5
	2.2 Renewable Power Source	5
	2.2.1 Solar Energy System	6
	2.2.2 Wind Energy System	6
	2.2.3 Fuel Cells System	6
	2.3 Inverter	7
	2.3.1 Current Source Inverter (CSI)	7
	2.3.2 Voltage Source Inverter (VSI)	7
	2.4 VSI Topologies	8
	2.4.1 Single-Phase Inverter Topology for PV Grid	8

	Connected System	
	2.4.1.1 Cascaded Multilevel Inverter Topology	8
	2.4.1.2 A Power Electronic Transformer (PET) with a Cycloconverter on The Grid Side Topology	9
	2.4.2 Transformer Inverter System	11
	2.4.3 Single-phase Inverter Transformerless Topology	11
	2.4.3.1 Split-capacitor H-bridge (SC-HB) Topology	11
	2.4.3.2 H6 single-phase Inverter Topology	12
	2.4.3.3 High Efficient and Reliable Inverter Concept (HERIC) Topology	13
	2.4.3.4 Single-phase Full-bridge Grid Connected PV Transformerless Inverter Topology	14
	2.5 Switching Techniques for Single-Phase Inverter Circuit	15
	2.5.1 Pulse-width-modulated Inverters	15
	2.5.2 Square-wave Inverters	16
	2.5.3 Single-phase Inverters with Voltage Cancellation	16
	2.6 Modulation Schemes	16
	2.6.1 SPWM with Bipolar Switching	17
	2.6.2 SPWM with Unipolar Switching	18
	2.6.3 PWM Consideration	19
	2.6.3.1 Frequency Modulation Ratio, m_f	19
	2.6.3.2 Amplitude Modulation Ration, m_a	20
	2.7 Harmonic Distortion Definition	20
	2.7.1 Relation Between Harmonic Voltage and Current	21
	2.7.2 Total Harmonic Distortion	21
	2.8 AC Filters	22
	2.9 Summary	22
3	DESIGN METHODOLOGY	24
	3.1 Introduction	24
	3.2 Research Methodology	24
	3.2.1 Flowchart	25

3.2.2	Milestone Research	26
3.2.3	Project Gantt Chart	27
3.3	Single-phase transformerless Inverter	28
3.3.1	Ground Leakage Current	28
3.3.2	Common-mode Voltage in Single-phase Transformerless Inverter	29
3.3.3	Parasitic Capacitance of PV Grid System	32
3.3.4	Hbridge inverter transformerless Control Switching Technique	33
3.3.5	Filter Design	38
3.4	Simulation of Single-Phase Transformerless Inverter	40
3.4.1	Simulink Parameter	41
3.5	Hardware Design	42
3.5.1	H-bridge transformerless Inverter Circuit	42
3.5.2	Gate Drive Circuit	43
3.5.3	XMC 4500 Microcontroller	44
3.6	Hardware Experimental Setup	46
3.7	Summary	47
4	RESULT AND DISCUSSION	48
4.1	Introduction	48
4.2	Simulation Result	48
4.2.1	Simulation of Single-phase Transformerless Inverter	48
4.2.2	Effect of Filter Design	58
4.2.3	Effect of Filter Impedance Matching	60
4.2.4	Effect of Parasitic Capacitance	65
4.2.5	Effect of Switching Frequency	67
4.3	Hardware Results	69
4.3.1	Pulse Width Modulation	69
4.3.2	Single Phase Transformerless Inverter	70
4.3.3	Effect of Filter Design	74
4.3.4	Effect of Filter Impedance Matching	75

4.3.5	Effect of Parasitic Capacitance	77
4.3.6	Effect of Switching Frequency	79
4.4	Comparison Result Between Simulation and Hardware	80
4.41	Analysis on LC Filter using One Inductance, LC Filter using Split Inductance, Parasitic Capacitance and Switching Frequency at Ground Leakage Current	82
4.5	Summary	84
5	CONCLUSION AND RECOMMENDATION	86
	REFERENCES	87
	APPENDICES	90



LIST OF FIGURE

FIGURE	TITLE	PAGE
2.1	Circuit Structure of CSI Inverter	7
2.2	Circuit Configuration of VSI Inverter	8
2.3	Cascaded Multilevel Inverter Topology	9
2.4	Power Electronic Transformer Topology For Integrating Multiple Renewable Energy	10
2.5	SC-HB Inverter Topology	12
2.6	H6 Inverter Topology	13
2.7	HERIC Topology	13
2.8	Single-phase Grid Connected Transformerless PV Inverter	14
2.9	(a) Switching Pattern (b) Output Waveform	17
2.10	Full Bridge Converter	18
2.11	Waveform Of Unipolar Modulation Scheme	18
2.12	Current Distortion Caused By Nonlinear Resistance	20
2.13	Relation between Harmonic Voltage and Current	21
3.1	Flowchart of Research Methodology	25
3.2	Transformerless Single-Phase Inverter With Parasitic Capacitance	29
3.3	The Common-Mode Model For The PWM Voltage Source Inverter System	30
3.4	Simplified Equivalent Model Of Common-Mode Resonant Circuit	31
3.5	Equivalent Circuit For The Common-Mode Leakage Current Path	32
3.6	(a) Maximum and (b) Minimum PV Module Earth Capacitance	33
3.7	Transformerless H-Bridge Inverter	34

3.8	Half-positive Cycle State i for Unipolar H-bridge Circuit	35
3.9	Half-positive Cycle State ii for Unipolar H-bridge Circuit	35
3.10	Half-positive Cycle State iii for Unipolar H-bridge Circuit	36
3.11	Positive Cycle State i for Bipolar H-Bridge Circuit	37
3.12	Positive cycle state ii for Bipolar H-Bridge Circuit	38
3.13	LC Filter With One Inductor (L_f)	39
3.14	LC Filter With Split Inductor (L_f)	39
3.15	MATLAB Simulink Model Of Single-Phase Transformerless Inverter For Bipolar Switching Scheme	40
3.16	Operation Mode Of The CD-Boost Converter In Switch-On Mode	41
3.17	Flowchart Of Hardware	42
3.18	IGBT G4PC50UD-E	42
3.19	Gate Drive circuit	44
3.20	Microcontroller XMC 4500	44
3.21	CCU4 circuit	45
3.22	Block Parameter Sine Wave	45
3.23	Block Parameter CCU4	46
3.24	Hardware Setup	47
4.1	(A) Common-Mode Voltage (V_{cm}), (B) V_{ao} And (C) V_{bo} That Obtained Using Unipolar Switching Technique	49
4.2	Output Inverter Voltage 30 V (V_{ab})	50
4.3	Output Inverter Current 24.48 mA (I_o)	50
4.4	Output Inverter Voltage 24.48 V (V_o)	51
4.5	THD current for unipolar H-bridge inverter (0.75 %)	51
4.6	THD Voltage For Unipolar H-Bridge Inverter (0.75 %)	52
4.7	Ground Leakage Current Using Unipolar Switching Technique (155.2 mA)	52
4.8	THD Ground Leakage Current For Unipolar H-Bridge Inverter (26761.36 %)	53
4.9	(a) Common-mode Voltage (V_{cm}), (b) V_{ao} and (c) V_{bo} That Obtained Using Unipolar Switching Technique	54
4.10	Output Inverter Voltage 30 V (V_{ab})	54

4.11	Output Inverter Current 24.98 mA (I_o)	55
4.12	Output Inverter Voltage 24.98 V (V_o)	55
4.13	THD Current For Bipolar H-Bridge Inverter (3.21 %)	56
4.14	THD Voltage For Bipolar H-Bridge Inverter (3.21 %)	56
4.15	Ground Leakage Current Using Bipolar Switching Technique (1.556 mA)	57
4.16	THD Ground Leakage Current For Bipolar H-Bridge Inverter (189.13 %)	57
4.17	The Effect Of Filter With One Inductor On Ground Leakage Current (3 A)	59
4.18	The Ground Leakage Current Spectrum When Used Filter With One Inductor (142138.91 %)	59
4.19	The Effect Of Filter With Split Inductor With Same Value On Ground Leakage Current (1.556 mA)	60
4.20	The Ground Leakage Current Spectrum When Used Filter With Split Inductor Same Value (189.13 %)	60
4.21	Ground Leakage Current Of Filter Ratio 1 (1.556 mA)	61
4.22	Ground Leakage Spectrum Filter Ratio 1 (189.13 %)	61
4.23	Ground Leakage Current Of Filter Ratio 1.2 (51.99 mA)	62
4.24	Ground Leakage Spectrum Filter Ratio 1.2 (8171.57 %)	62
4.25	Ground Leakage Current Of Filter Ratio 1.4 (63.69 mA)	63
4.26	Ground Leakage Spectrum Filter Ratio 1.4 (11218.36 %)	63
4.27	Ground Leakage Current Of Filter Ratio 2 (158.7 mA)	64
4.28	Ground Leakage Spectrum Filter Ratio 2 (25782.03 %)	64
4.29	Ground Leakage Current Of Filter Ratio 5 (4460.8 mA)	65
4.30	Ground Leakage Spectrum Filter Ratio 5 (85271.87 %)	65
4.31	Ground Leakage Current ($1.556 \text{ mA}_{\text{peak}}$) Using Parasitic Capacitor = 10 nF	66
4.32	Ground Leakage Current ($3.21 \text{ mA}_{\text{peak}}$) Using Parasitic Capacitor = 30 nF	66
4.33	Ground Leakage Current ($3.772 \text{ mA}_{\text{peak}}$) Using Parasitic Capacitor = 40 nF	67
4.34	Ground Leakage Current ($3.928 \text{ mA}_{\text{peak}}$) Using Parasitic	67

	Capacitor = 50 nF	
4.35	Ground Leakage Current (1.556 mA _{peak}) using 8 kHz Switching Frequency	68
4.36	Ground Leakage Current (1.1 mA _{peak}) using 16 kHz Switching Frequency	68
4.37	Ground Leakage Current (529.4 μA _{peak}) using 24 kHz Switching Frequency	68
4.38	Bipolar Switching Scheme Using XMC 4500	69
4.39	Unipolar Switching Scheme Using XMC 4500	70
4.40	(a) V _{ao} Using Unipolar Switching Technique (b) V _{bo} Using Unipolar Switching Technique	70
4.41	Output Inverter Voltage Using Unipolar Switching Technique 30V _{peak} (10 V/div)	71
4.42	AC Waveform For Unipolar H-Bridge Inverter. Output Voltage 12 V _{peak} (Blue Trace 5 V/div) and Output Current 600 mA _{peak} , (Purple Trace 500 mA/div)	71
4.43	THD Voltage (0.5 %) For Unipolar H-Bridge Inverter Using Fluke 43B Power Quality Analyzer	71
4.44	Ground Leakage Current Using Bipolar Switching Technique 100 mA _{peak} (100 mA/div)	72
4.45	(a) V _{ao} Using Bipolar Switching Technique (b) V _{bo} Using Bipolar Switching Technique	73
4.46	Output Inverter Voltage Using Bipolar Switching Technique 30 V _{ab} (10 V/div)	73
4.47	AC Waveform For Bipolar H-Bridge Inverter. Output Voltage 24 V _{peak} (Blue Trace 10.0 V/div) and Output Current 1.2 A _{peak} (Purple Trace 1 A/div)	73
4.48	THD Voltage (1.7 %) For Bipolar H-Bridge Inverter Using Fluke 43B Power Quality Analyzer	74
4.49	Ground Leakage Current Using Bipolar Switching Technique (1.8 mA _{peak})	74
4.50	The Effect Of Filter With One Inductor On Ground Leakage Current 2 A _{peak} (1 A/div)	75

4.51	The Effect Of Filter With Split Inductor With Same Value On Ground Leakage Current $1.8 \text{ mA}_{\text{peak}}$ (2 mA/div)	75
4.52	Ground Leakage Current $40 \text{ mA}_{\text{peak}}$ Using Filter Ratio 1.2 (20 mA/div)	76
4.53	Ground Leakage Current $55 \text{ mA}_{\text{peak}}$ Using Filter Ratio 1.4 (50 mA/div)	76
4.54	Ground Leakage Current $160 \text{ mA}_{\text{peak}}$ Using Filter Ratio 2 (100 mA/div)	76
4.55	Ground Leakage Current $500 \text{ mA}_{\text{peak}}$ Using Filter Ratio 5 (250 mA/div)	77
4.56	Ground Leakage Current $1.8 \text{ mA}_{\text{peak}}$ With Parasitic Capacitor Value 10 nF (2 mA/div)	77
4.57	Ground Leakage Current $2 \text{ mA}_{\text{peak}}$ With Parasitic Capacitor Value 30 nF (2 mA/div)	78
4.58	Ground Leakage Current $3 \text{ mA}_{\text{peak}}$ With Parasitic Capacitor Value 40 nF (2 mA/div)	78
4.59	Ground Leakage Current $4.4 \text{ mA}_{\text{peak}}$ With Parasitic Capacitance Value 50nF (20 mA/div)	79
4.60	Ground Leakage Current $1.556 \text{ mA}_{\text{peak}}$ Using 8 kHz Switching Frequency (2 mA/div)	79
4.61	Ground Leakage Current $0.6 \text{ mA}_{\text{peak}}$ Using 16 kHz Switching Frequency (1 mA/div)	80
4.62	Ground Leakage Current $529.4 \mu \text{ A}_{\text{peak}}$ Using 24 kHz Switching Frequency (1 mA/div)	80
4.63	Ground Leakage Current Levels Against L_r (L_{f1}/L_{f2})	83
4.64	Parasitic Capacitance Vs. Ground Leakage Current	83
4.65	Comparison Effect Of Switching Frequency Between Simulation And Experiment Hardware	84

LIST OF TABLE

TABLE	TITLE	PAGE
2.1	Switching Control	19
3.1	Gantt Chart of Research Methodology	27
3.2	Half-positive cycle operation mode of transformerless H-Bridge inverter	34
3.3	Operation mode of transformerless H-Bridge inverter	37
3.4	Simulation Parameter of single-phase transformerless inverter	41
3.5	Parameter of IGBT IHW15N120R3	43
3.6	The parameter of XMC 4500	45
4.1	Simulations result for unipolar SPWM and bipolar SPWM	58
4.2	Unipolar switching technique comparison result between simulation and hardware	81
4.3	Bipolar switching technique comparison result between simulation and hardware	81
4.4	The comparison between simulation and hardware by using LC filter with one inductance and split inductance with same value	83
4.5	Calculation of inductance value	84

LIST OF APPENDICES

APPENDIX	TITLE	PAGE
A	INFINEON-UTeM FYP Competition Poster	91



CHAPTER 1

INTRODUCTION

1.1 Background

Inverter is the power electronic circuit that converts direct current (DC) to alternating current (AC). In specifically, inverters convert power from a DC source to an AC source. The inverters are commonly used to supply AC fed from DC source such as grid-connected PV systems, grid connected fuel cell system and batteries. The grid-connected inverters play a crucial role in providing the electric power supply in an eco-friendly manner. Grid connected system required a galvanic isolation to prevent from ground leakage current. Nowadays, the technology of transformerless for grid-connected PV systems are introduced due to offer the high efficiency power conversion, less weight and low cost.

In the transformerless grid-connected PV systems, the path for the ground leakage current to flow, which is the parasitic capacitor is appear between positive and negative terminal of PV grid with the ground. Ground leakage current can produce serious electromagnetic interference either through directed or radiated emission that cause safety issues. In view of the VDE-0126-1-1 standard, the level of ground leakage current must be lower than $300 \text{ mA}_{\text{rms}}$, the level that can cause ventricular fibrillation and involuntary muscle contractions. Therefore, the topologies, switching algorithm, AC filter design have been proposed by previous researchers.

In the AC signal, the quality of signal is important parameter to consider. In electrical power distribution system, there are many non-linear loads drawing non-sinusoidal current is exists. It cause serious problem to power quality of the power

distribution system. The harmonic of the voltage and current will affect the power system components. Moreover, the harmonic can cause extra losses, overheating and over-loading to the system.

1.2 Problem Statement

Mostly, the commercial grid connected photovoltaic inverter will use line-frequency transformer, which is provide galvanic isolation and safety. However, the line-frequency transformers are big and weighty that causes the system bulky and makes the system become complex. Besides using line-frequency transformer, high-frequency isolation transformers also can be used which is cheaper, small size and weight. But, the inverters with high-frequency transformers have a several power stages that make the system complexity and decrease the system efficiency. Therefore, to make the system become more efficiency, the transformerless grid is used due to small loss. The advantages of the system are smaller size, lower cost, weight and high power density.

Due to the capacitance between the Photovoltaic grid- connected system and earth, potential differences enforced by switching actions of the inverter introduce a ground leakage current. The leakage current is appearing because there is no galvanic isolation when using transformerless. Factor effected ground leakage current is based on the topology used, switching strategy, parasitic capacitor and filter design. Appearing leakage current is causes the safety problem and increased system losses.

Low-power PV applications have limited input voltage range. Therefore, an expansive number of PV modules are joined in series to get high dc input voltage. Even though this setup is meets the target input voltage anyhow, it influence the power output level of the PV modules [12]. Thus, the single-phase transformerless inverter is used to extract power from the PV modules.

1.3 Objective

The objectives of this project are:

1. To model and analyze the single-phase transformerless inverter using Matlab/Simulink.
2. To design and develop hardware of single-phase transformerless inverter.
3. To verify the performance of single phase transformerless inverter between the simulation and hardware result.

1.4 Scope

The aim of this project is to focus the performance of single-phase transformerless inverter on reducing ground leakage current less than 300mA_{rms} based on VDE0126-1-1 German Standard but at the same time maintain the THD below 5% based on IEEE Standard 519. The Matlab Simulink is used to model and analyze the performance of ground leakage current by using simulation approach that are switching technique, parasitic capacitor, filter design and topology used. The single-phase transformerless inverter is tested using R loads. The single-phase transformerless inverter is simulated to determine the factor that effected ground leakage current.

The performance of the single-phase transformerless are analyze by using bipolar switching schemes. The purpose of this simulation is to compare the performance of the single-phase transformerless inverter in terms of ground leakage current and total harmonic distortion (THD).

The experiment single-phase transformerless inverter will be developed after the simulation result is obtained. The equipment contain of gate drive to turn ON and OFF IGBT. The H-Bridge involves of Insulated Gate Bipolar Transistor (IGBT) type G4PC50UD-E and connected with LC filter. For the control plan of the power switches, the PWM algorithm will be transferred to the microcontroller XMC 4500 as the fundamental controller. At long last, the information and result from the equipment will be studied and compare with the simulation result from the MATLAB Simulink.

1.5 Report Outline

This report consist five chapters that is start with the introduction of the project and the following five chapters of this report are arranged as follows:

Chapter 1 covers a little explanation of the background project, problem statement, objectives and scope of the project.

Chapter 2 covers the theoretical background of this project including the detail about the general renewable energy, basic type of single-phase inverter, the general topologies of single-phase transformerless inverter, PWM consideration, common mode leakage current definition and total harmonic distortion definition.

Chapter 3 covers about the project methodology. This chapter consists of the flowchart of the project, milestone, Gantt chart, factor that affects the ground leakage current, simulation model, hardware design and the switching method used in this project.

Chapter 4 discusses the simulation result by using PWM switching technique, filter design, parasitic capacitor analysis, ground leakage current analysis and the harmonic analysis to evaluate the performance of the inverter.

Chapter 5 is the summary of this project and the recommendation for the further research.

CHAPTER 2

LITERATURE REVIEW

2.1 Introduction

Inverter is a circuit that converts a direct current (DC) power to an alternating current (AC) power at a desired output voltage and frequency. The output powers are fully come from DC source. DC source that used is coming from local energy source such as fuel cell, photovoltaic cell (PV), small turbines and small hydroelectric plants. Single-phase inverters are mostly used in numerous applications involving variable voltage and variable frequency AC supply. The examples of several main applications are adjustable-speed AC motor drives, DC motor drive, induction heating, standby power supply, uninterruptible power supplies (UPS) and high voltage DC transmission systems. The inverter can be designed using transformer or transformerless.

2.2 Renewable Power Source

Renewable energy is energy that is produced from natural processes that are nonstop replenished. Such as sunlight, geothermal heat, wind, tides, and water. Renewable energy sources have been taken the place of the traditional sources and especially rapidly developments of photovoltaic (PV) technology and Fuel cell (FC) technology have been put forward these renewable energy sources in all others renewable energy source. The common renewable power source used is solar energy system, wind energy system and fuel cell system.

2.2.1 Solar Energy System

The most available source energy is the solar energy. Sun powered energy is non-pollution since it non-conventional source of energy. Energy from sun is one of the alternatives for power source as it is accessible all over the place. Energy from sun can be created through the sunlight based photovoltaic modules (PV). The PV comes in different power output to meet the load requirement. The benefits of solar energy are it has better protection, dependability, smaller cost, high efficiency, and monitoring features [19].

2.2.2 Wind Energy System

Wind energy is the slightest costly source of new sustainable power source that is perfect with condition protection programs [19]. The wind turbine catches the wind motor energy in a rotor comprises of at least two sharp edges mechanically coupled to an electrical to be utilized for the framework control.

2.2.3 Fuel Cells System

Fuel cell systems electrochemically oxidize a fuel source, which may consist of hydrogen or a simple hydrocarbon to produce electricity [20]. Fuel cell is able to deliver high electrical efficiency thru a wide range of sizes and part-load conditions. This system can be applied in small size. Therefore it can be positioned closed to electrical loads. Additional, fuel cell produce very small levels of regulated air pollutants plus reduced carbon dioxide emission due to better efficiency and low to no-carbon fuel sources. This system operates silently compared to solar and wind. Fuel cell systems are same with generating devices such as batteries and photovoltaic (PV) cells. The different between batteries and fuel cell is fuel cell can produced constant power as long as fuel cell and oxidant are contributed.

2.3 Inverter

In order to produce a sinusoidal ac output which magnitude and frequency can be controlled, a switch-mode dc to ac are used [1]. There are two kinds of essential inverter that is voltage source inverter (VSI) and current source inverter (CSI). The contrasts between these two sorts of inverters are as in the info source is of steady voltage or consistent current character.

2.3.1 Current Source Inverter (CSI)

Current source inverter is bolstered by a steady current source with an inductor in arrangement with a DC source. In this manner, the supply current does not change rapidly. Figure 2.1 demonstrates the square chart of CSI inverter. The CSI inverters are built with thyristor and GTOs and this is because the inverter is referred to high power levels. The thyristor and GTOs have the high rated current compared to the IGBT and MOSFET. By controlling the DC input voltage to the CSI, the load current is varied. The advantages of CSI are the peak current flow through thyristor is limited to save value and thyristor used for commutation are simpler. CSI is used in a extremely high-power AC drives [2].

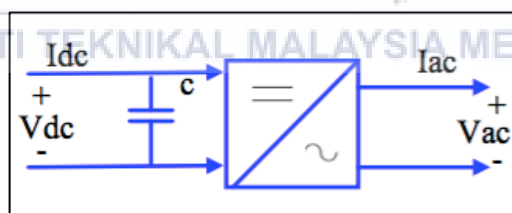


Figure 2.1: Circuit Structure of CSI Inverter

2.3.2 Voltage Source Inverter (VSI)

Voltage source inverter is served by a DC source of small inside impedance. VSI inverters are generally built with GTOs, thyristor or IGBTs. Figure 2.2 shows the block diagram of VSI inverter. Thus, to provide the constant DC voltage, the input voltage was parallel with capacitor. The AC terminal output voltage is continuous irrespective of the load current drawn. The advantages of VSI are the

input voltage is maintained constant, output voltage does not depend on the load and the size is small. The VSI can be classified to PWM inverter, square wave inverter and Single-phase inverters with voltage cancellation [2].

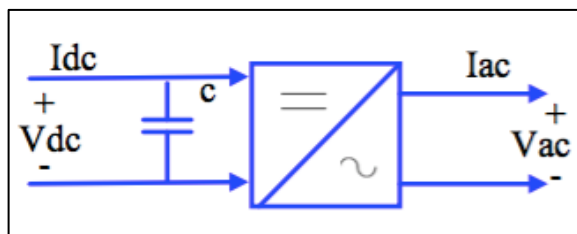


Figure 2.2: Circuit Configuration of VSI Inverter

2.4 VSI Topologies

PWM is connected to variable speed drives that are used as a part of various undeniably in new mechanical applications. The most generally utilized for VSI is sinusoidal heartbeat width regulation (SPWM). The classifications of VSI can be arranged into two section that is with transformer establishment and without transformer establishment.

2.4.1 Single-phase Inverter Topology for PV Grid Connected System

PV grid connected system usually use line frequency transformer or high frequency transformer to produce galvanic isolation. There are several topologies that used PV grid connected such as cascaded multilevel inverter topology and a power electronic transformer (PET) with a Cycloconverter on The Grid Side Topology.

2.4.1.1 Cascaded Multilevel Inverter Topology

Cascaded H-bridge may be a magnetic result to grid associated PV system. This topology may be associated with one DC-DC flyback converter on accomplishes best maximum power point tracking and in addition utilized to galvanic isolation in place will move forward system effectiveness [17]. DC-DC

flyback converters need aid cascaded to intensify dc voltage that utilized for medium and high voltage systems, which is those output voltage may be applied as input on H-bridge inverter. Then, H-bridge inverter cascaded on produce multilevel output voltage.

Figure 2.3 indicates the H-bridge comprises for four MOSFETs. Two upper MOSFETS would operating during line frequency and at same time alternate the other two operate at switching frequency. Therefore, it will lessen switching losses and moving forward system effectiveness. Besides, this topology likewise attain isolation during high frequency, eliminating the leakage current because of parasitic capacitance between PV module and ground, decoupling those second harmonic voltage ripple and decreasing the switching losses in the inverters.

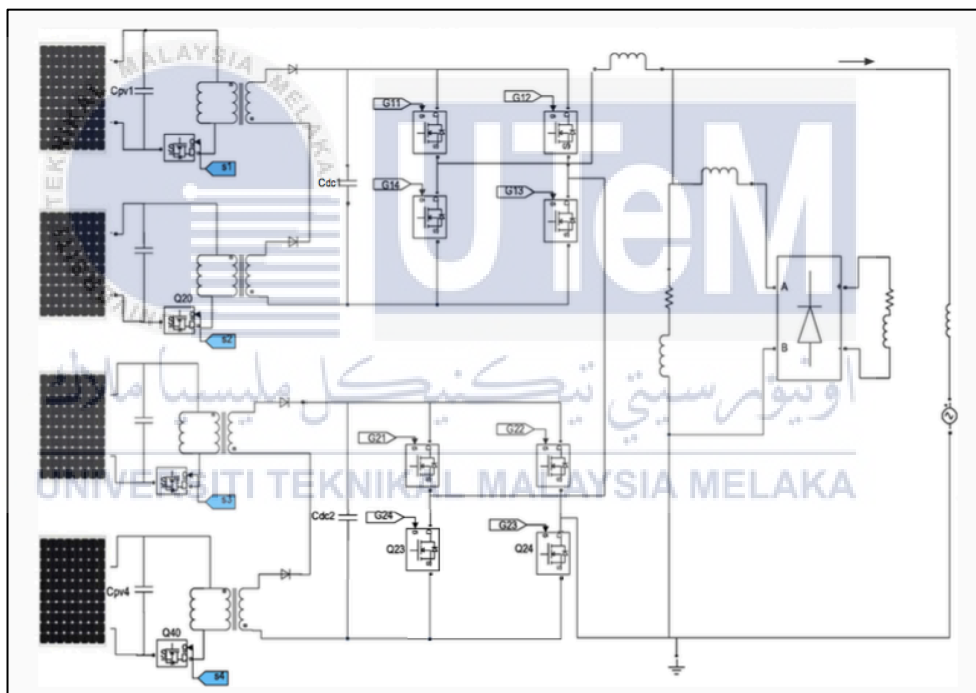


Figure 2.3: Cascaded Multilevel Inverter Topology

2.4.1.2 A Power Electronic Transformer (PET) with a Cycloconverter on The Grid Side Topology

An energy electronic transformer with a cycloconverter on the grid side will be used to coordination a few renewable energy source of the grid [18]. This topology is utilization thyristor-based phase-controlled cycloconverters as the grid side converters. It needs a single-phase multi winding high frequency transformer to

incorporate different renewable energy sources of the grid through the grid side converters.

Figure 2.4 shows the grid side converter is a thyristor-based cycloconverter. Advantage of thyristor is it ready to deal with a high measure of energy, arrangement and parallel operation of the gadgets isn't required bringing about lower number of gadgets and less difficult rationale circuit. At that point, the cycloconverter works in circling current mode bringing about a nonstop current supply and diminished symphonious substance in the yield voltage. The high recurrence transformer is a multi-winding transformer having various auxiliary windings to interface different sustainable power sources, and three essential winding, which fill in as the info supplies to the cycloconverters. Accordingly, the utilization of a solitary high recurrence transformer is to numerous line recurrence transformers result in a considerable lessening in size and weight. Then again, the spillage inductance of the transformer goes about as a short pass channel for the current across it, bringing about smooth and nonstop streams, which help the common compensation of the leakage energy of the transformer.

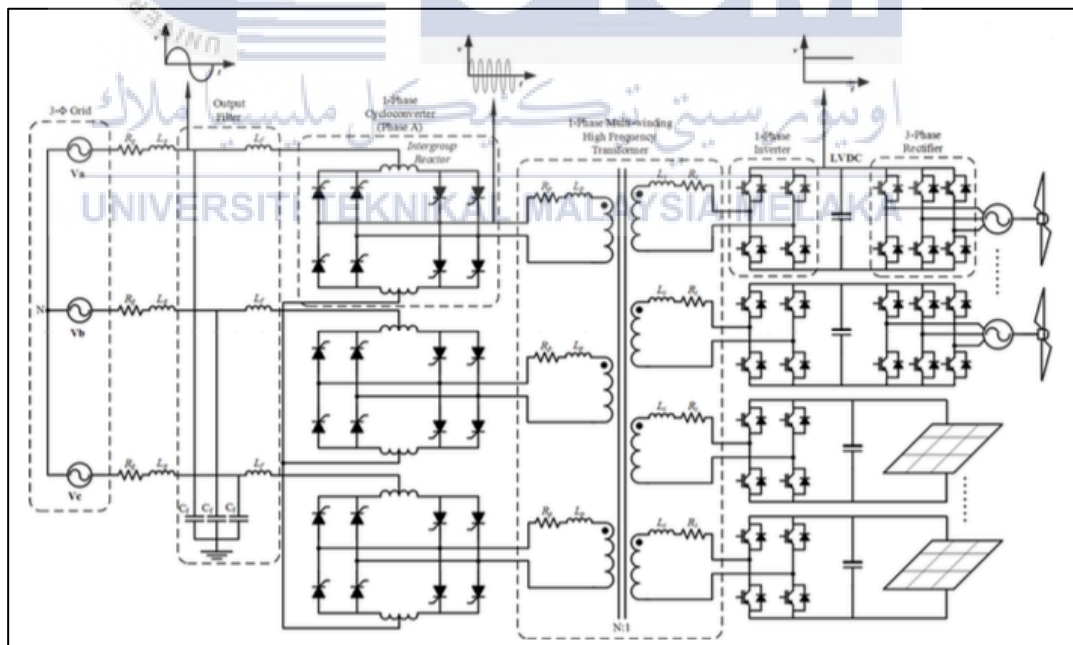


Figure 2.4: Power Electronic Transformer Topology for Integrating Multiple Renewable Energy

2.4.2 Transformer Inverter System

PV grid usually uses a line transformer to provide galvanic isolation and for safety issued. However, the line frequency transformer is big and heavy that cause the system bulky and complex. Therefore, high-frequency isolation is used due to lower cost, smaller size and weight. However, the inverter that uses high frequency transformer use numerous power stages, which is increase the system complexity and reduce the system efficiency. Thus, the transformerless inverter was introduced to make the system more efficiency due to low loss.

2.4.3 Single-phase Inverter Transformerless Topology

There are many single-phase inverter transformerless topologies for the selections of inverters. The single phase full bridge inverter is commonly used for modern power conversion in various applications for example hybrid/electric vehicles (HEVs/EVs), photovoltaic applications (PV) and bridge less power factor corrector [4]. There are several types of topologies for transformerless system such as single-phase full-bridge five-level grid connected PV transformerless inverter topology, split-capacitor H-bridge (SC-HB) topology, a single-phase bipolar sinusoidal pulse width modulation (SPWM) H-Bridge power inverter configuration with a DC/DC high gain conversion-boosting (CD-Boost) topology, H6 single-phase inverter topology and High Efficient and Reliable Inverter Concept (HERIC) topology.

2.4.3.1 Split-capacitor H-bridge (SC-HB) Topology

Split-capacitor H-bridge (SC-HB) topology is works to accomplish higher efficiency, lower cost, lighter weight, smaller size. Usually, bipolar SPWM system to the H-bridge inverter might have been utilization diminish the ground leakage current. But, those exchanging system provides for twice the grid present swell Furthermore higher THD contrasted with unipolar SPWM strategy [11]. By utilizing the unipolar SPWM, those low leakage current might even now make achieved for

these topologies when those PV exhibit disengage starting with the grid during zero vector state.

Therefore, those SC-HB may be a topology that to be used to suppressing ground leakage current. SC-HB used those unipolar SPWM switching technique. Figure 2.5 indicates the SC-HB inverter topology that needs a grounded association during those mid-point of its two-arrangement DC-link capacitor [11]. By utilizing this method, those common-mode voltages practically consistent. The common-mode voltage must chance to be kept consistent throughout at communication states of the inverter exchanging system on prevent from ground leakage current. DC-DC converter might have been utilized within this topology because of the utilization about series-connected capacitor. The DC-link capacitor need to split into two and interfacing the DC-link mid-point to the ground, this topology able on produce near-constant common-mode voltage and extremely low leakage ground current [11]. SC-HB topology is produce low leakage current and higher conversion efficiency.

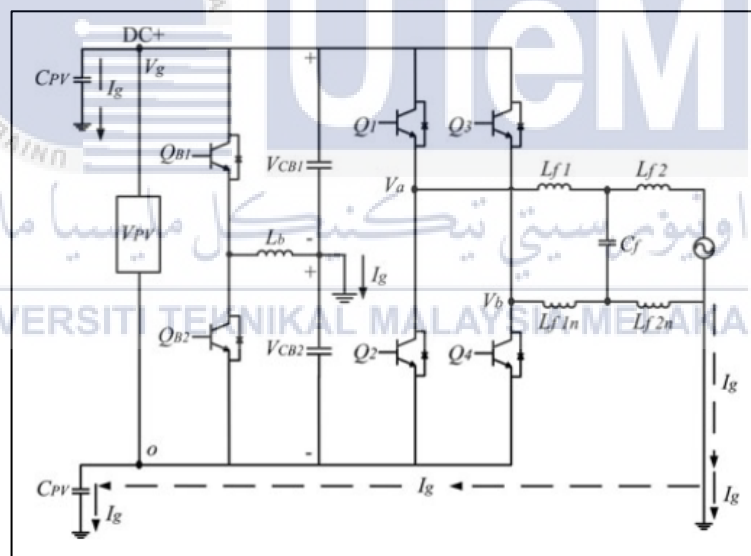


Figure 2.5: SC-HB Inverter Topology

2.4.3.2 H6 Single-phase Inverter Topology

H6 single-phase inverter topology is able to remove common-mode leakage current in the transformerless photovoltaic grid-connected system. This topology is a three level inverter with SPWM technique and capable of withstanding the low input voltage [13]. Reactive power (VAR) control is used.

Two additional switches are decoupled on the DC side to make this system higher efficiency and suitable thermal design as shown in Figure 2.6. The H6 inverter topology has two-phase legs similar to H4 inverter topology. A controller is used for the grid-tied inverter that is consisting three segments which is current controller, utility grid synchronizer and DC voltage controller.

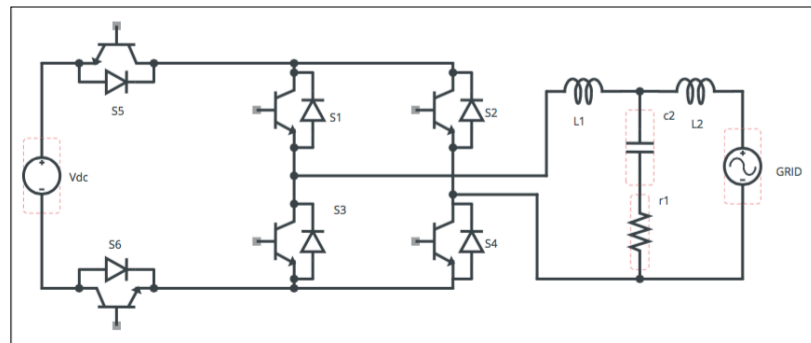


Figure 2.6: H6 Inverter Topology

2.4.3.3 High Efficient and Reliable Inverter Concept (HERIC) Topology

The HERIC topology is derived from the H-bridge converter where AC bypass leg is added. Figure 2.7 shows the HERIC topology that is two switches has been connected parallel to the bridge. The two switches work may be on isolating those photovoltaic board from the grid, and keeping those reactive power between the filter inductors and capacitors during those zero voltage state, in this manner expanding effectiveness [14]. The disadvantage of HERIC topology is high number of switches that leads to higher complexity and switching losses.

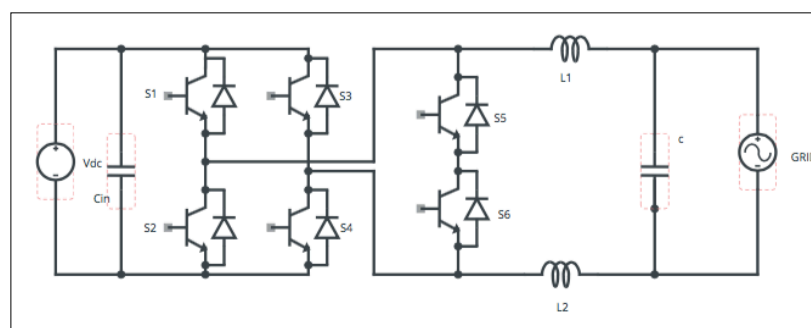


Figure 2.7: HERIC Topology

2.4.3.4 Single-phase Full-bridge Grid Connected PV Transformerless Inverter Topology

The main point of this topology is to eliminate the common mode leakage current. The modulation technique used third harmonic injection with multicarrier phase-shifted pulse width modulation. The modulation technique practical to single-phase full-bridge five-level grid connected PV transformerless inverter topology [10]. Two extra switches on the DC side were added to the single-phase full-bridge inverter that functioned to produce five-level output. This topology was produces low spectrum in the grid current and the leakage current are detected at the securer acceptable limits.

Figure 2.8 shows the single-phase five-level grid connected transformerless PV inverter topology that consists of full bridge inverter with switches S_1 , S_2 , S_3 , and S_4 with additional double switches S_5 and S_6 located near the dc side. Function of this two extra switch is to controls the current flow to and from the neutral of the photovoltaic system. When the inverter is isolated between the grid and the PV panel through zero voltage state, the common mode leakage current is reduced. This system also reduces harmonics. The modulation technique performs well in reducing the production of common mode voltage in the transformerless PV system.

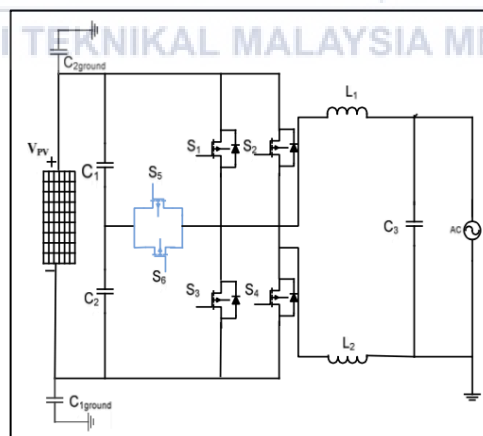


Figure 2.8: Single-phase Grid Connected Transformerless PV Inverter

2.5 Switching Technique for Single-Phase Circuit

AC signal that is generated from inverter circuit is controlling by switching technique. The several switching techniques are pulse width modulated inverters, square wave inverter and single-phase inverter with voltage cancellation.

2.5.1 Pulse-width-modulated Inverters

Pulse-width-modulation (PWM) gives an approach to decline the total harmonic distortion of load current. The amplitude of the output voltage could make regulated for the modulating waveforms. Lessened filter necessities will diminish harmonics and the control of the output voltage amplitude is two different favorable circumstances about PWM. A pure sin wave is gotten after passing the sign through a low pass filter. The reasons PWM have a wide application in modern electronics and the reasons are [5]:

- Reduction Power Loss – those switches circuits have a tendency to have more level energy utilization a direct result those switching devices need aid very nearly dependably off (low present which is low force) or hard-on (low voltage which may be low force).
- Simple to Produce – A percentage about microcontroller that employments chip that incorporate PWM run in the foundation without meddling with executing code.
- Digital to Analogue Conversation – PWM signal could be regulated faultlessly by simple counting procedures, which will be used to fulfill digital-to-analogue change.
- The characteristic of the desired PWM technique [5]:
 - Great use for DC supplies voltage conceivably a high voltage gain.
 - Linearity about voltage control.
 - Low amplitude from claiming low order harmonic for output voltage on minimizes those harmonic substances from output current.
 - Addition time recompense for corrects operation of the inverter switches and control system.

Two signals are compared in SPWM (Sinusoidal Pulse Width Modulation). Control of the switches to sinusoidal PWM output needs a reference signal that is sinusoid and a carrier signal [3]. The pulse wave were generated toward contrasting those two signals and the width from claiming every pulse will be differed may be extent of the amplitude of the sine wave. The frequency of the reference signal determines that inverter output frequency and the references peak amplitude controls that modulation index and the RMS quality of the output voltage [5].

2.5.2 Square-wave Inverters

The input dc voltage is controlled with a command goal to control the greatness of the output magnitude voltage, and accordingly the inverter needs to control just the recurrence of the output voltage. The output of ac voltage has a waveform like a square wave, subsequently these inverters are called square-wave inverter [1].

2.5.3 Single-phase Inverters with Voltage Cancellation

If there should arise an occurrence of inverters with single-stage output, it is conceivable to control the magnitude and the frequency of the inverter output voltage, despite the fact that the contribution to the inverter is a steady DC output voltage and the inverter switches are not pulse width modulated. Along these lines, these inverters consolidate the characteristic for the past two inverters. The voltage cancellation method works only thru single-phase inverter [1].

2.6 Modulation Schemes

There are many modulation methods and the three main modulation scheme widely used are bipolar PWM, unipolar PWM and hybrid PWM. Some of PWM have advantages in reducing EMI by spreading spectrum, or reduced switching loss, they fare not used frequently due to either complex control strategy, difficulty in calculation or realization. In bipolar and unipolar modulation schemes, the four main

switches are switching at same carrier frequency. For hybrid PWM, two out of four switches are driven by high switching frequency PWM signals for great quality sinusoidal output and the other two commutated at the low fundamental frequency [4].

2.6.1 SPWM with Bipolar Switching

The different among control signal, V_r with the triangular signal, V_c create the switching pulse or PWM for the switching devices. When the control signal, V_r is larger than triangular signal, V_c , the output is $+V_d$ and when the control signal, V_r is smaller than triangular signal, V_c the output is $-V_d$ as shown in figure 2.9.

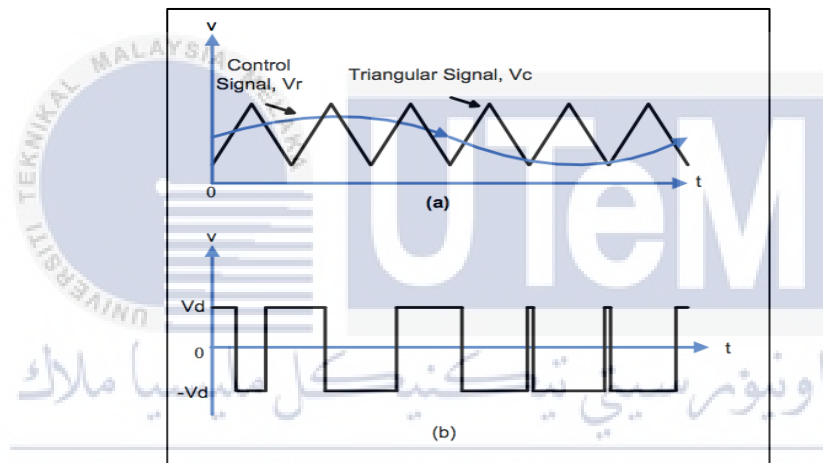


Figure 2.9: (a) Switching Pattern (b) Output Waveform

The output alternates the middle of in addition to and less dc supply voltage, accordingly this will be bipolar. The figure 2.10 indicates full bridge converter to bipolar PWM, which will be S_1 and S_2 are on when $V_r > V_c$ ($V_o = +V_d$) same time S_3 and S_4 are on when $V_r < V_c$ ($V_o = -V_d$). To those full-bridge circuit application, the askew pairs about switches S_1 and S_2 and S_3 and S_4 would switched then again in those switching frequency [16]. Though the switching movements need aid conveyed at the same time, no progressions show up in the common-mode voltage furthermore no leakage current are produced. But, IGBTs What's more diodes need aid switching at the switching frequency with that entire information voltage that reasons multiplying the switching losses.

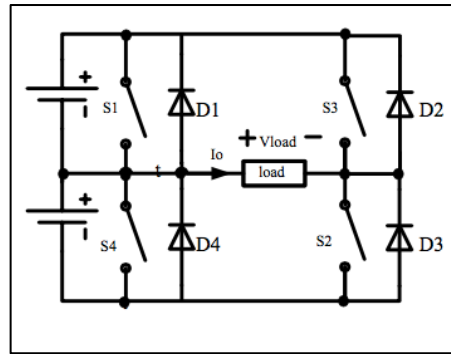


Figure 2.10: Full Bridge Converter

2.6.2 SPWM with Unipolar Switching

Unipolar another switching plan close to bipolar that the output is changed either from high to zero or from low to zero, instead of amongst high and low as in bipolar switching [3]. The switch sets $((S_1, S_4)$ and (S_2, S_3) are correlative. One sets of switches is working at the carrier frequency while the other match works at the reference frequency, in this manner having two high-frequency switches and two low-frequency switches [3].

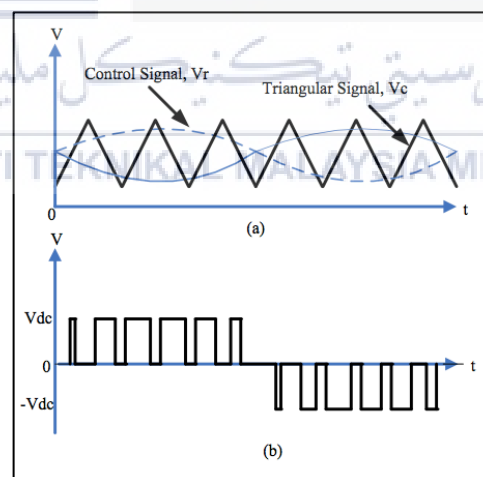


Figure 2.11: Waveform of Unipolar Modulation Scheme

Figure 2.11 (a) shows the SPWM with unipolar switching with the comparison between control signal, V_r and triangular signal, V_c . Figure 2.12 (b) shows the output waveform where $+V_d$ when $V_r > V_c$ and $-V_d$ when $V_r < V_c$. For the full bridge circuit application, only two switches are on at the same time, and only one IGBT and one diode commutate at the switching frequency with the whole input

voltage [16]. This technique can be applied when use a line transformer but if there is no transformer used, the leakage current would not be controlled.

Unipolar switching scheme has switch control as shown in Table 2.1.

Table 2.1: Switching Control

Signal Condition	Switching Control
$V_r > V_C$	S_1 is ON
$-V_r < V_C$	S_2 is ON
$-V_r > V_C$	S_3 is ON
$V_r < V_C$	S_4 is ON

2.6.3 PWM Consideration

There are some definition and considerations when using a PWM in an inverter. The considerations are based on frequency modulation ratio, m_f and amplitude modulation ratio, m_a .

2.6.3.1 Frequency Modulation Ratio, m_f

Those Fourier arrangement of the PWM output voltage need an essential frequency that is same like those reference signal. Harmonic frequencies exist at around multiples of the switching frequency. m_f to be an odd basic and assuming that m_f may be not an integer, there might exist sub- sounds at output voltage. Harmonic frequencies exist toward and around multiples of the switching frequency. Expanding the carrier frequency (increase m_f) builds those frequencies in which the harmonics happen [3]. The Frequency modulation is represent in Equation 2.1.

$$m_f = \frac{f_{carrier}}{f_{reference}} = \frac{f_{tri}}{f_{sine}} \quad (2.1)$$

2.6.3.2 Amplitude Modulation Ratio, m_a

The amplitude of the fundamental frequency of the PWM output is thus measured by m_a . Alternatively, m_a can be varied to modify the amplitude of the output. However, if m_a is greater than 1, the amplitude of the output rises with m_a but not linearly [3]. The amplitude modulation ratio m_a is defined as a ratio of frequency ratio and reference signals as represented in Equation 2.2. If $m_a \leq 1$, the fundamental output voltage will be designed as illustrated in Equation 2.3.

$$m_a = \frac{V_{m,reference}}{V_{m,carrier}} = \frac{V_{m,sine}}{V_{m,tri}} \quad (2.2)$$

$$V_1 = m_a V_{dc} \quad (2.3)$$

2.7 Harmonic Distortion Definition

Harmonic distortion happens by nonlinear devices in the power system. A nonlinear device is one in which current may not be proportional to the connected voltage. Figure 2.12 illustrates this idea of a voltage sine wave connected to a straightforward nonlinear resistor to which the voltage and current fluctuate according to the curve [6]. Those voltage connected may be perfectly sinusoidal yet the resulting current will be distorted.

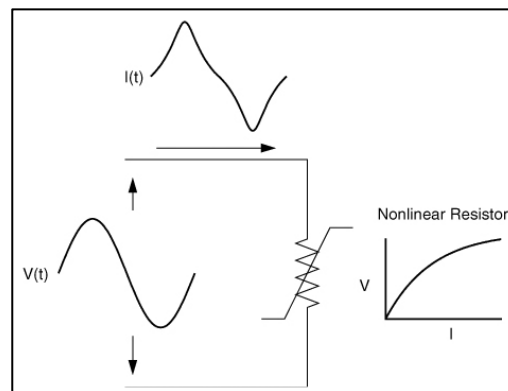


Figure 2.12: Current Distortion Caused By Nonlinear Resistance

2.7.1 Relation Between Harmonic Voltage and Current

The equipment producing the harmonics generates harmonic currents. The current flows through the conductor between power supply and equipment and produces harmonic voltage at the source. Figure 2.13 shows a switchboard that is supplying a UPS or VSD. The UPS or VSD produce harmonic currents and generate harmonic voltage at the switchboard because the harmonic current flow through the cable impedance [7].

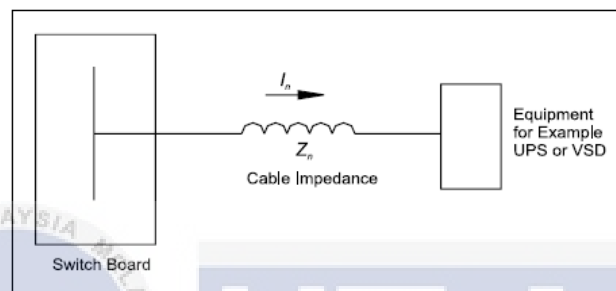


Figure 2.13: Relation Between Harmonic Voltage and Current

2.7.2 Total Harmonic Distortion

Total harmonic distortion (THD) is the metering and examination of sounds substance of current and voltage waveform. At the end of the day, THD is utilized to depict the nature of the air conditioner yield voltage or current. The nature of a non-sinusoidal wave can be communicated as far as aggregate consonant contortion (THD). Each of frameworks will deliver diverse THD for current and voltage relying upon the heap associated with the appropriation control supply [3]. Condition 2.4 and condition 2.5 portray the voltage THD (THD_v) and current THD (THD_i), where V_1 and I_1 are the major voltage and current. Expecting no dc part in the output,

$$\text{Total harmonic distortion in voltage: } THD_V = \frac{\sqrt{\sum_{n=2}^{\infty} (V_{n,rms})^2}}{V_{1,rms}} \quad (2.4)$$

$$\text{Total harmonic distortion in current: } THD_I = \frac{\sqrt{\sum_{n=2}^{\infty} (I_{n,rms})^2}}{I_{1,rms}} \quad (2.5)$$

The value of current THD changes from a couple of percent to over 100 % relying upon the sort of non-direct load appended to the power dispersion system. Typically, the voltage THD is differed inside fewer than 5 % is extensively satisfactory. In any case, the adequate range is diverse as indicated by nation [8]. The present consonant will change the shape factor of the current waveform and diminish the effective power factor on the dispersion power supply. The viable power factor is run from 0.5 to 1.0. The lessening of the power factor will build the power losses in appropriation power supply. Electronic segment that especially sensitive to the voltage harmonic, for example capacitor suffer effects the lifetime because of expanded warming from warming current [9]. Harmonic voltage additionally essentially influencing to the DC to c motors.

2.8 AC Filters

AC filters usually used to avoid harmonic currents from flowing into the ac network impedance affecting voltage distortion and induced phone obstruction in the capable of being heard frequency range. AC filter channel give a low-impedance way to ground at the harmonic frequencies. The AC filter consist a high-voltage capacitor banks and lower voltage reactors, resistors, and capacitors that form a circuit tuned to the characteristic harmonic [15]. This filter design is based on the harmonic currents generated and estimating harmonic impedance characteristic of the ac network across the whole range of operating conditions and tolerances.

2.9 Summary

This chapter begins by discussing the type of renewable energy that commonly used which is solar energy system, wind energy system and fuel cells system. This is followed by an overview of single-phase inverter connected to PV grid topology, which are cascaded multilevel inverter topology and a power electronic transformer (PET) with a Cycloconverter on the grid side. Thus, the transformer inverter system was explained. Here, the single-phase transformerless

inverter topology also had been review. Then, the switching techniques for single-phase inverter are reviewed. Lastly, modulation schemes, harmonic distortion and AC filter are discussed.



CHAPTER 3

DESIGN METHODOLOGY

3.1 Introduction

Project will done within planned by following the sequence. This chapter will discuss about the methodology of this project and also the flowchart will be used to guide the process of designing and step to analyzed the result. There are severe factor that affected the ground leakage current. As required in VDE-0126-1-1, the ground leakage current must be below $300 \text{ mA}_{\text{rms}}$. Thus, this chapter explains about the factor that effect ground leakage current and how to reduce the leakage current. The simulation is use MATLAB/Simulink to analyzed the factor affected ground leakage current.

3.2 Research Methodology

In order to ensure this project done within planned time, this project must be followed by sequence. Therefore, in this chapter flowcharts, milestone and Gantt chart that will assist the explanation about the process and steps or procedures in conducting this research. Also, the Simulink for both bipolar and unipolar switching scheme are modeled by MATLAB/SIMULINK.

3.2.1 Flowchart

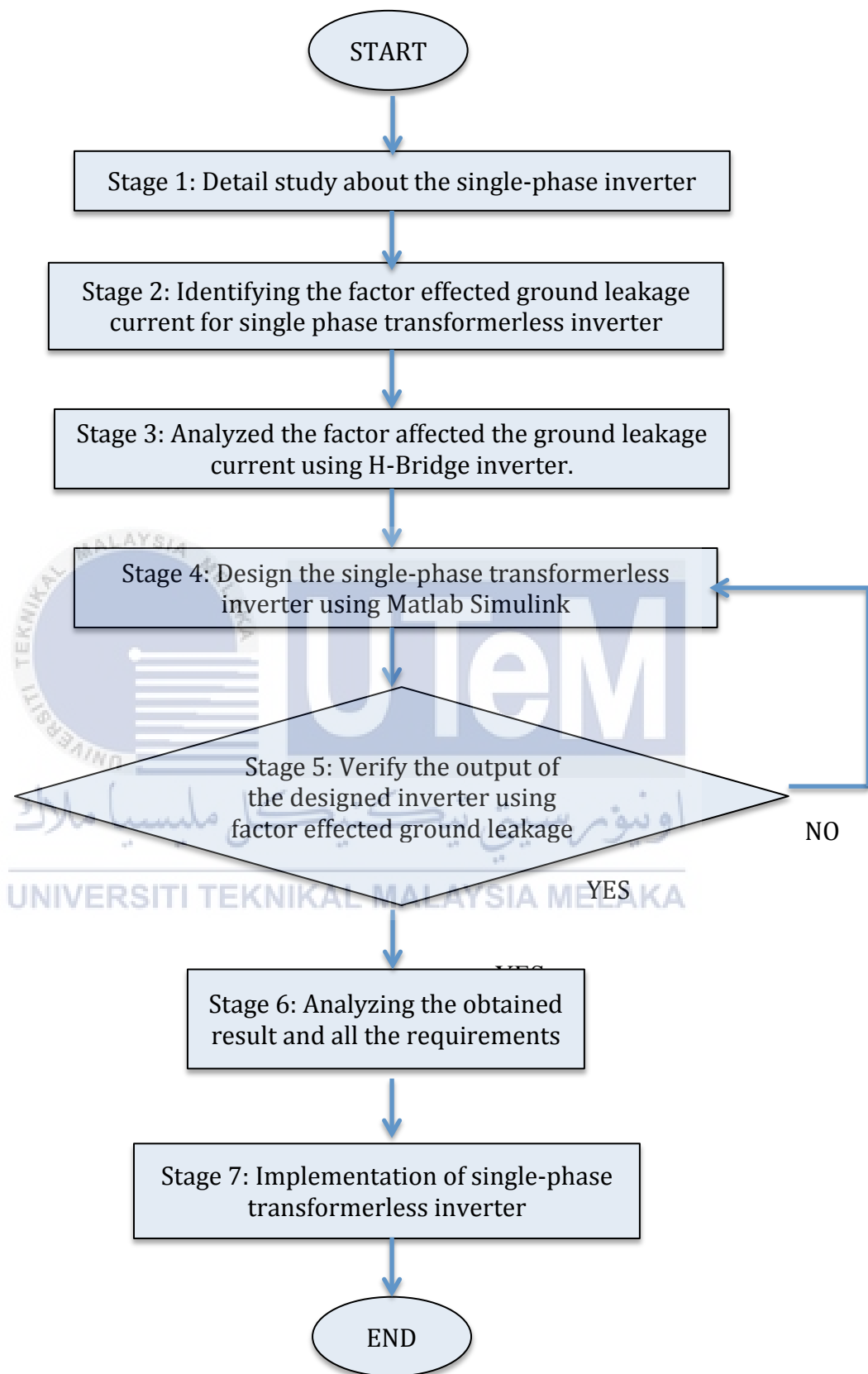


Figure 3.1: Flowchart of Research Methodology

Figure 3.1 displays the flow of the process guided upon completion of this project. Firstly, to conduct this project, all information and data required need to be gathered. The information and data that are achieved is very important to get a full understanding about this project and to ensure this project runs smoothly. The gathered information will assist in identifying the factors that affect ground leakage current for a single-phase transformerless inverter.

Then, after identifying the factors that affect ground leakage current, the simulation of a single-phase transformerless inverter is conducted. The performance of a single-phase transformerless inverter was analyzed using unipolar and bipolar switching schemes. The purpose of the simulation is to analyze the factors of the ground leakage current. MATLAB and Simulink were used to implement the simulation and to analyze the obtained results. After analyzing the effect of ground leakage current, a single-phase transformerless inverter was proposed.

In the elaboration of this research, the analysis on ground leakage current and THD has been carried out for a single-phase transformerless inverter. This simulation is simulated to investigate the effect of leakage current and the effect of THD.

Finally, after completing the modeling of a single-phase transformerless inverter, the hardware for a Single-phase Transformerless Inverter will be implemented according to the designed characteristics in the MATLAB/Simulink simulation.

3.2.2 Milestone Research

There are 7 milestones set for this project to ensure this project runs smoothly.

Milestone 1: Research on single-phase inverter.

The first milestone is to study the concept and the topology of a single-phase inverter. It is also to study the pulse width modulation (PWM) switching method.

Milestone 2: Simulation on the single-phase transformerless inverter.

The milestone is to analyze the factors that affect ground leakage current using an H-bridge inverter. Unipolar and bipolar were used for the switching technique.

Milestone 3: Design a single-phase transformerless inverter based on the factors that affect the ground leakage current.

Milestone 4: Validate the data obtained from the simulation.

Milestone 5: Development of single-phase transformerless inverter. The design of circuit and hardware of single-phase transformerless inverter was developed and hardware is analyzed.

Milestone 6: Validate the data obtained from hardware.

Milestone 7: Report writing.

3.2.3 Project Gantt Chart

Table 3.1: Gantt chart of Research Methodology

Milestone	Year	2017				2018				
	Task	9	10	11	12	1	2	3	4	5
1	Research on single-phase inverter	█	█	█						
2	Analyzed factor effected the ground leakage current using H-Bridge inverter		█	█						
3	Simulate the single-phase inverter				█					
4	Validate the data get from simulation		█	█						
5	Development of single-phase transformerles inverter						█	█	█	
6	Validate the records obtain from hardware							█	█	█
7	Report writing		█	█	█	█	█	█	█	█

Table 3.1 shows the Gantt chart of activities conducted according to the month upon completing of this project. Based on this chart, this project starting on September 2017. The first step of this project is research on single-phase inverter. This research has been done for three months. Two month is required to do

simulation for the single-phase transformerless inverter. The simulation is focused on the factor that affects the ground leakage current of single-phase transformerless inverter using bipolar and unipolar. After the factor that affects the ground leakage current is analyzed, a single-phase transformerless inverter was proposed and the performance will analyze within two month. Then, after the simulation is completed, the hardware will implement and approximately five months require completing the hardware. The data obtain from hardware will validate and four month is required to do this project. Lastly, the report writing is conducted along the way of the project start.

3.3 Single-phase Transformerless Inverter

Single-phase transformerless inverter is a connection of H-bridge with DC source. Single-phase transformerless inverter that linked with PV grid has a ground leakage current problem due to no galvanic isolation. Leakage current is the main focus of the grid linked PV inverters. There are four factor that effect the ground leakage current which is switching technique, parasitic capacitance, type of filter and topology used.

3.3.1 Ground Leakage Current

In order to reduce cost, size, losses of power PV application system, line frequency transformer or high frequency transformer is removed. When there is no transformer, a galvanic connection between the ground of the grid and the PV array exist. The parasitic capacitor appears between the output terminal of PV grid and the ground, which is creating a low impedance path for leakage current to flow as shown in Figure 3.2. The potential different imposed on the parasitic capacitance through switching actions of the inverter inject a capacitive ground leakage current. The ground leakage current is measured between neutral (N) point and ground.

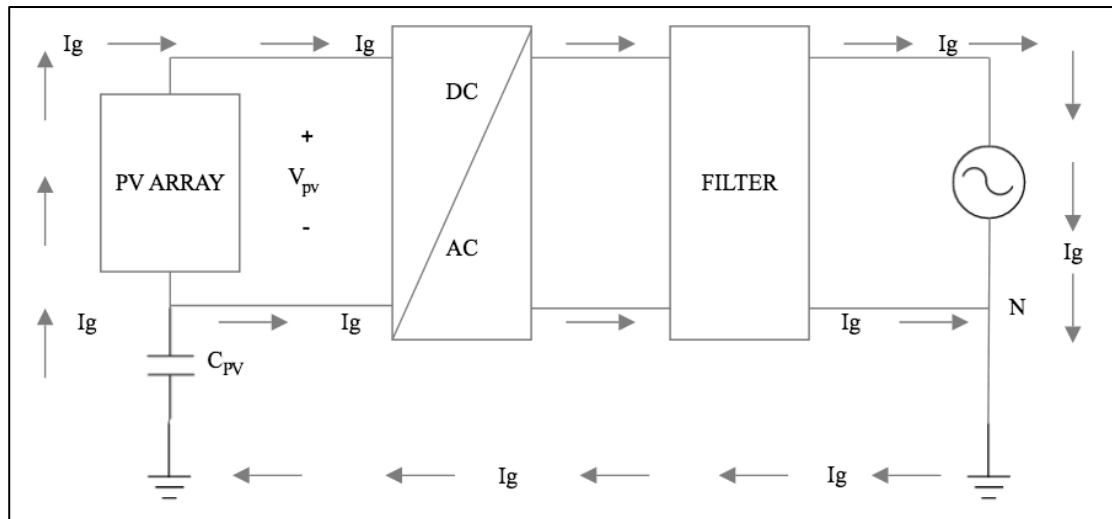


Figure 3.2: Transformerless Single-phase Inverter With Parasitic Capacitance

The estimation of ground leakage current relies upon the frequency substance of the voltage variance of the PV terminal that is through the parasitic capacitance. In order to minimize the ground leakage current, the values of capacitance need to reduce by decreasing the grounding frame of the PV grid. Next, pick the exchanging strategy that is no voltage vary and utilize an appropriate channel plan. Finally, pick a topology that lessening the voltage vacillation between PV system and ground. The VDE 0126-1-1 standard is alluded to observed the security issues of operation transformerless PV grid-connected system.

3.3.2 Common-mode Voltage in Single-phase Transformerless Inverter

A common-mode resonant circuit appears when the PV panel and grid are not isolated that is consist of parasitic capacitance (C_{pv}), H-Bridge inverter, LC Filter and utility grid. The behavior of a common-mode resonant circuit model system is represent in Figure 3.3. This model shows the common-mode voltage (V_{cm}) and differential-mode voltage (V_{dm}). Output voltage can be measure at point a and b. The ground leakage current can be investigating through the both power inverter voltages (V_{cm} and V_{dm}). Equation (3.1) indicates the common-mode voltage is the middling of output voltage.

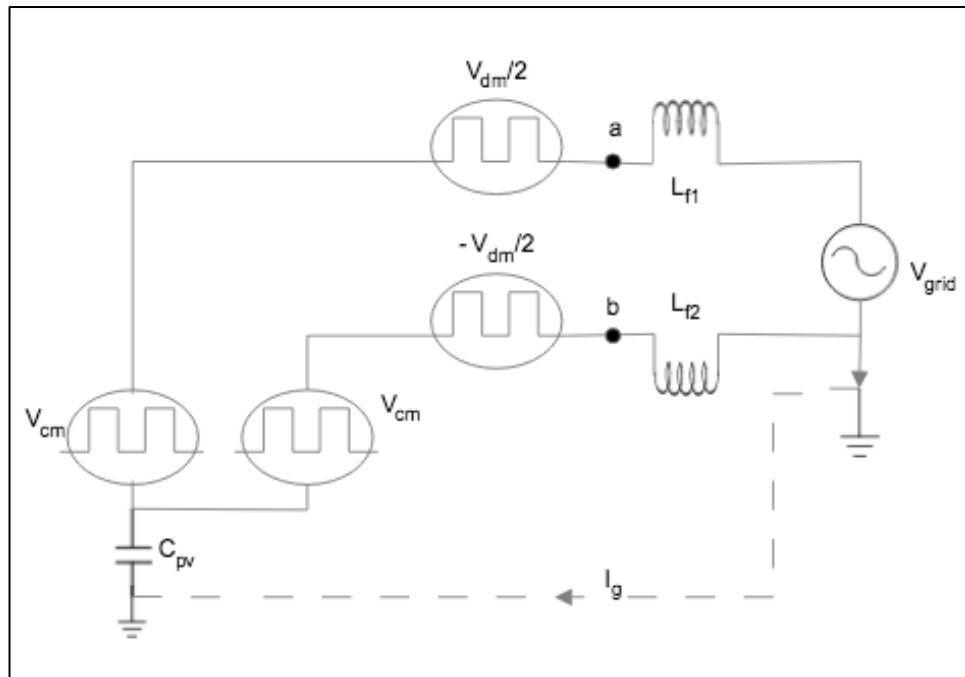


Figure 3.3: The Common-mode Model For The PWM Voltage Source Inverter



System

$$V_{cm} = \frac{V_a + V_b}{2} \quad (3.1)$$

The differential mode voltage (V_{dm}) is the voltage difference among two-output power inverter as defined in Equation (3.2).

$$V_{dm} = V_a - V_b \quad (3.2)$$

The output power inverter voltage terminals and negative terminal can be expressed as in (3.3) and (3.4) from the Equation (3.1) and (3.2).

$$V_a = \frac{V_{dm}}{2} + V_{cm} \quad (3.3)$$

$$V_b = -\frac{V_{dm}}{2} + V_{cm} \quad (3.4)$$

The model of Figure 3.4 can be arranged by using Thevenin's theorem and shortened equal model of common-mode resonant circuit [23]. Equation (3.5) defined the inverter equivalent common-mode voltage (V_{ecm}).

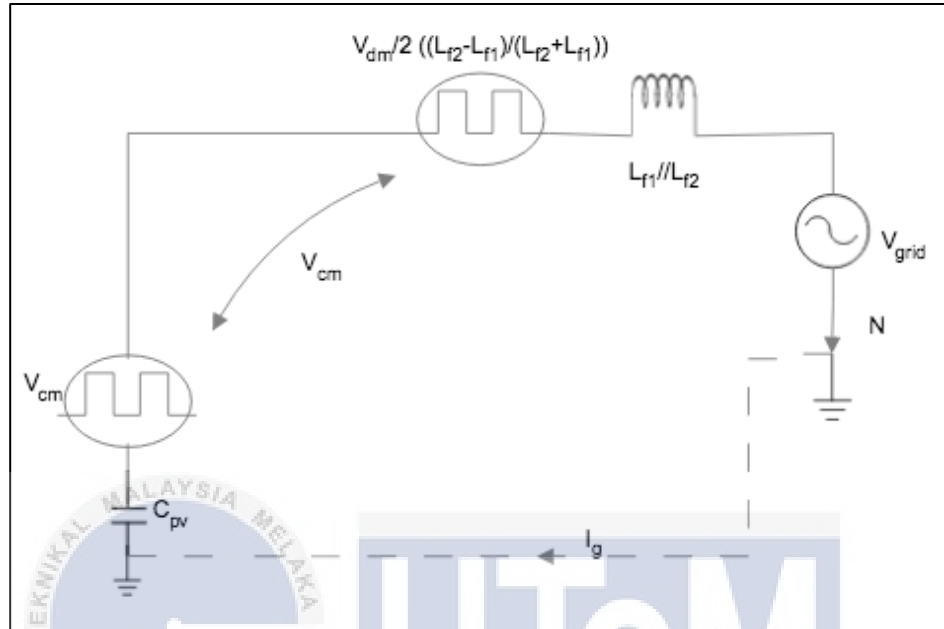


Figure 3.4: Simplified Equivalent Model of Common-mode Resonant Circuit

$$V_{ecm} = V_{cm} + \frac{V_{dm}}{2} \left(\frac{L_{f2} - L_{f1}}{L_{f2} + L_{f1}} \right) \quad (3.5)$$

The filter inductors (L_{f1} and L_{f1}) usually used the similar values. As an effect, the inverter same common-mode voltage is only expressed by inverter common-mode voltage (V_{cm}) as shown in Equation (3.5) and modeled in Figure 3.5.

$$V_{ecm} = V_{cm} = \frac{V_a + V_b}{2} \quad (3.6)$$

From the model of Figure 3.5, it shows the ground leakage current (I_g) is excited by the stated inverter common-mode voltage (V_{cm}) circuit.

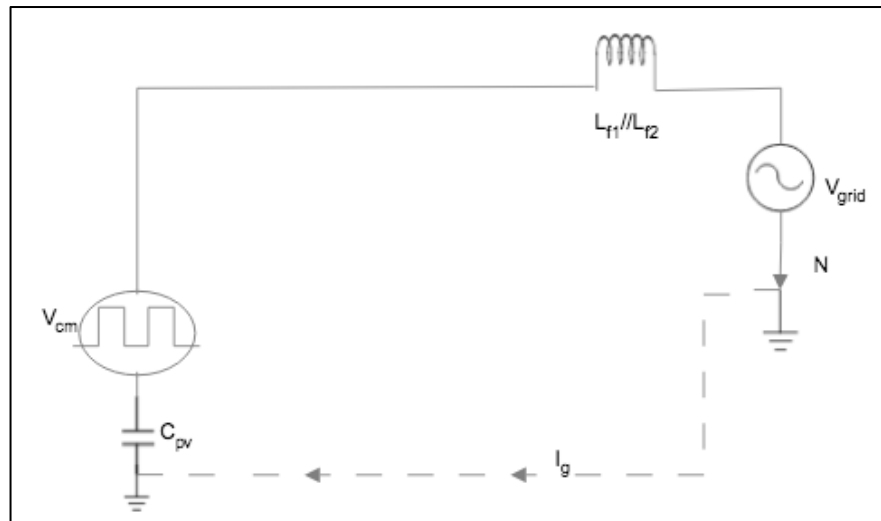


Figure 3.5: Equivalent Circuit For The Common-mode Leakage Current Path

Thus, the ground leakage current relies only on the varieties of the inverter common-mode voltage, which may be characteristic in (3.7) [12]. To prevent high flowing current through the common-mode model circuit, the common-mode voltage ($\frac{dV_{cm}}{dt}$) necessity to kept continuous.

$$I_g = C_{pv} \frac{dV_{cm}}{dt} \quad (3.7)$$

3.3.3 Parasitic Capacitance of PV Grid System

The parasitic capacitance (C_{pv}) produced among the output terminal of PV grid and ground as shown in Figure 3.2. The value of the parasitic capacitor is depends on the weather conditions, gap among the PV cell to the module and the atmospheric conditions [12]. Figure 3.6(b) show the one electrode of the capacitance is produced by the photovoltaic cells while the other by the grounded frame [21]. The worst case of the whole surface of the PV array is shielded by a conducting layer rising the area of the grounded electrode of the array as shown in Figure 3.6 (a).

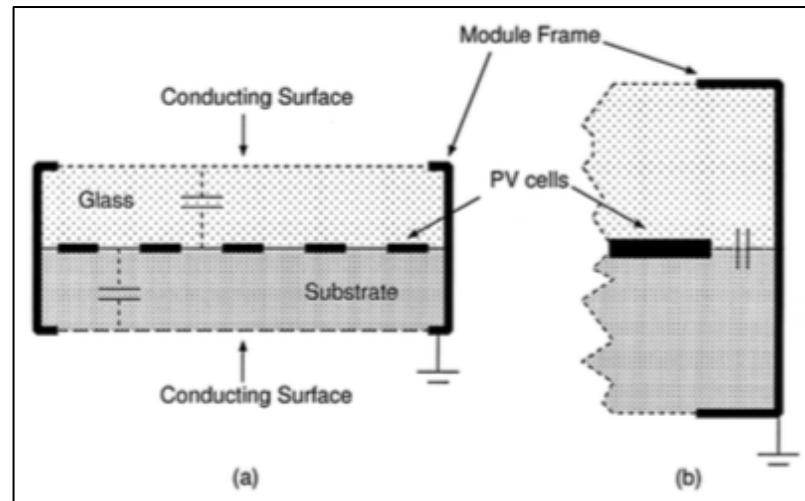


Figure 3.6: (a) Maximum and (b) Minimum PV Module Earth Capacitance

The value of parasitic capacitance for simulation is used between 50-150nF/kW [11]. The simulation using MATLAB/Simulink is to analyze the effect of parasitic capacitance value towards the ground leakage current. The ground leakage current can reach at higher levels due to potential variations of parasitic capacitance in the transformerless inverter. Thus, the ground leakage current can cause additional losses to the system and safety issues. German VDE0126-1-1 standard specified that the ground leakage current need to be below than 300 mA_{rms} value to prevent possible electrical hazards from any unintended touching of the PV array. Therefore, to minimize the ground leakage current, the common mode voltage needs to be continuous through all commutation situations.

3.3.4 H-bridge Inverter Transformerless Control Switching Technique

There are various modulation control schemes in single-phase transformerless inverter. The basic control pulse width modulation (PWM) scheme is used in this project. The H-bridge inverter transformerless is simulated using bipolar and unipolar switching schemes. This simulation is to investigate the common-mode voltage of the switching technique. The result obtained from the simulation will be compared between the bipolar switching and unipolar switching in terms of output voltage and common-mode voltage.

The transformerless H-Bridge inverter design is shown in Figure 3.7. Unipolar switching scheme that implemented on H-bridge inverter have three level

inverter voltages, which is zero state, positive state and negative state. Double voltage references (V_{ref1} and V_{ref2}) and single triangle carrier signal (V_c) are used for the signal generation. V_{ref2} is set to negative value of V_{ref1} . Table 3.2 shows the output voltage and common-mode voltage of the operation mode of half-positive cycle

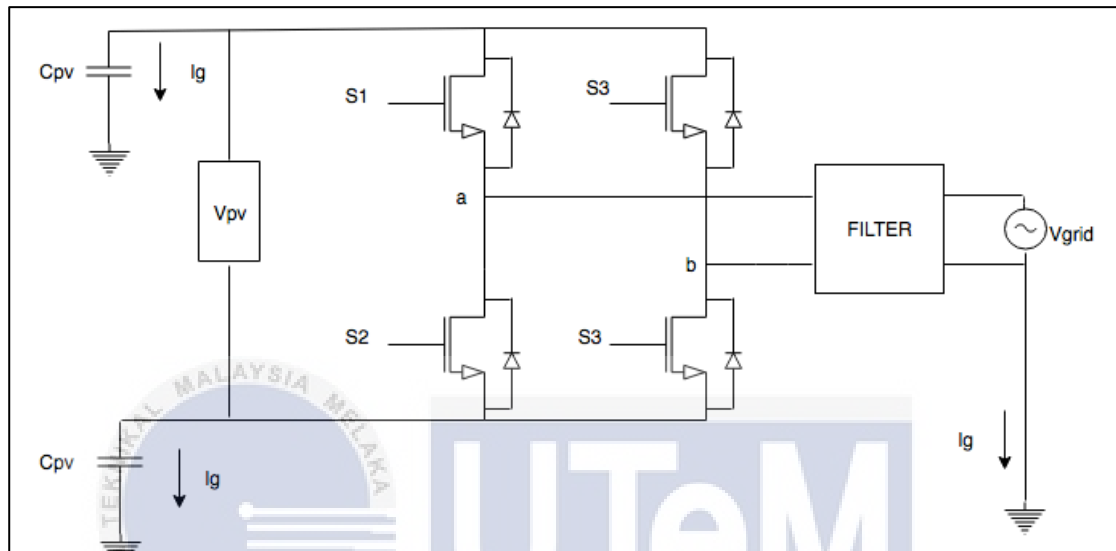


Figure 3.7: Transformerless H-Bridge Inverter

Table 3.2: Half-positive cycle operation mode of transformerless H-Bridge inverter

State	S ₁	S ₂	S ₃	S ₄	V_{dm}	V_{cm}
i	ON	OFF	OFF	ON	V_{dm}	$\frac{V_{dm}}{2}$
ii	ON	OFF	ON	OFF	0	V_{dm}
iii	OFF	ON	OFF	ON	0	0

During S₁ and S₄ ON at state I, the current is flow to the load as shown in figure 3.8. Figure 3.9 and 3.10 show the state ii and iii that got by short-circuiting the output of the inverter.

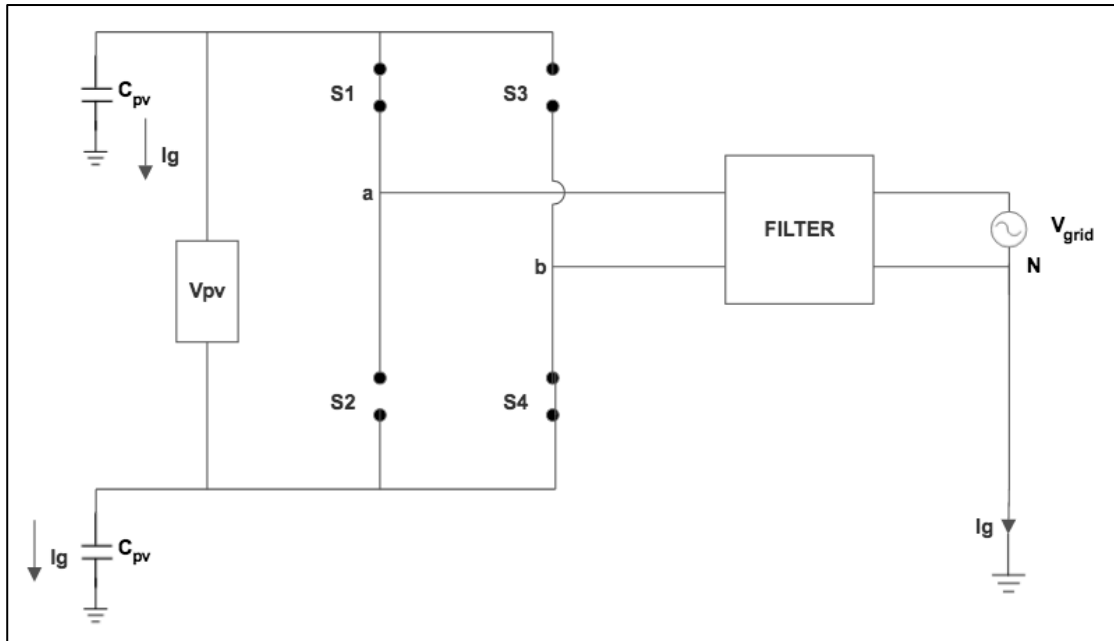


Figure 3.8: Half-positive Cycle State i For Unipolar H-bridge Circuit

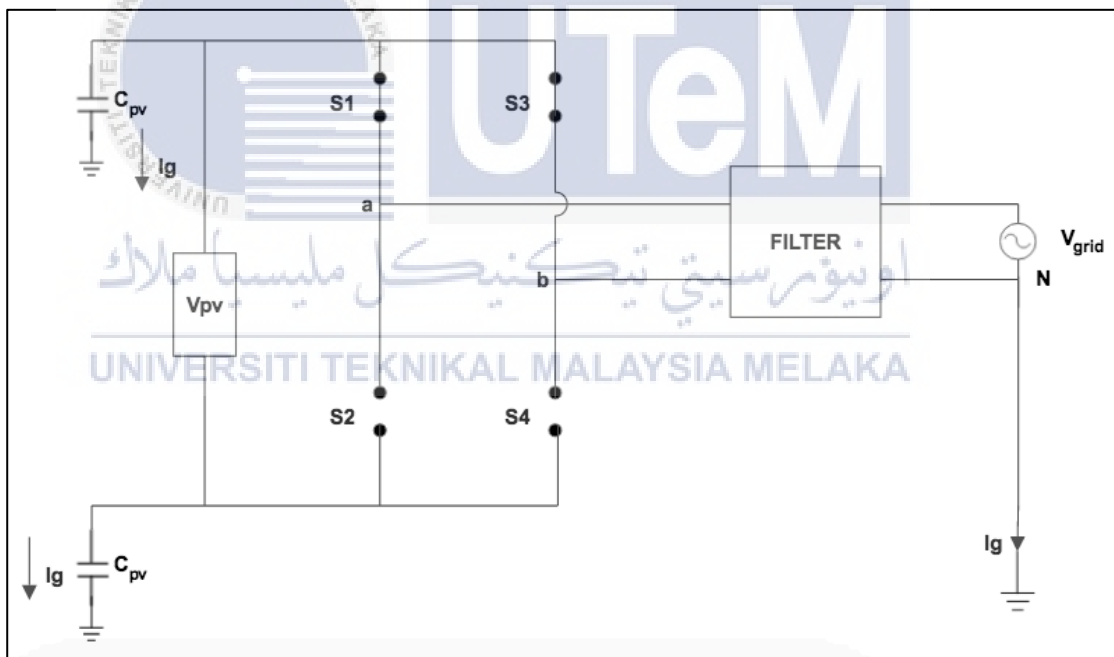


Figure 3.9: Half-positive Cycle State ii For Unipolar H-bridge Circuit

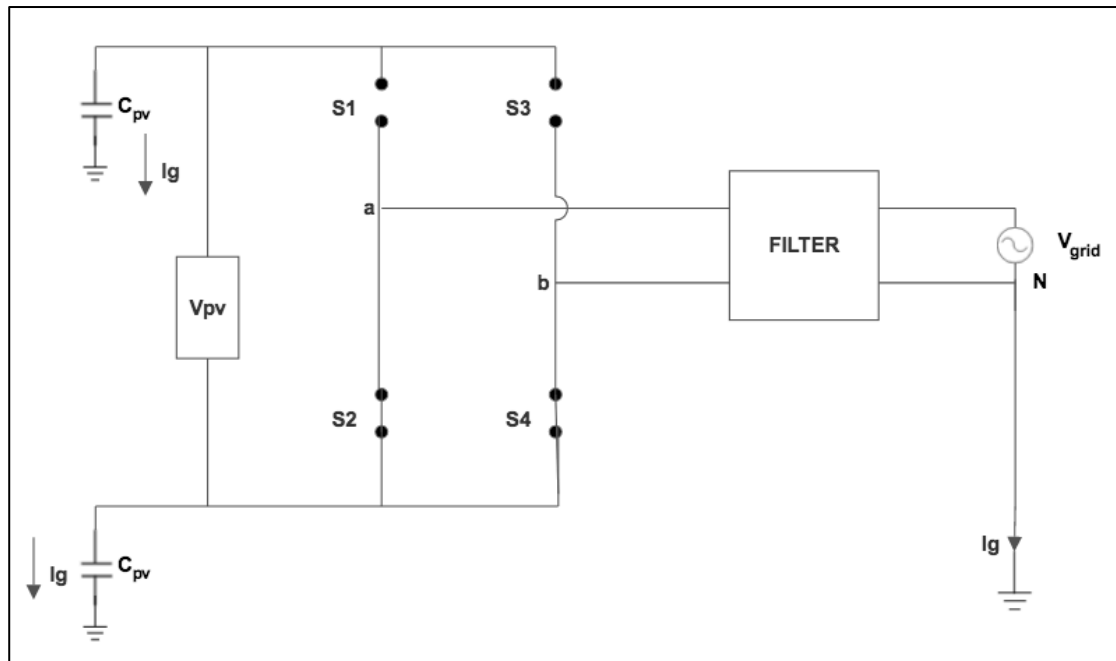


Figure 3.10: Half-positive Cycle State iii For Unipolar H-bridge Circuit

The common-mode voltage is measured at point a and b that can defined in Equation (3.1). Equation (3.8), (3.9) and (3.10) are show the details commutation state of the common-mode voltage.

$$\text{State i: } V_a = V_{dm} \text{ and } V_b = 0; V_{cm} = \frac{V_{dm}}{2} \quad (3.8)$$

$$\text{State ii: } V_a = V_{dm} \text{ and } V_b = V_{dm}; V_{cm} = V_{dm} \quad (3.9)$$

$$\text{State iii: } V_a = 0 \text{ and } V_b = 0; V_{cm} = 0 \quad (3.10)$$

Unipolar switching scheme showing that the common-mode voltage fluctuates between V_{dm} , $\frac{V_{dm}}{2}$ and 0 as shown in Equation (3.8), (3.9) and (3.10). When the common-mode voltage is fluctuated, it is unsafe for the transformerless PV grid-connected application system.

Bipolar switching scheme that implemented on H-bridge inverter also analyzed and have two level inverter voltages, which is positive state and negative state. Bipolar switching scheme was implement using same circuit as unipolar as shown in Figure 3.4. Voltage references (V_{ref}) and triangle carrier signal (V_c) are used for the signal generation. Table 3.3 shows the output voltage and common-

mode voltage of the operation mode. Figure 3.11 and 3.12 shows the output voltage and common-mode voltage of the operation mode.

Table 3.3: Operation mode of transformerless H-Bridge inverter

State	S ₁	S ₂	S ₃	S ₄	V_{dm}	V_{cm}
i	ON	OFF	OFF	ON	V_{dm}	$\frac{V_{dm}}{2}$
ii	OFF	ON	ON	OFF	0	V_{dm}

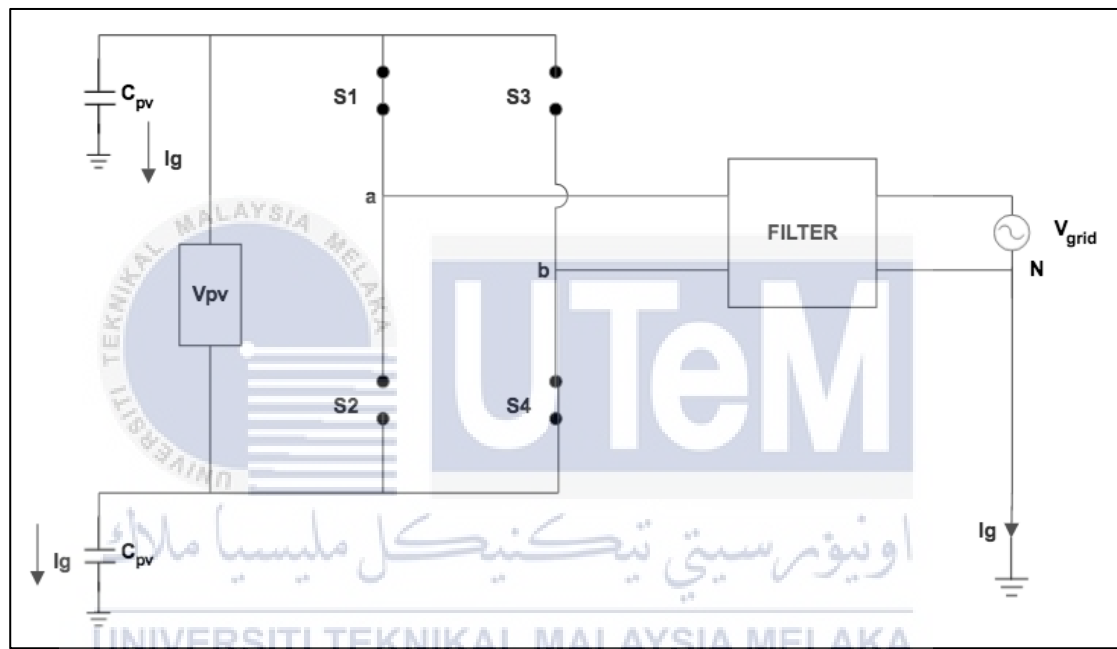


Figure 3.11: Positive Cycle State i For Bipolar H-Bridge Circuit

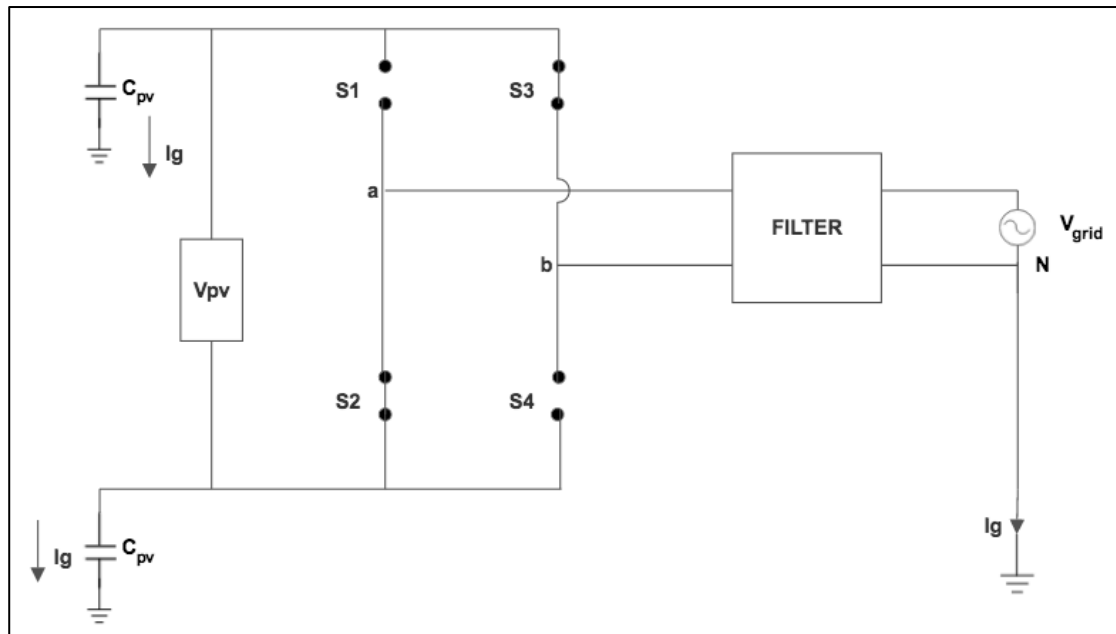


Figure 3.12: Positive Cycle State ii For Bipolar H-Bridge Circuit

Equation (3.11) and (3.12) show the details commutation state of the common-mode voltage for bipolar scheme.

$$\text{State i: } V_a = V_{dm} \text{ and } V_b = 0; V_{cm} = \frac{V_{dm}}{2} \quad (3.11)$$

$$\text{State ii: } V_a = 0 \text{ and } V_b = V_{dm}; V_{cm} = \frac{V_{dm}}{2} \quad (3.12)$$

Equations (3.11) and (3.12) show the voltage is constant to $\frac{V_{dm}}{2}$. The transformerless inverter is safe with the constant common mode voltage.

3.3.5 Filter Design

Two LC filters can be considered at the grid side as shown in Figure 3.13 and Figure 3.14. Single inductor (L_f) connected at line branch for LC filter in Figure 3.13. In Figure 3.14, the split inductor (L_f) is joined between line and neutral branch. The two LC filters are simulated to analyze the effect towards ground leakage current. The split inductor (L_f) with a different ratio also been analyzed.

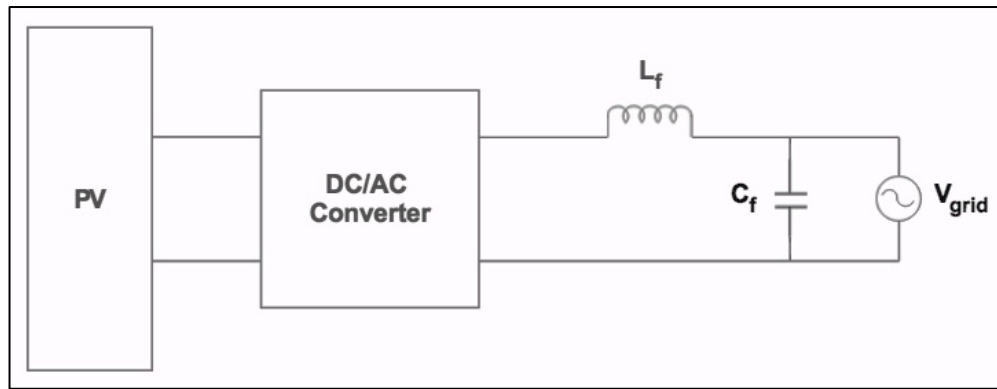


Figure 3.13: LC Filter With One Inductor (L_f)

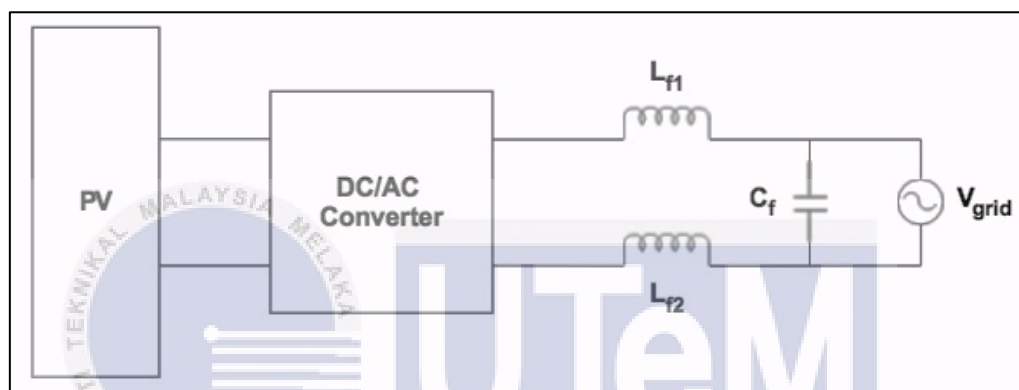


Figure 3.14: LC Filter With Split Inductor (L_f)

The calculation of filter inductor (L_f) is given in Equation (3.13). The maximum ripple current was chosen to be 5%-20% [22].

$$L = \frac{V_{dc}}{8\Delta I_{L,ripple,max} f_s} \quad (3.13)$$

Filter capacitance (C_f) is controlled by the reactive power assimilated in the filter capacitor is communicated in condition (3.14) with ∞ being the reactive power factor and its value is chosen to be under 5 % [22]. Prated is the rated power of the inverter and Vrated is its rated voltage.

$$C_f = \frac{\infty P_{rated}}{2\pi f_{line} V_{rated}^2} \quad (3.14)$$

3.4 Simulation of Single-Phase Transformerless Inverter

The single-phase transformerless inverter is simulated by using bipolar and unipolar switching schemes. This simulation is to analyze the factor of the ground leakage current which is switching technique, parasitic capacitance and LC filter. The simulation is based on $V_d = 30$ V, $m_a = 0.8$, $f_{ref} = 50$ Hz, $f_{sw,bi} = 8$ kHz and $f_{sw,uni} = 4$ kHz. Figure 3.15 shows the MATLAB Simulink model of transformerless inverter for bipolar switching scheme and Figure 3.16 shows the MATLAB Simulink model of transformerless inverter for unipolar switching scheme.

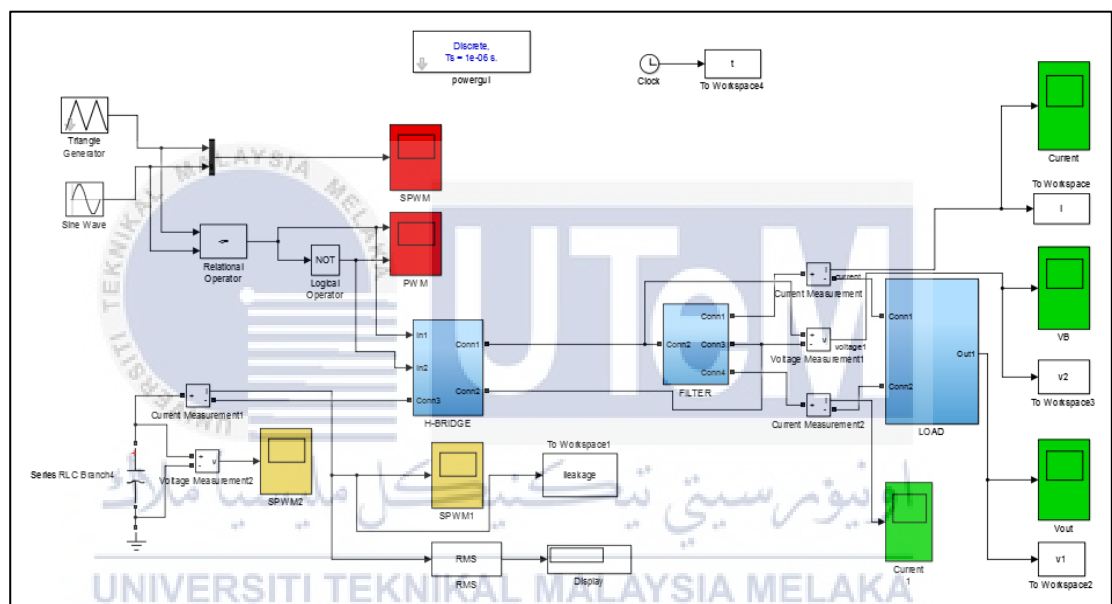


Figure 3.15: MATLAB Simulink Model of Single-phase Transformerless Inverter For Bipolar Switching Scheme

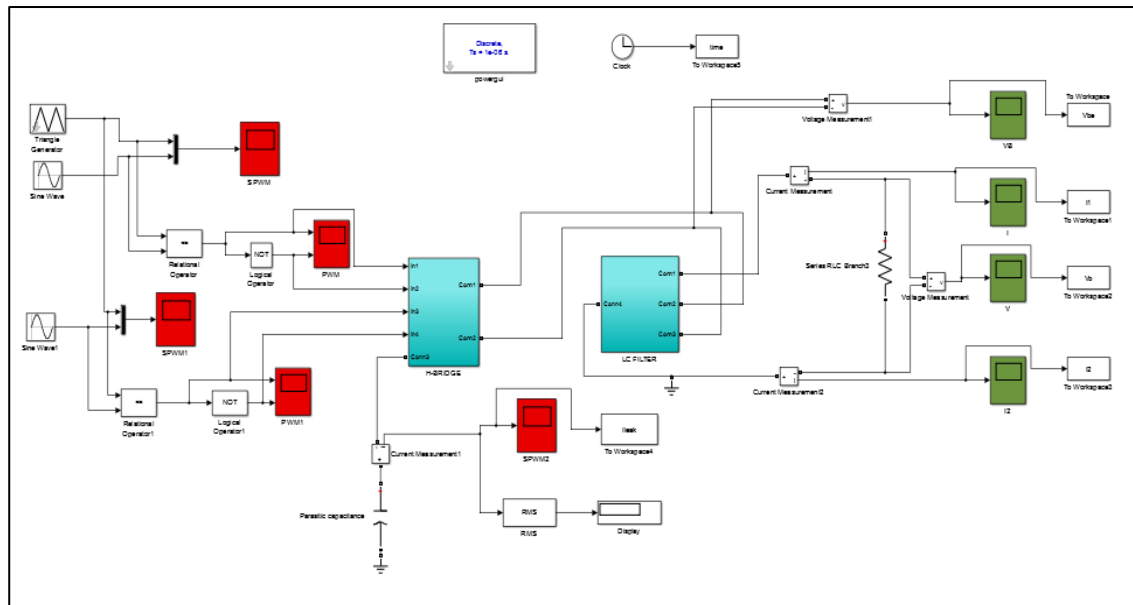


Figure 3.16: MATLAB Simulink Model Of Single-phase Transformerless Inverter For Unipolar Switching Scheme

3.4.1 Simulink Parameter

A reference signal or sine wave and a carrier signal are required to control switching frequency to produce the PWM control signal. The simulation parameters are designed based on Table 3.4.

Table 3.4: Simulation Parameter of single-phase transformerless inverter

PARAMETER	VALUE
V_{in}	30 V
Carrier Frequency (Bipolar)	8 kHz
Carrier Frequency (Unipolar)	4 kHz
Reference Frequency	50 Hz
M_a	0.8
L_{f1}	5 mH
L_{f2}	5 mH
C_f	10 μ F
R load	100 Ω
C_{pv}	10 nF

3.5 Hardware Design

This section will present the proposed circuit design for the single-phase transformerless inverter. The circuit structures are constructed using DC source, H-bridge transformerless inverter circuit, gate drive, microcontroller, LC filter and R load. Figure 3.17 shows the hardware flowchart.

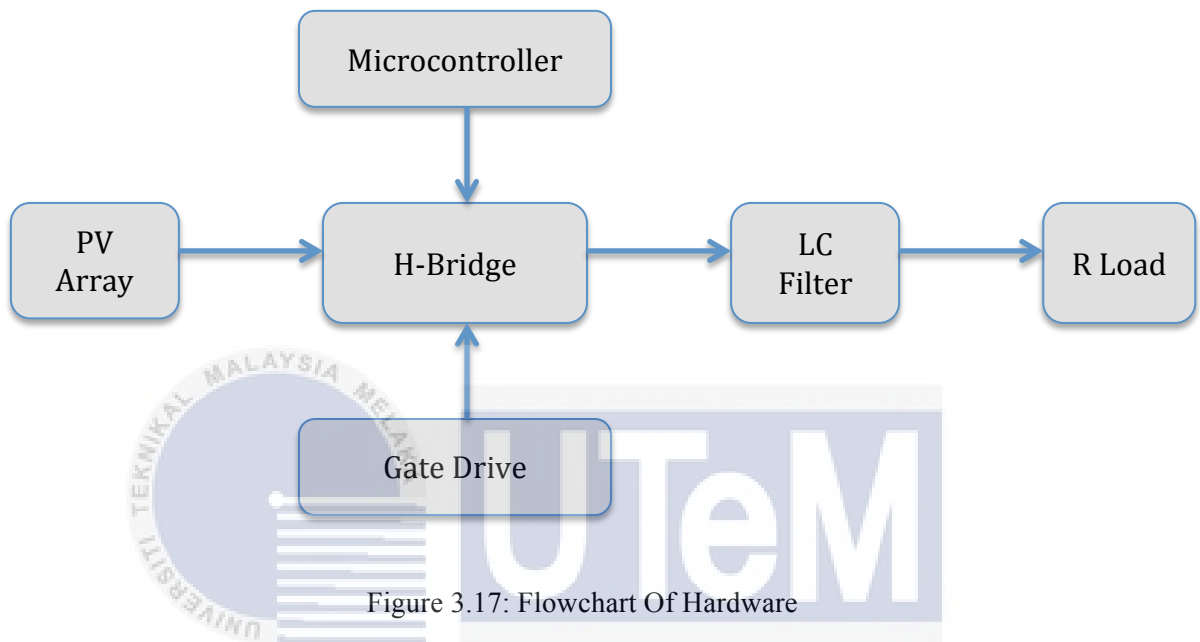


Figure 3.17: Flowchart Of Hardware

3.5.1 H-bridge Transformerless Inverter Circuit

Basically, the H-Bridge inverter circuit was constructed with four set of power electronic switching device such as Insulated-Gate Bipolar Transistor (IGBT) or Metal Oxide Semiconductor Field Effect Transistor (MOSFET). For this project, the power switching device chosen is IGBT type G4PC50UD-E. The picture and image of IGBT type G4PC50UD-E are show in Figure 3.18 [24]. This IGBT will get a switching signal from microcontroller through the gate drive circuit. Table 3.5 shows the parameter of IGBT IHW15N120R3.

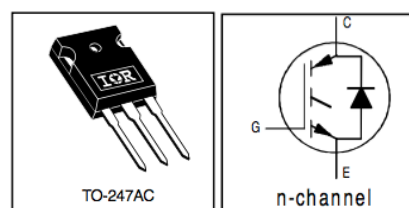


Figure 3.18: IGBT G4PC50UD-E

Table 3. 5: Parameter of IGBT IHW15N120R3

Parameter	Symbol	Value	Unit
Collector-emitter voltage	V_{CE}	600	V
Gate-emitter voltage	V_{GE}	± 20	
DC collector current $T_C = 25^\circ\text{C}$ $T_C = 100^\circ\text{C}$	I_C	55 27	A
Pulsed collector current	$I_{C_{puls}}$	227	
Diode Continuous Forward Current	I_F	25	
Diode Maximum Forward Current	I_{Fmax}	220	
Power dissipation $T_C = 25^\circ\text{C}$ $T_C = 100^\circ\text{C}$	P_{tot}	200 78	W
Operating junction temperature and Storage temperature	T_j	-55 to +150	$^\circ\text{C}$
Soldering temperature, 1.6mm (0.063 in.) from case for 10s	-	300	$^\circ\text{C}$

3.5.2 Gate Drive Circuit

Gate driver circuit is a circuit integral part of power electronics converters, which is used to drive IGBT. Function of this gate drive in this project is to isolate signal from microcontroller and switching devices. Microcontroller will generate the PWM signal. The IGBT power switch needs 15 V to turn ON and the signal from microcontroller is only 5 V. Hence, the 15 V supply is connected to the gate drive as a desired voltage to turn ON the IGBT. Gate drive that used for this project is HCPL3120-000E. Figure 3.19 shows the gate drive circuit design for half-bridge IGBT. DC/DC converter is connected to the gate drive HCPL3120-000E in this circuit is because to convert from 5 V to 15 V.

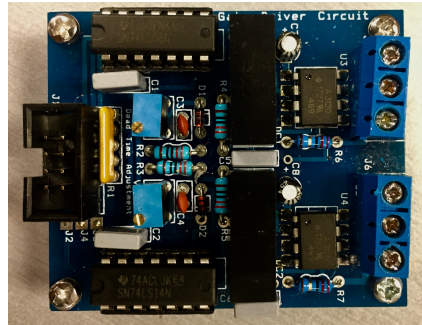


Figure 3.19: Gate Drive Circuit

3.5.3 XMC 4500 Microcontroller

The main controller that will be used in this project is XMC 4500. Figure 3.20 shows the microcontroller XMC 4500. The XMC 4500 will generate the switching signal that will be used to operate of turn ON and OFF the IGBT power switching. Table 3.6 shows the parameter of XMC 4500 [25]. Microcontroller XMC 4500 was use to generate bipolar SPWM and unipolar SPWM. Besides, the XMC 4500 easy to use because direct memory access. Figure 3.21 shows the circuit of CCU4 that used to generate unipolar SPWM and bipolar SPWM. Figure 3.22 shows the block parameter that has been used to set the sine wave parameter. CCU4 block was used to generate triangle single. Therefore, Figure 3.23 is use to setting the triangle parameter. Based on Equation 3.15, the switching frequency can be calculated.

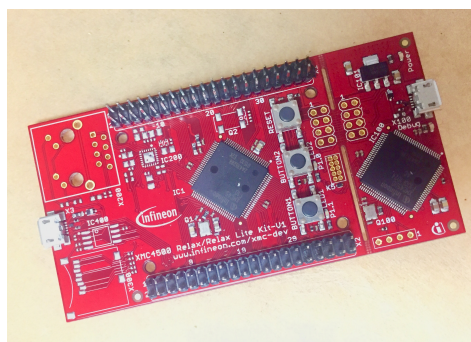


Figure 3.20: Microcontroller XMC 4500

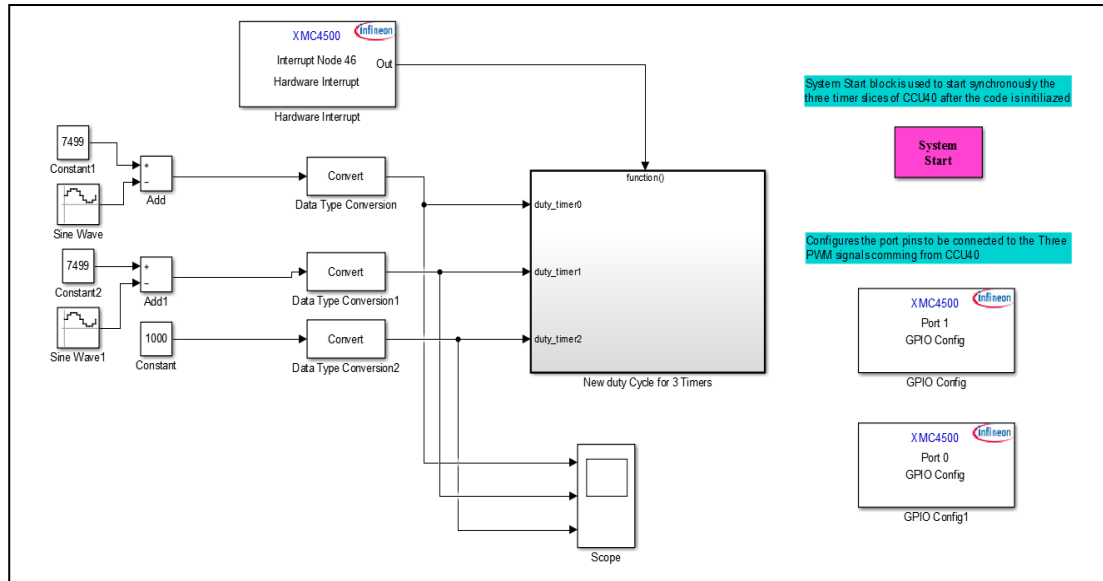


Figure 3.21: CCU4 Circuit

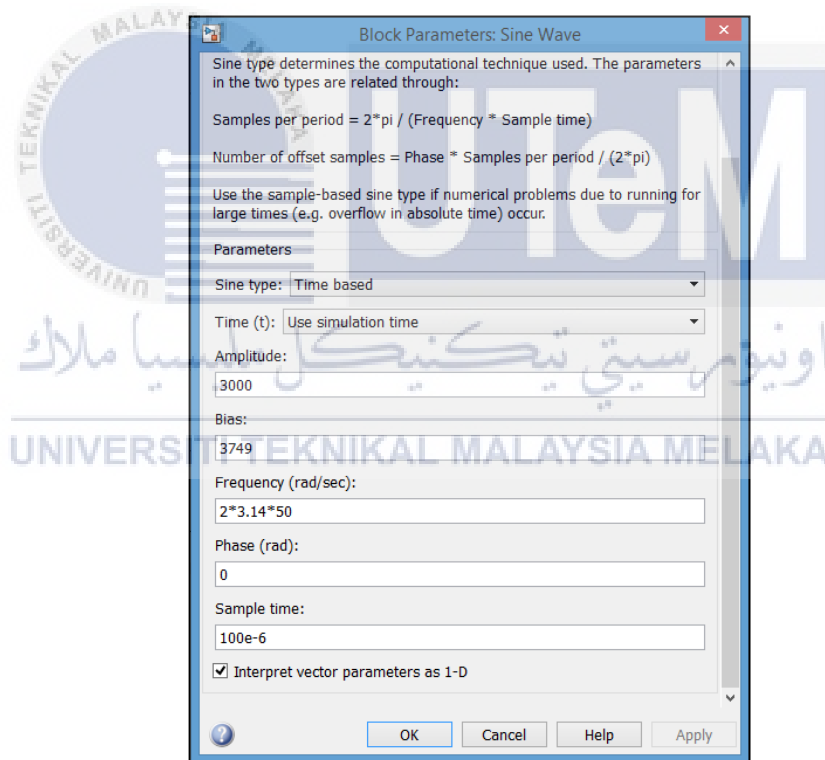


Figure 3.22: Block Parameter Sine Wave

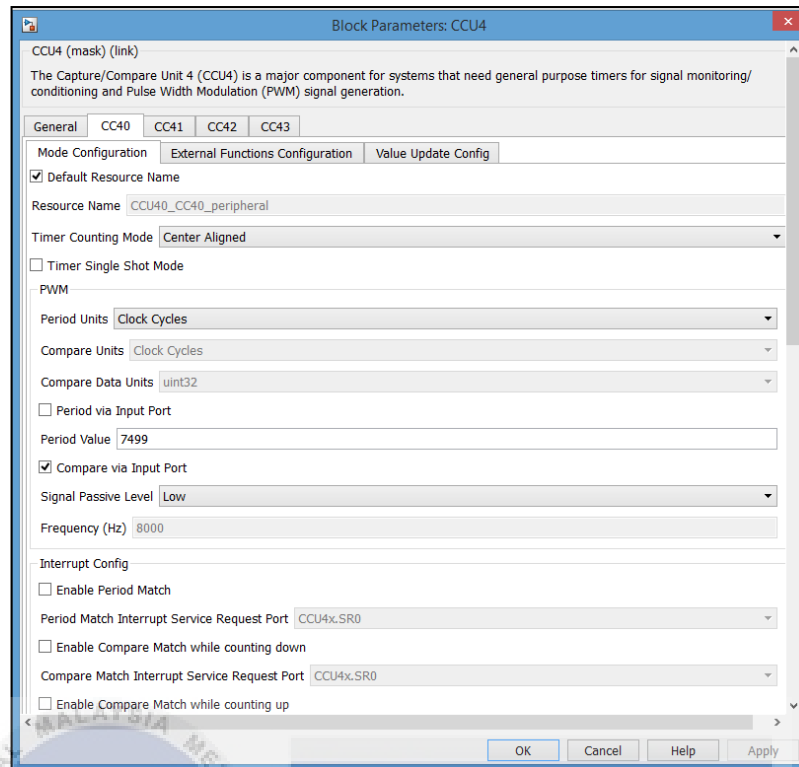


Figure 3.23: Block Parameter CCU4

$$\text{Switching Frequency (Fs)} = \frac{1}{\text{Period Value} \times \text{Resolution}} \times \frac{1}{2} \quad (3.16)$$

Table 3.6: The parameter of XMC 4500

Parameter	
Microcontroller	XMS 4500
Operating voltage	3.3 V
Input Voltage	3 - 5 V
Flash Memory	1024 kB
SRAM	160 kB
Speed Grade	80 MHz

3.6 Hardware Experimental Setup

The hardware development of this project is focused on development of single-phase transformerless inverter. Figure 3.21 shows the hardware setups that are

consist of H-bridge circuit, gate drive, microcontroller and LC filter. Heat sink used for purpose of cooling system due to high switching frequency.



Figure 3.21: Hardware Setup

3.7 Summary

This chapter is briefly explained the research methodology using flow chart, milestone and Gantt chart. Ground leakage current is explained in details in this chapter. Then, method to determine the factors that affect the ground leakage current also has been explained. Simulation of single-phase transformerless inverter was discussed. After determine the factor that affected ground leakage current, single-phase transformerless inverter was proposed. Finally, the chapter is ended with hardware design.

CHAPTER 4

RESULT AND DISCUSSION

4.1 Introduction

This chapter is about the preliminary result of the single-phase transformerless inverter. The simulation was simulated after determine the several factor that cause a ground leakage current. The discussion will focus on the ground leakage current and total harmonic distortion (THD)

4.2 Simulation Results

The result of the simulation will be presented in this section. The result was obtained from the simulation of the single-phase transformerless inverter that using bipolar and unipolar switching scheme. The single-phase transformerless inverter was simulated to identify the factors that affect ground leakage current which is switching technique, parasitic capacitance value, filter design and topology. The simulation was simulated by using a various parameter such as parasitic capacitor value C_{pv} and inductor filter value L_f .

4.2.1 Simulation results of Single-phase Transformerless Inverter

Single-phase transformerless inverter operates with the PWM switching pulse to turn ON the power switching device IGBT. The unipolar switching technique is simulated using H-Bridge topology. The common-mode voltage signals resulting from unipolar switching technique is depicted in Figure 4.1. The unipolar switching

scheme has a fluctuated common-mode voltage. Figure 4.2 show the three level output inverter voltage $30 V_{\text{peak}}$ (V_{dc} , 0 , $-V_{dc}$). AC current output ($24.48 \text{ mA}_{\text{peak}}$) and AC voltage output ($24.48 V_{\text{peak}}$) is shown in Figure 4.3 and 4.4. The current THD and voltage THD of unipolar H-bridge is given as 0.75% as shown in Figure 4.5 and 4.6. A high ground leakage current ($155.2 \text{ mA}_{\text{peak}}$) and THD ground leakage current (26761.36%) are shown in Figure 4.7 and 4.8 due to fluctuate common-mode voltage.

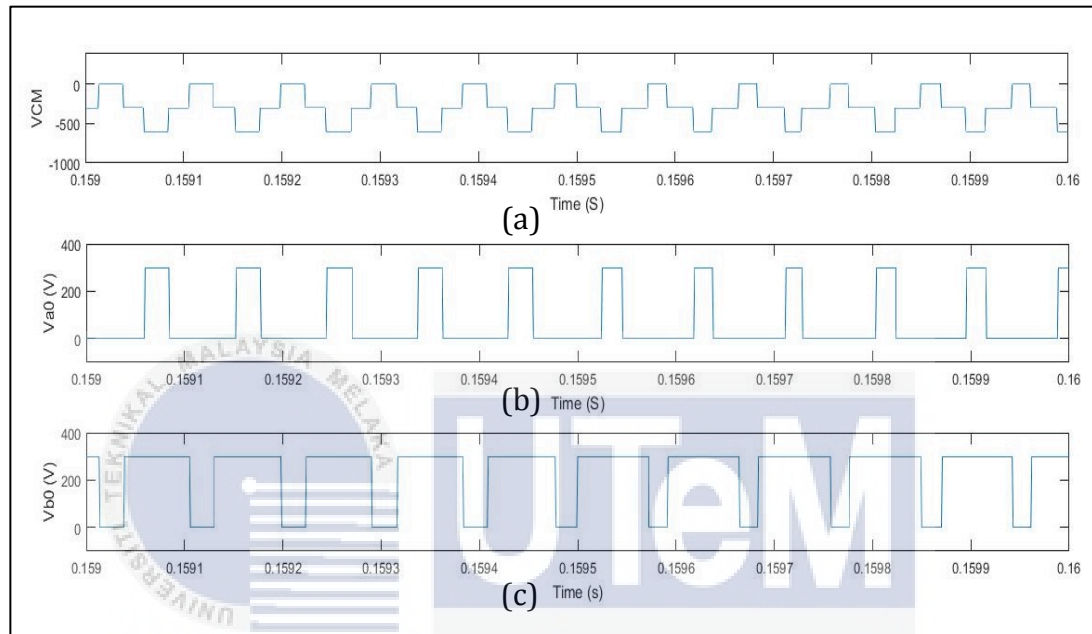


Figure 4.1: (a) Common-mode Voltage (V_{cm}), (b) V_{ao} and (c) V_{bo} That Obtained Using Unipolar Switching Technique

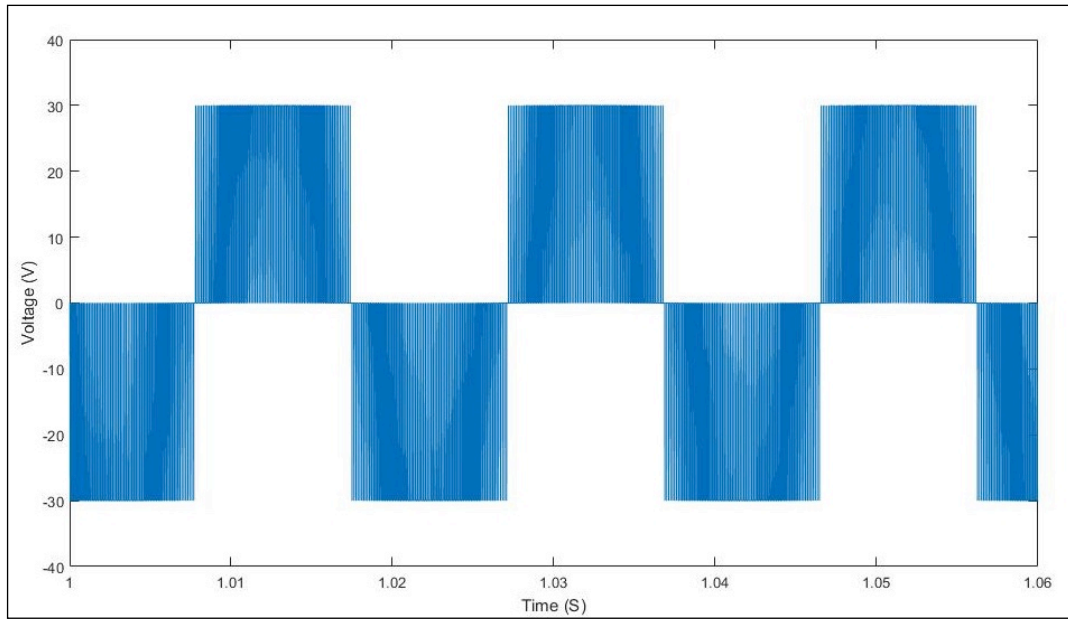


Figure 4.2: Output Inverter Voltage $30 V_{\text{peak}} (V_{ab})$

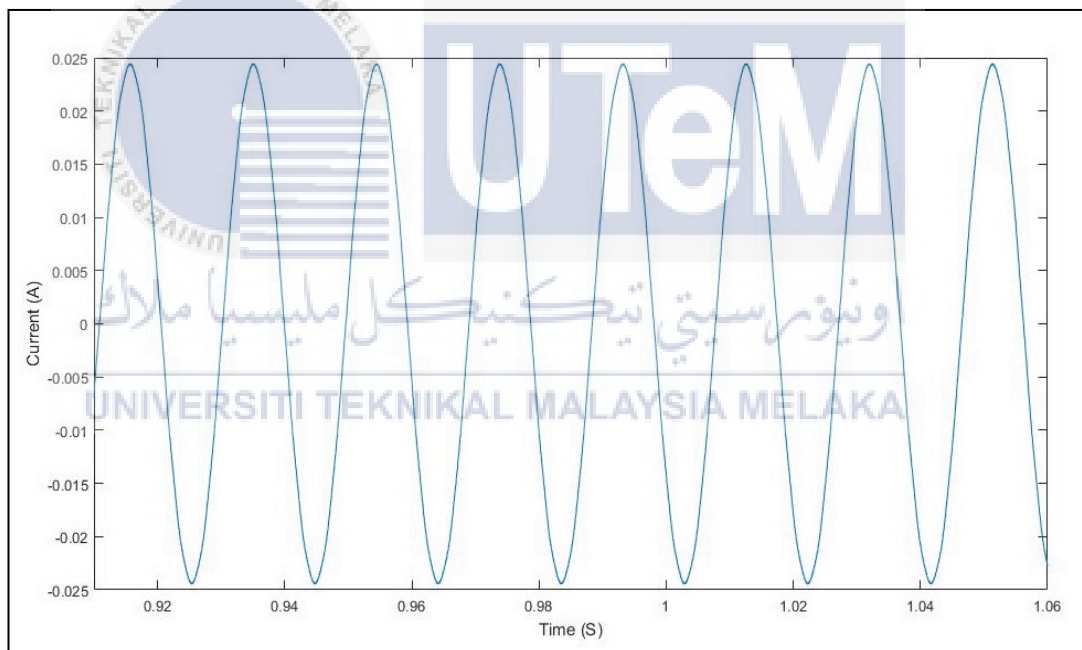


Figure 4.3: Output Inverter Current $24.48 \text{ mA}_{\text{peak}} (I_o)$

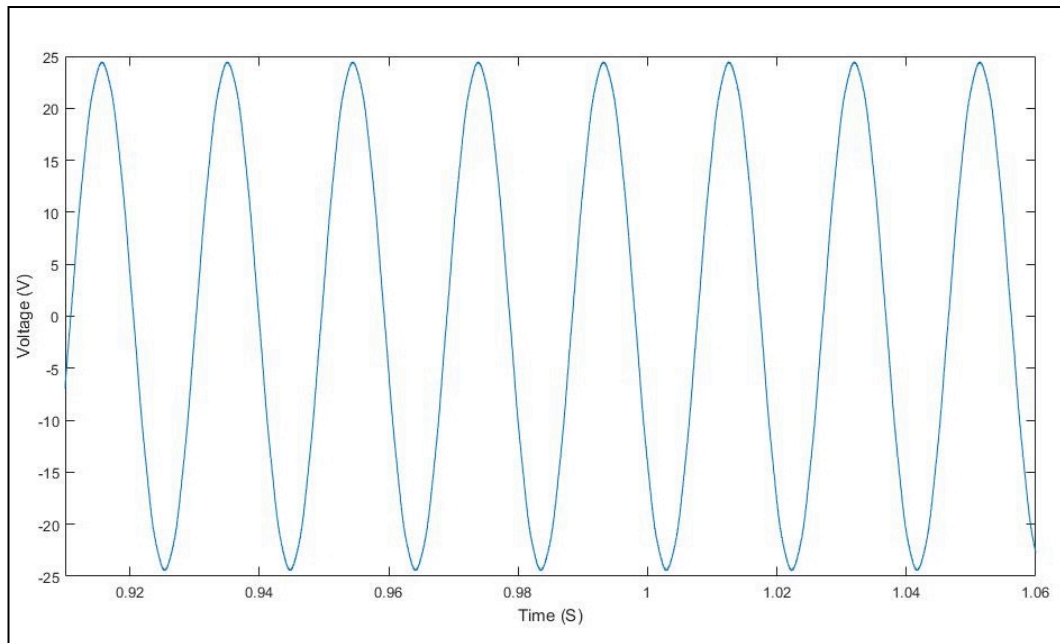


Figure 4.4: Output Inverter Voltage 24.48 V_{peak} (Vo)

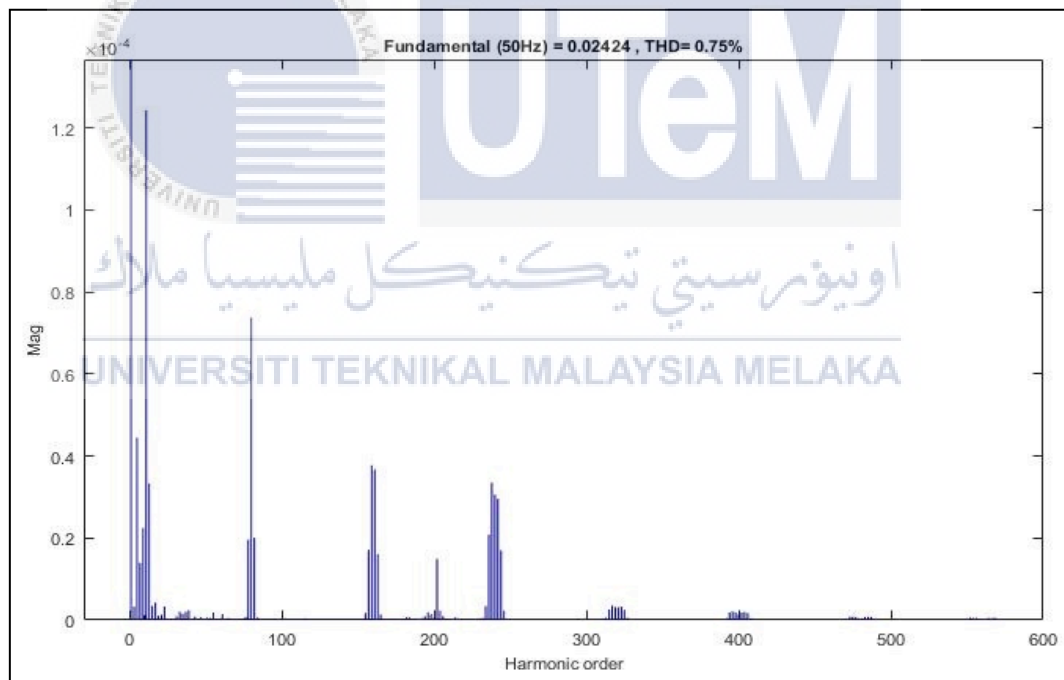


Figure 4.5: THD Current For Unipolar H-bridge Inverter 0.75 %

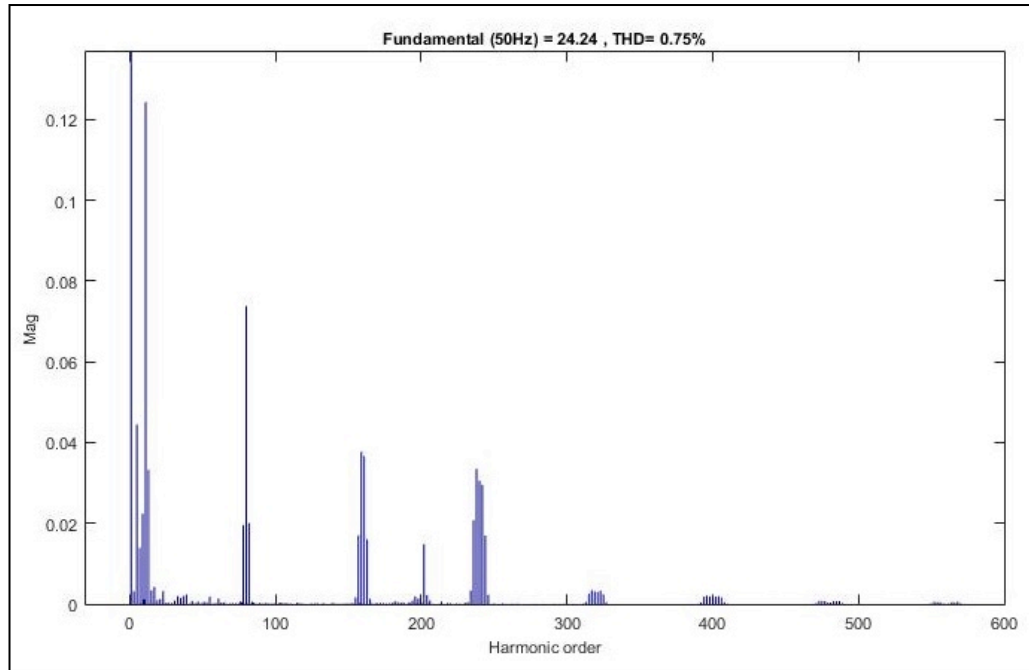


Figure 4.6: THD Voltage For Unipolar H-bridge Inverter 0.75 %

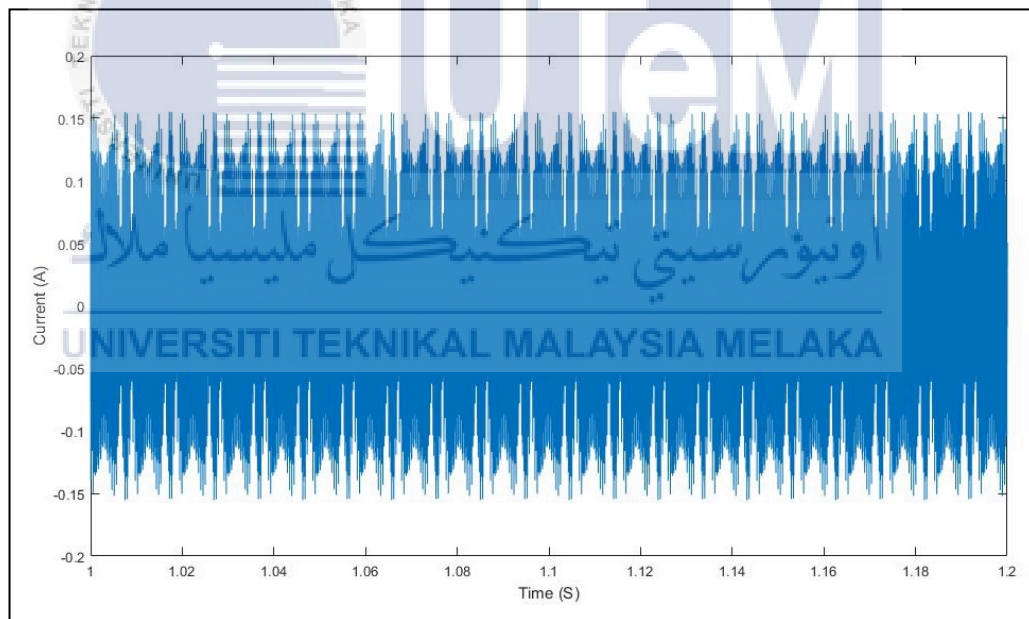


Figure 4.7: Ground Leakage Current Using Unipolar Switching Technique 155.2

mA_{peak}

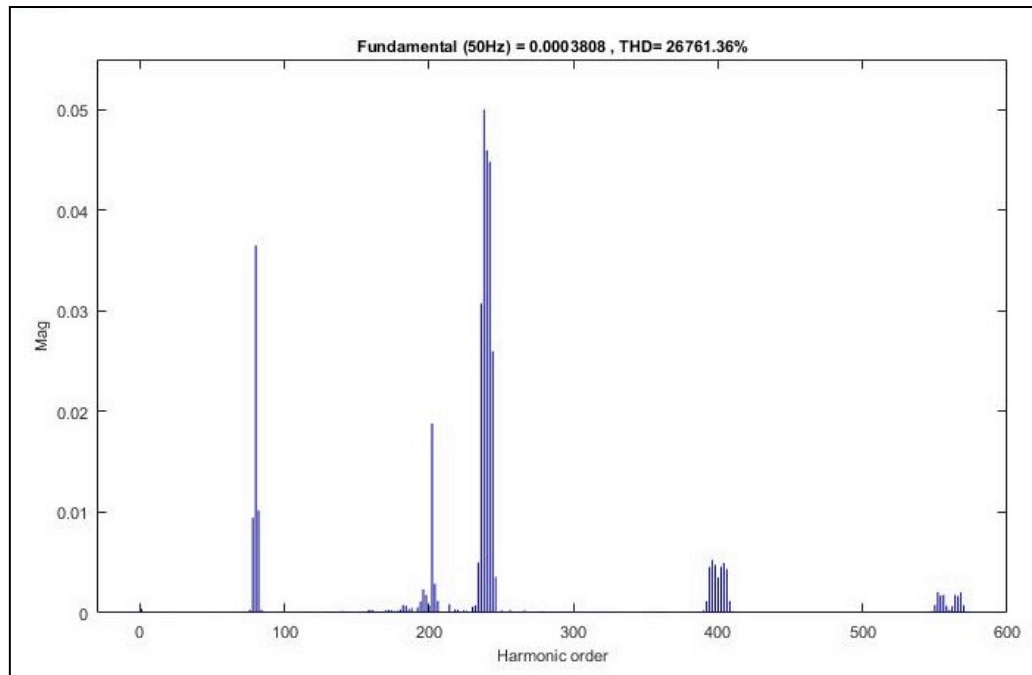


Figure 4.8: THD Ground Leakage Current For Unipolar H-bridge Inverter

26761.36 %

The bipolar switching technique is simulated using H-Bridge inverter topology. The common-mode voltage signals resulting from bipolar switching technique is illustrated in Figure 4.9. The bipolar switching scheme has a constant common-mode voltage. Figure 4.10 shows the output voltage $30 V_{\text{peak}}$ (V_{dc} and $-V_{dc}$). The switching frequency is double the frequency of unipolar SPWM due to maintain the filter value as used in unipolar. AC current output ($24.98 \text{ mA}_{\text{peak}}$) and AC voltage output ($24.98 V_{\text{peak}}$) is shown in Figure 4.11 and 4.12. Next, the current THD and voltage THD of bipolar H-bridge is given as 3.21 % as shown in Figure 4.13 and 4.14. The common-mode voltage is constant with a small value of leakage current ($1.556 \text{ mA}_{\text{peak}}$) because of bipolar switching pattern behavior as shown in Figure 4.15. THD ground leakage current (189.13 %) is shown in Figure 4.16.

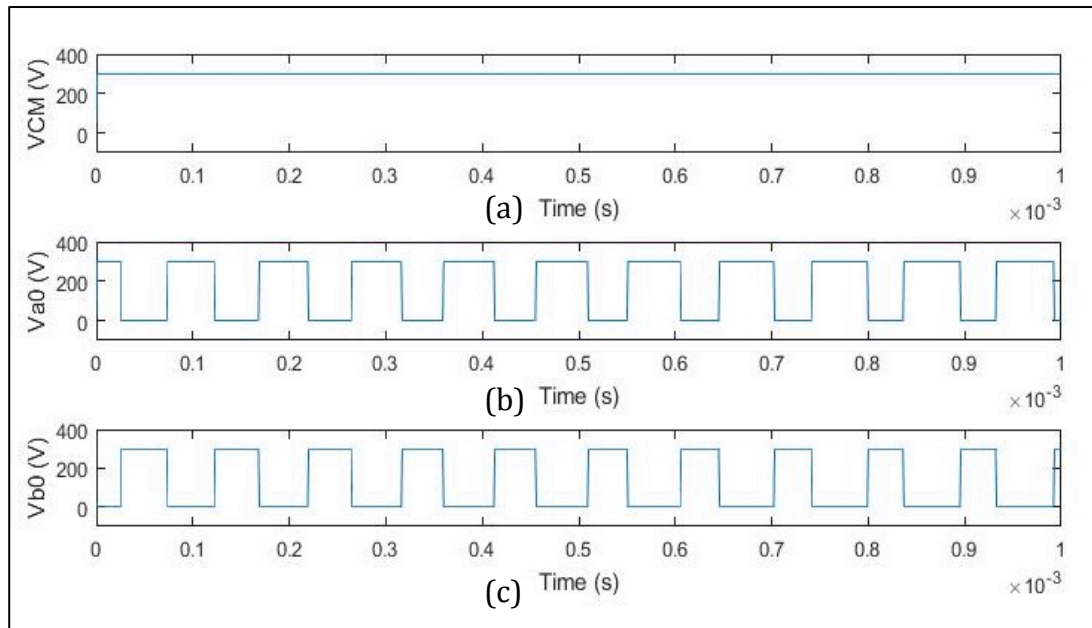


Figure 4.9: (a) Common-mode Voltage (V_{cm}), (b) V_{ao} and (c) V_{bo} That Obtained Using Bipolar Switching Technique

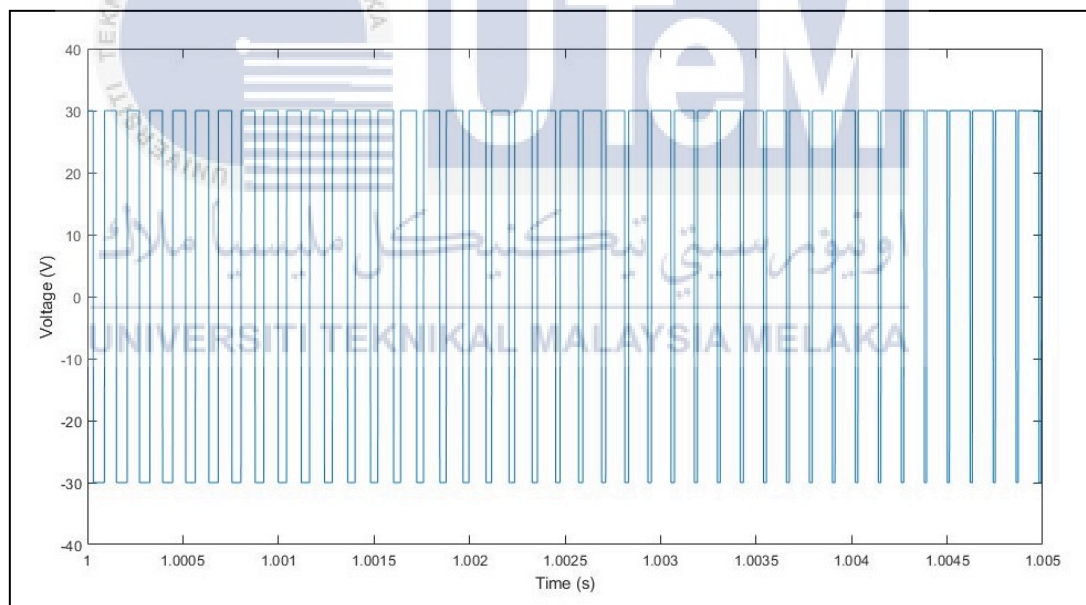


Figure 4.10: Output Inverter Voltage $30 V_{peak}$ (V_{ab})

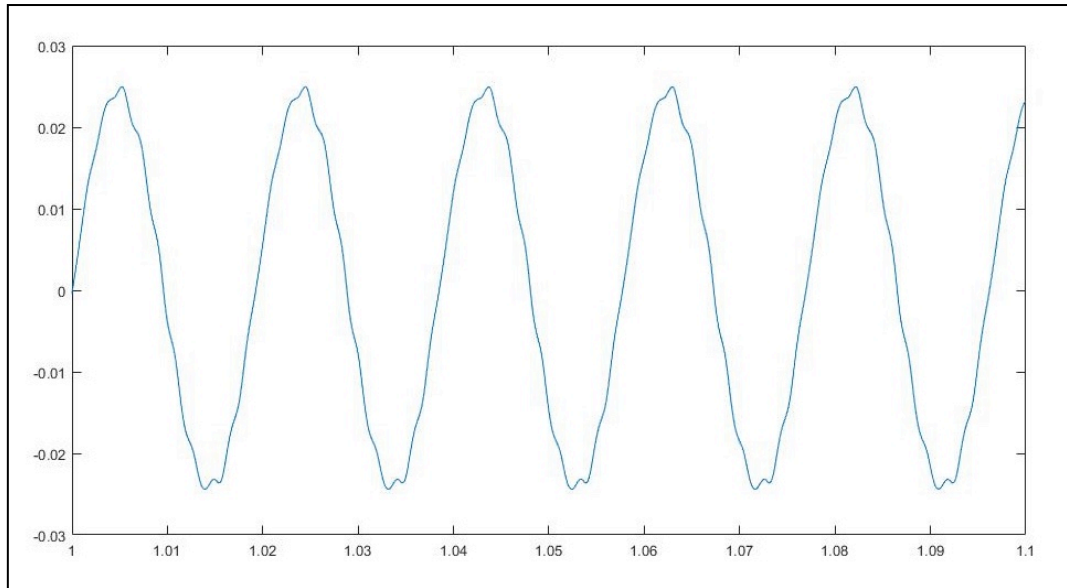


Figure 4.11: Output Inverter Current 24.98 mA_{peak} (I_o)

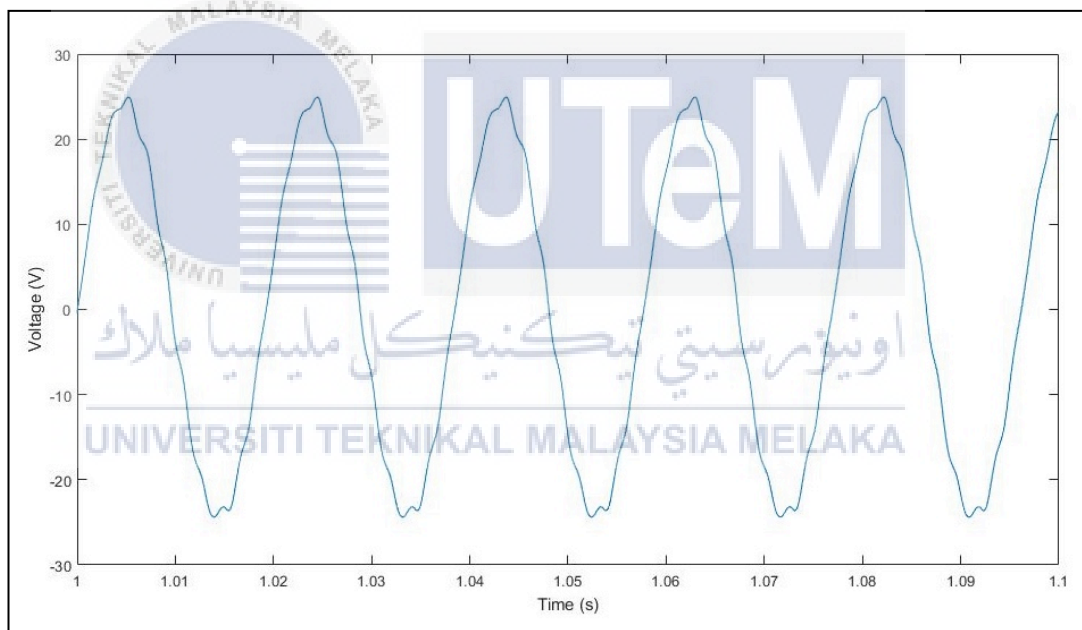


Figure 4.12: Output Inverter Voltage 24.98 V_{peak} (V_o)

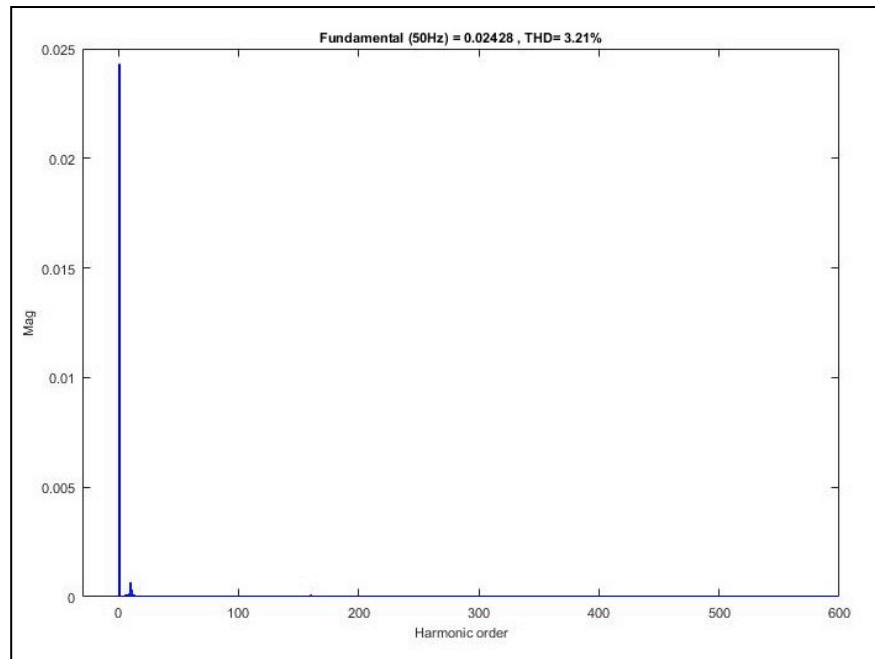


Figure 4.13: THD Current For Bipolar H-bridge Inverter 3.21 %

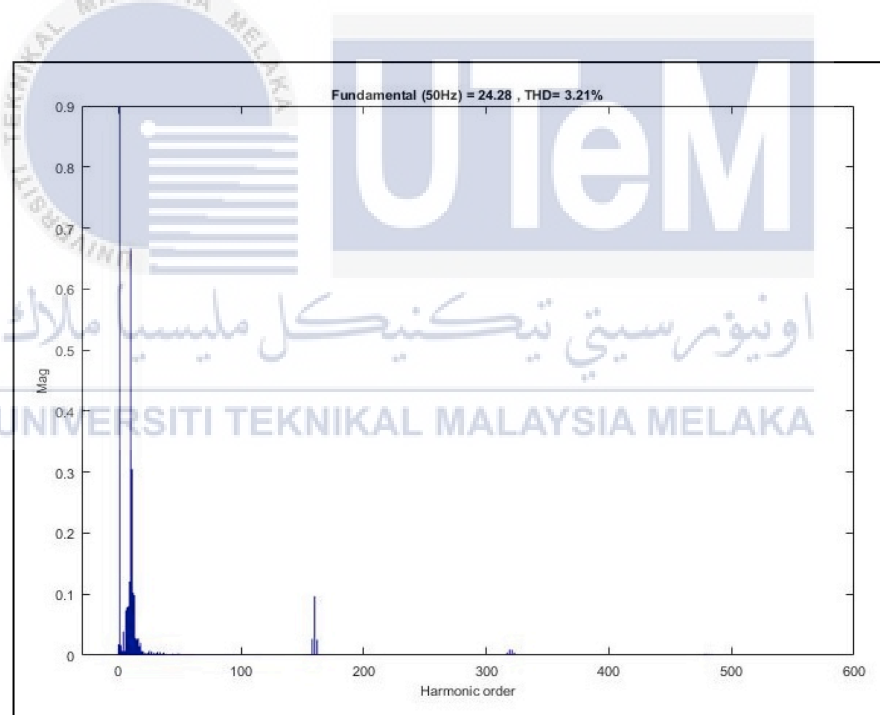


Figure 4.14: THD Voltage For Bipolar H-bridge Inverter 3.21 %

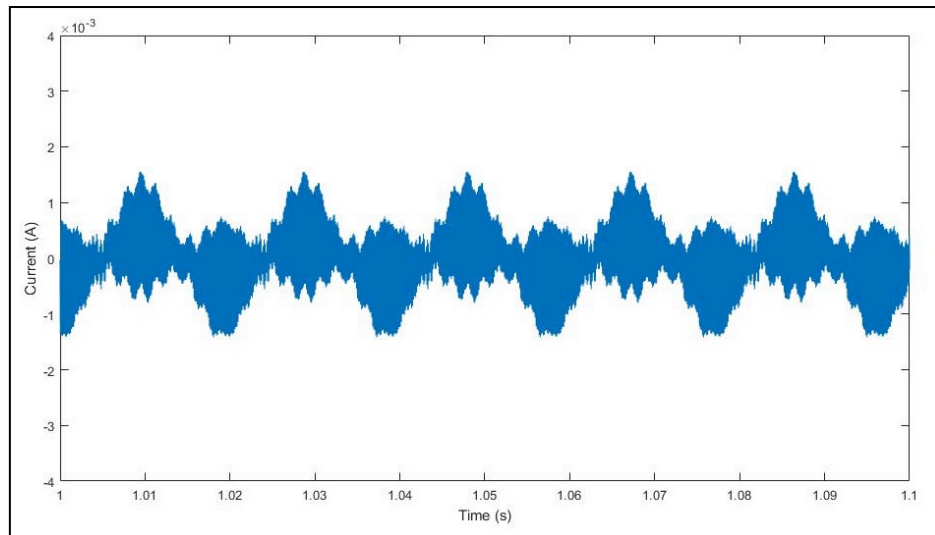


Figure 4.15: Ground Leakage Current Using Bipolar Switching Technique

1.556 mA_{peak}

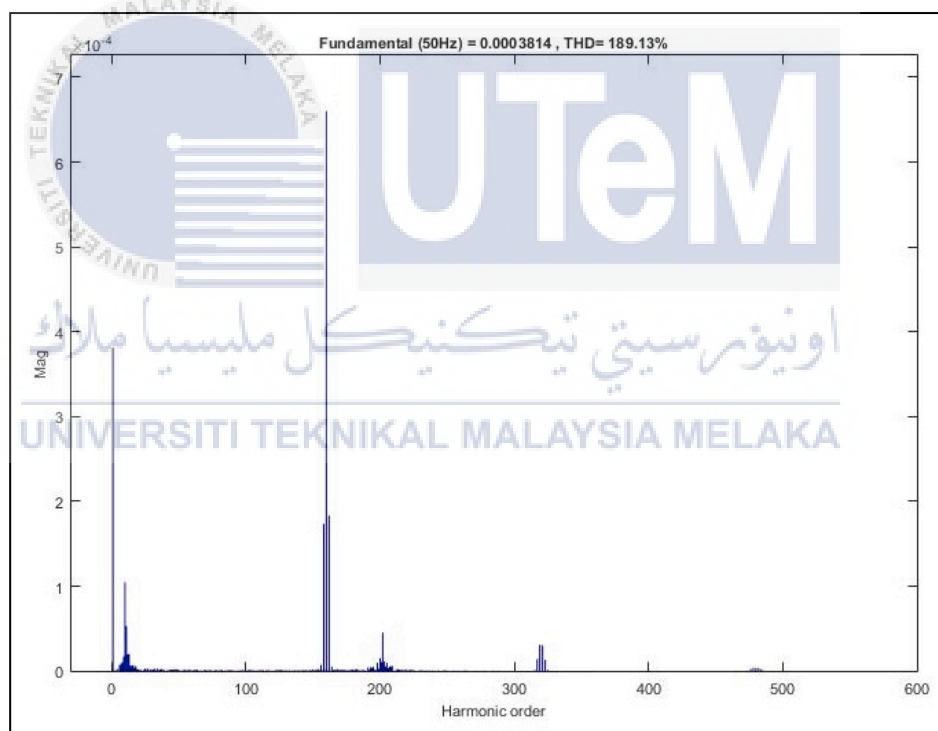


Figure 4.16: THD Ground Leakage Current For Bipolar H-bridge Inverter 189.13 %

The result can be summaries in the Table 4.1 below. It shows that the unipolar switching technique and bipolar switching technique have same value for output voltage before filter, which is 30 V. Value for output current (24.48 mA for unipolar and 24.9 mA for bipolar) and output voltage (24.48 V for unipolar and 24.98 V for bipolar) almost same. THD_i and THD_v for unipolar is equal 0.75 % same

goes to bipolar 3.21 %. Due to behavior of unipolar, the fluctuated common-mode voltage causes a high ground leakage current and high $THD_{leakage}$. Due to behavior bipolar, the common-mode voltage bipolar is constant thus, the ground leakage current is low and $THD_{leakage}$ is also low.

Table 4.1: Simulations result for unipolar SPWM and bipolar SPWM

	Unipolar SPWM	Bipolar SPWM
Common-mode Voltage Characteristic	Fluctuated	Constant
Voltage Output (V_{peak})	30	30
Current Output (mA_{peak})	24.48	24.89
AC Voltage Output (V_{peak})	24.48	24.89
THD_i (%)	0.75	3.21
THD_v (%)	0.75	3.21
Ground Leakage Current (mA_{peak})	155.2	1.556
$THD_{leakage}$ (%)	26761.36	189.13

4.2.2 Effect of Filter Design

Based on low ground leakage current ($1.556mA_{peak}$) of bipolar H-bridge inverter as shown in Figure 4.15 the effect of filter design is analyzed. There are two type of filter design that has been analyzed which is LC filter with one inductor and LC filter with split inductor with same value as shown in Figure 3.13 and 3.14. On the effect of filter with one inductor it shows on Figure 4.17 that the ground leakage current is high $3 A_{peak}$ that is more than $300 mA_{rms}$. Figure 4.18 shows a detailed THD (142138.89 %) of the ground leakage current with very high harmonic contents when using one inductor.

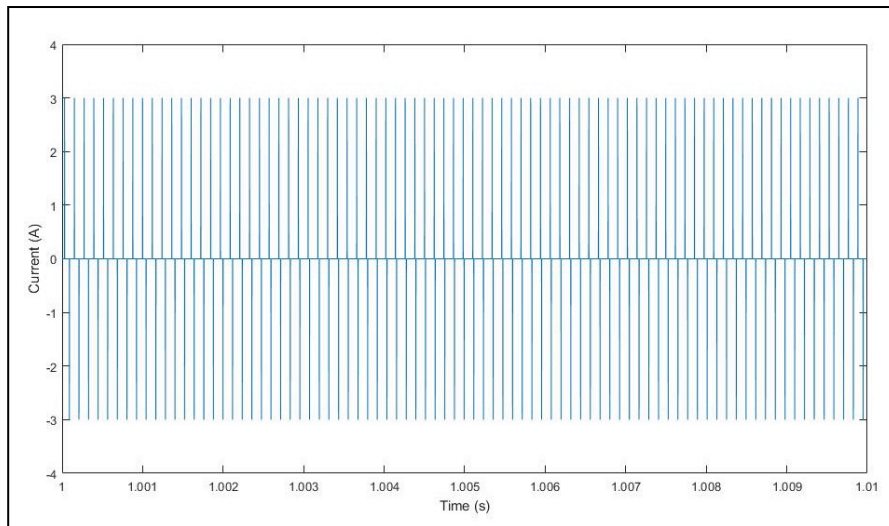


Figure 4.17: The Effect Of Filter With One Inductor On Ground Leakage Current
(3 A_{peak})

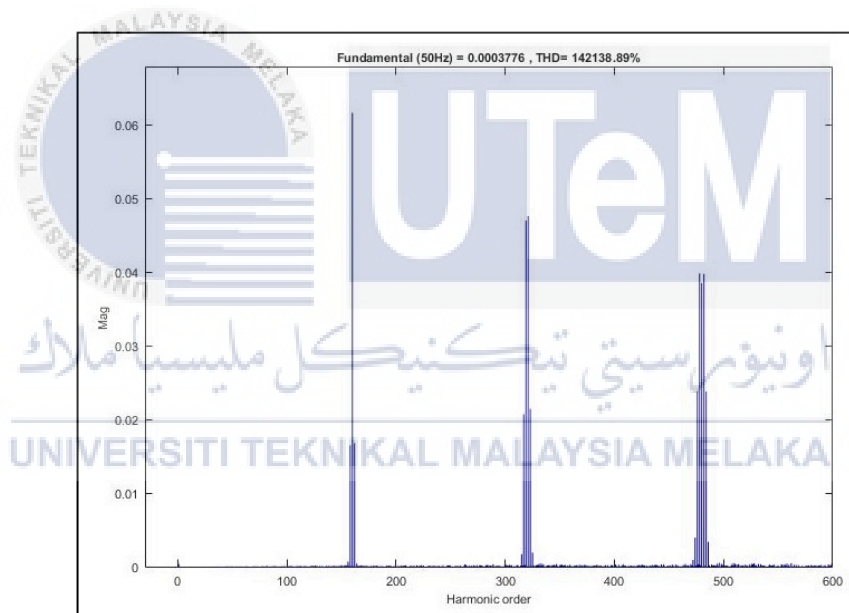


Figure 4.18: The Ground Leakage Current Spectrum When Used Filter With One Inductor (142138.89 %)

The ground leakage current is low (1.556 mA_{peak}) when using split inductor with same value as shown in Figure 4.19. Figure 4.20 show a spectrum of the ground leakage current with a low harmonic content (189.13 %).

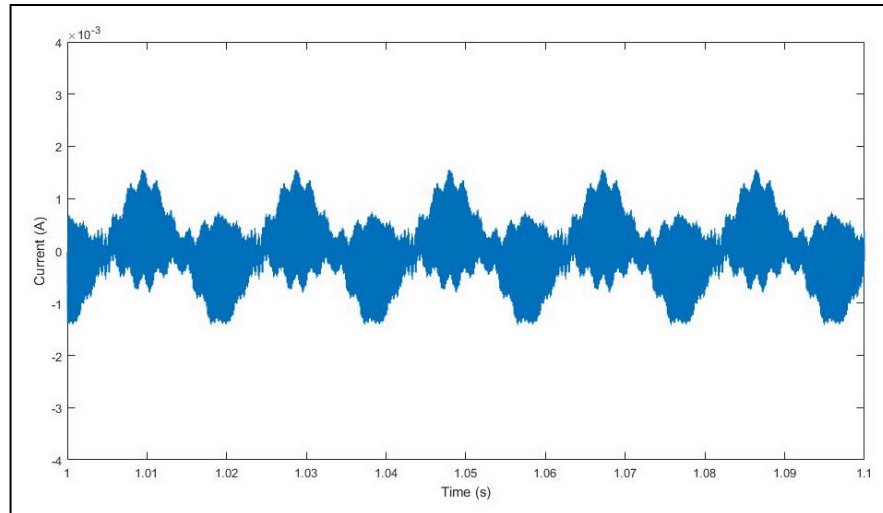


Figure 4.19: The Effect Of Filter With Split Inductor With Same Value On Ground
Leakage Current $1.556 \text{ mA}_{\text{peak}}$

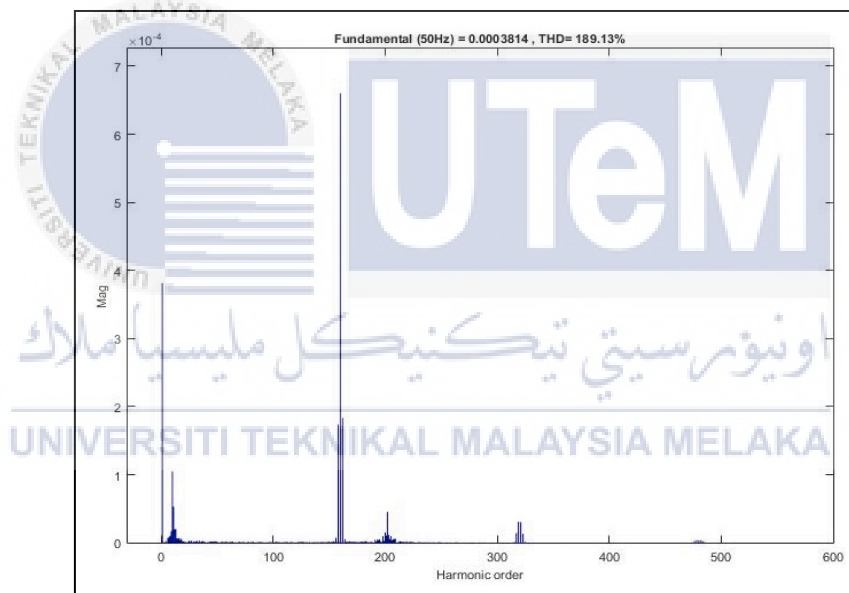


Figure 4.20: The Ground Leakage Current Spectrum 189.13 % Using Filter With
Split Inductor Same Value

4.2.3 Effect of Filter Impedance Matching

Due to low ground leakage current ($1.556 \text{ mA}_{\text{peak}}$) of filter using split inductor with same value as shown in Figure 4.19 compared to filter with one inductor ($3 \text{ A}_{\text{peak}}$) as shown in Figure 4.17, the effect of filter impedance matching has been analyzed. Firstly, the simulation is start with filter ratio ($L_r = 1$) as shown in Figure 4.21 (ground leakage current $1.556 \text{ mA}_{\text{peak}}$) and the spectrum (189.13 %)

shown in Figure 4.22. The mismatch impedance value between L_{f1} and L_{f2} produced effect as shown in Figure 4.23 (ground leakage current $51.99 \text{ mA}_{\text{peak}}$), 4.25 (ground leakage current $63.69 \text{ mA}_{\text{peak}}$) and 4.27 (ground leakage current $158.7 \text{ mA}_{\text{peak}}$) which are the value of ground leakage current increasing due to increasing filter ratio. Figure 4.29 shows the ground leakage current ($460.8 \text{ mA}_{\text{peak}}$) is more than $300 \text{ mA}_{\text{rms}}$ when using high filter ratio. Figure 4.24 (ground leakage spectrum 8171.57%), 4.26 (ground leakage spectrum 11218.36%), 4.28 (ground leakage spectrum 25782.03%) and 4.30 (ground leakage spectrum 85271.87%) shows the THD of the ground leakage current, which is produced a very high harmonic content.

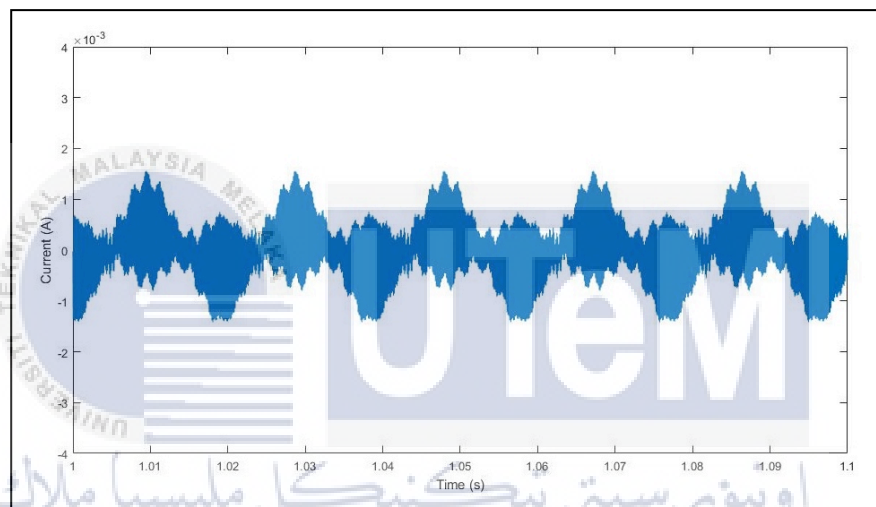


Figure 4.21: Ground Leakage Current Of Filter Ratio 1 ($1.556 \text{ mA}_{\text{peak}}$)
UNIVERSITI TEKNIKAL MALAYSIA MELAKA

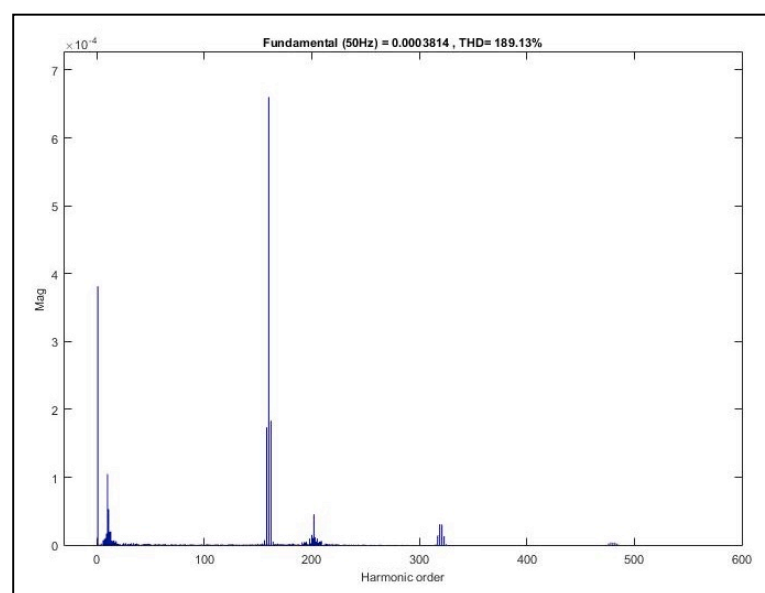


Figure 4.22: Ground Leakage Spectrum Filter Ratio 1 (189.13 %)

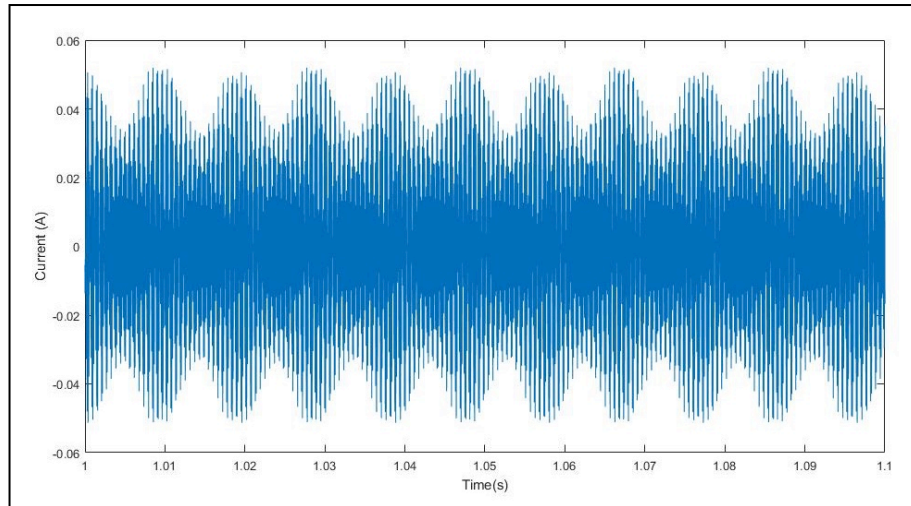


Figure 4.23: Ground Leakage Current Of Filter Ratio 1.2 ($51.99 \text{ mA}_{\text{peak}}$)

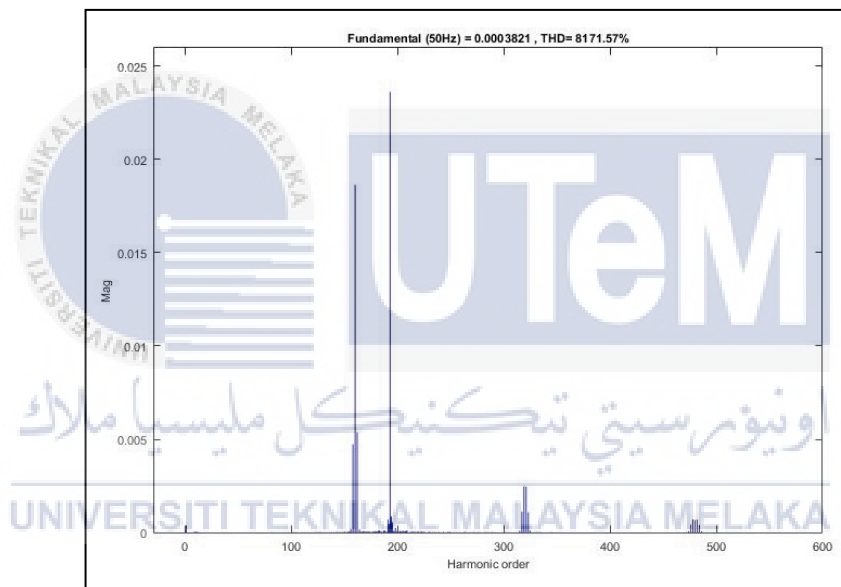


Figure 4.24: Ground Leakage Spectrum Filter Ratio 1.2 (8171.57 %)

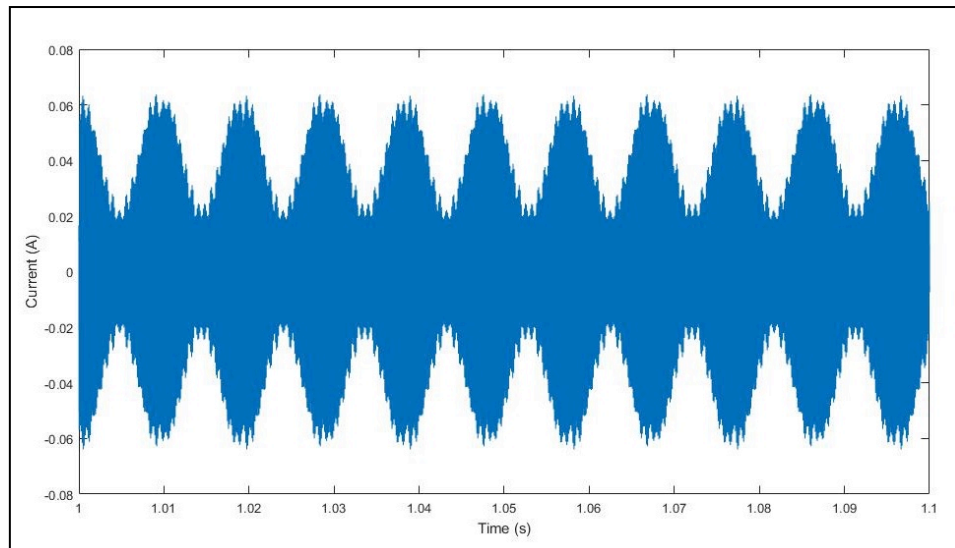


Figure 4.25: Ground Leakage Current Of Filter Ratio 1.4 (63.69 mA_{peak})

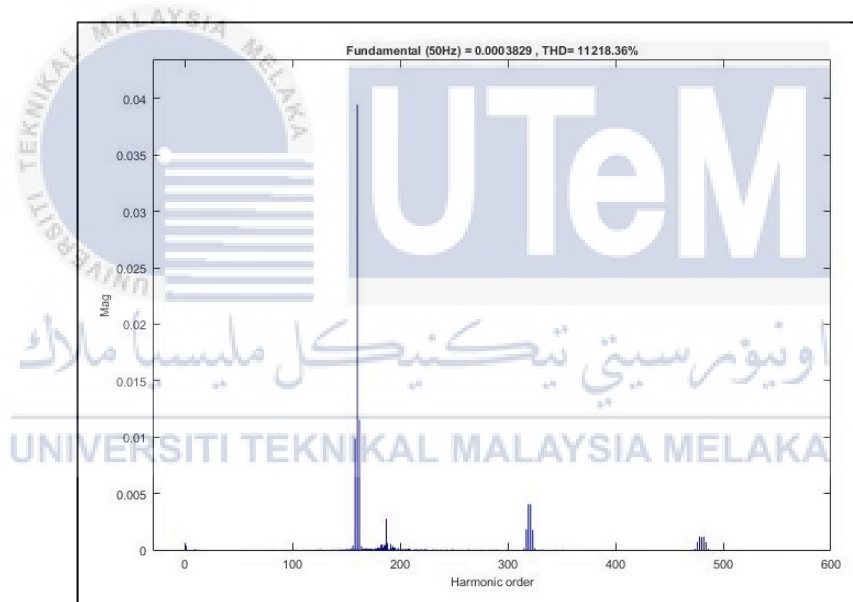


Figure 4.26: Ground Leakage Spectrum Filter Ratio 1.4 (11218.36 %)

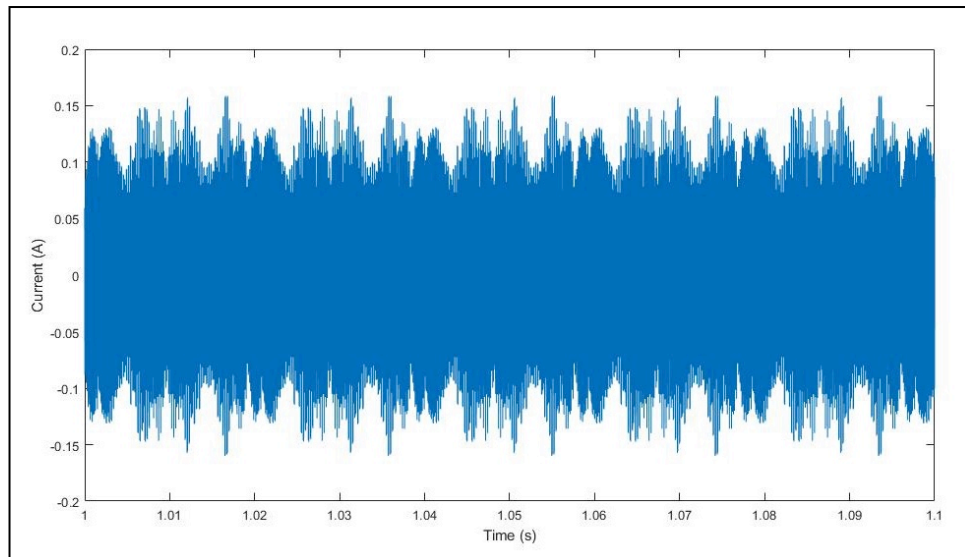


Figure 4.27: Ground Leakage Current Of Filter Ratio 2 (158.7 mA_{peak})

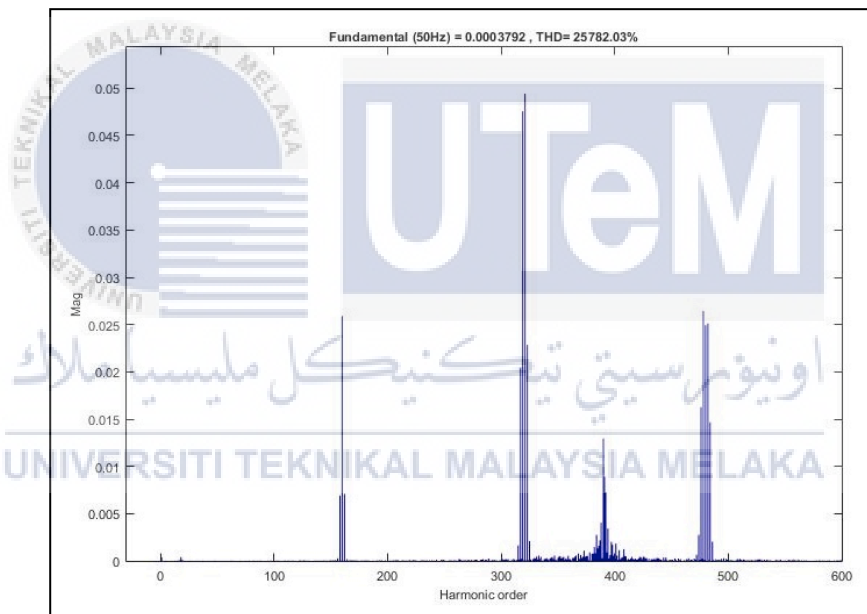


Figure 4.28: Ground Leakage Spectrum Filter Ratio 2 (25782.03 %)

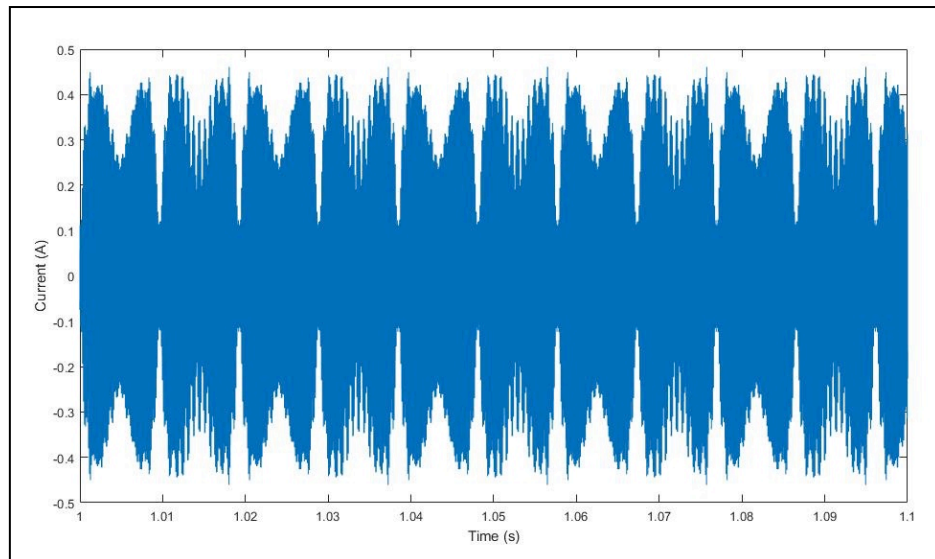


Figure 4.29: Ground Leakage Current Of Filter Ratio 5 ($460.8 \text{ mA}_{\text{peak}}$)

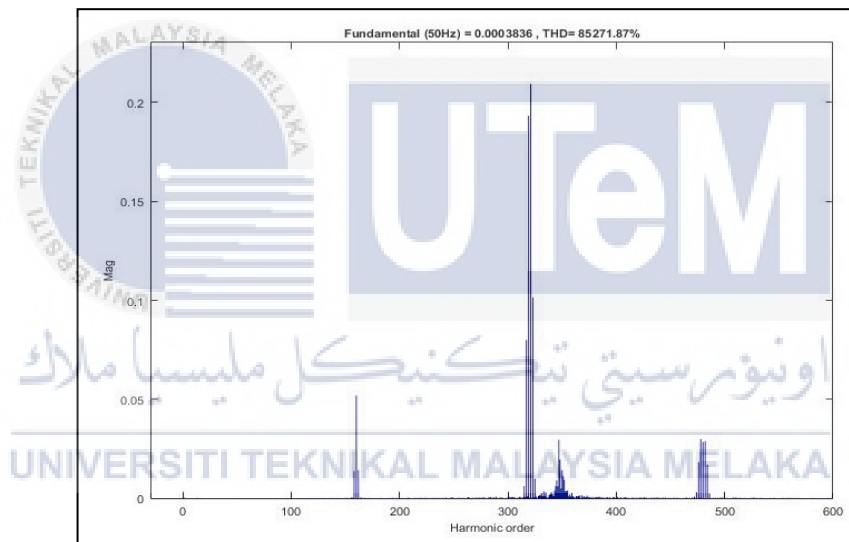


Figure 4.30: Ground Leakage Spectrum Filter Ratio 5 (85271.87 %)

4.2.4 Effect of Parasitic Capacitance

Effect of parasitic capacitance is analyzed using bipolar switching technique. Thus, the parasitic capacitance (C_{pv}) value was analyzed based on range 10-50nF/kW. Figure 4.31 (ground leakage current $1.556 \text{ mA}_{\text{peak}}$), 4.32 (ground leakage current $3.21 \text{ mA}_{\text{peak}}$), 4.33 (ground leakage current $3.772 \text{ mA}_{\text{peak}}$) and 4.34 (Ground leakage current $3.928 \text{ mA}_{\text{peak}}$) shows the result simulation of using a range value from 10nF to 50nF of parasitic capacitance. Based on the simulation results, it shows

that the higher value of parasitic capacitance will produce higher ground leakage current.

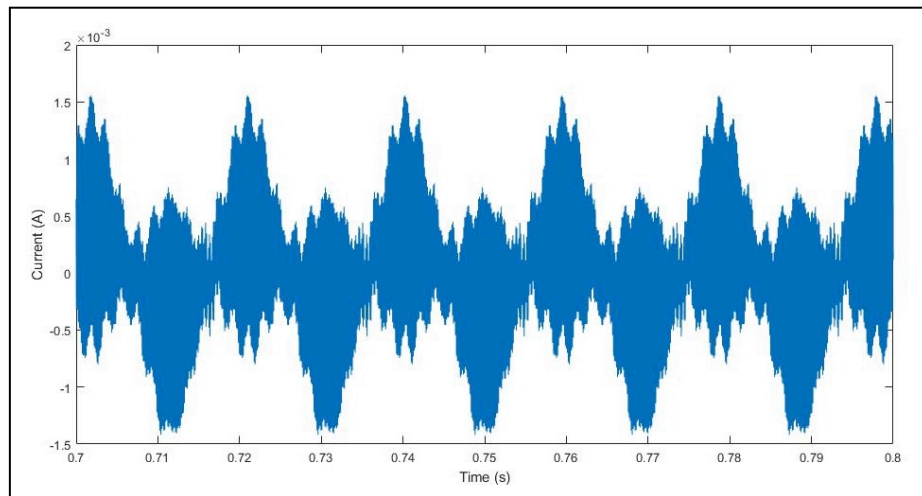


Figure 4.31: Ground Leakage Current ($1.556 \text{ mA}_{\text{peak}}$) Using Parasitic Capacitor = 10 nF

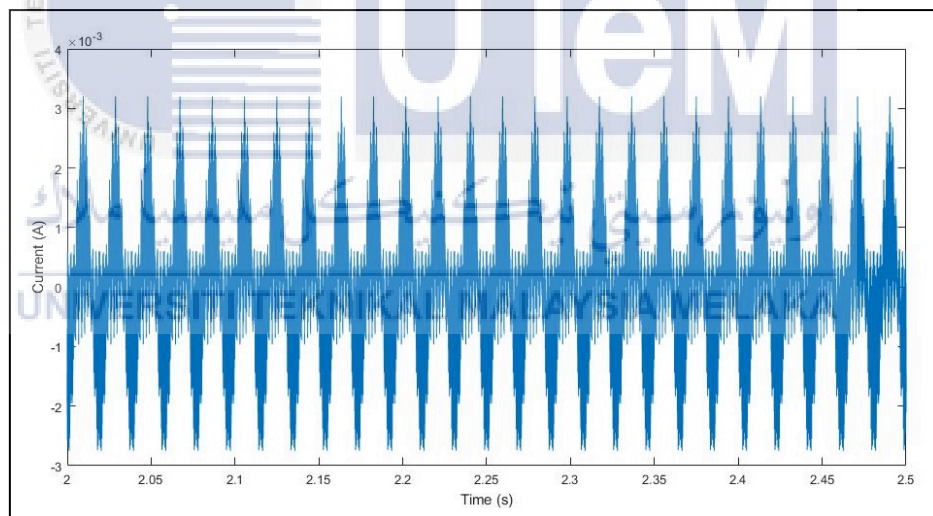


Figure 4.32: Ground Leakage Current ($3.21 \text{ mA}_{\text{peak}}$) Using Parasitic Capacitor = 30 nF

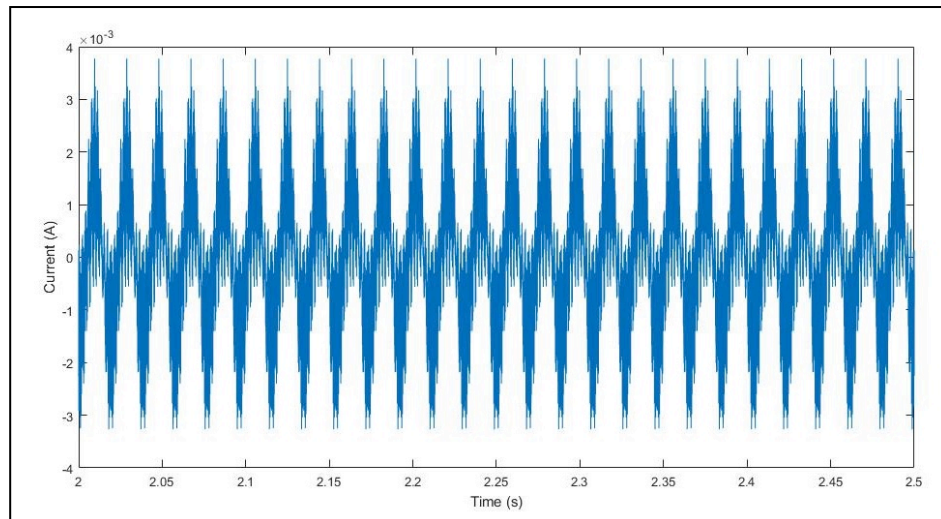


Figure 4.33: Ground Leakage Current ($3.772 \text{ mA}_{\text{peak}}$) Using Parasitic Capacitor = 40 nF

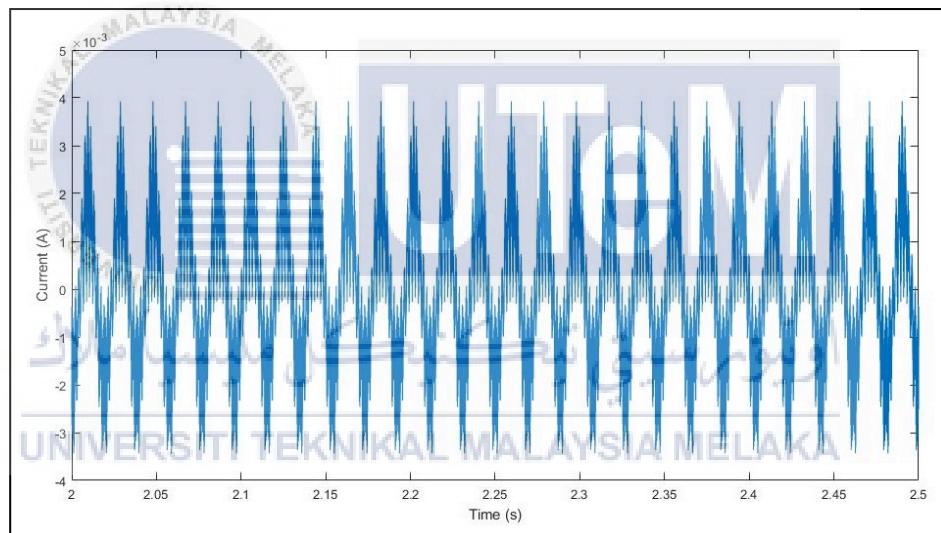


Figure 4.34: Ground Leakage Current ($3.928 \text{ mA}_{\text{peak}}$) Using Parasitic Capacitor = 50 nF

4.2.5 Effect of Switching Frequency

Switching frequency was analyzed to observe the ground leakage current. There are three values that have been used to analyze the ground leakage current which are 8 kHz, 16 kHz and 24 kHz. Based on Figure 4.35 (ground leakage current $1.556 \text{ mA}_{\text{peak}}$), 4.36 (ground leakage current $1.1 \text{ mA}_{\text{peak}}$) and 4.37 (ground leakage current $529.4 \mu \text{ A}_{\text{peak}}$) shows that the ground leakage current decreases due to increasing of switching frequency.

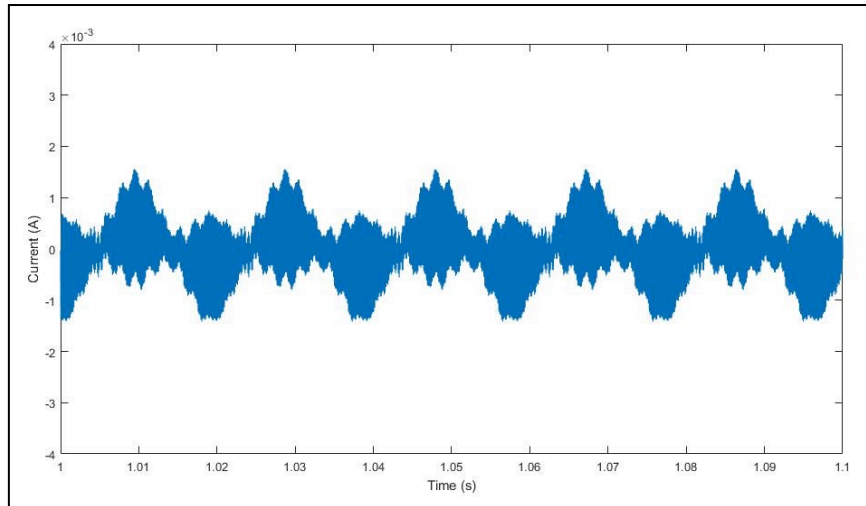


Figure 4.35: Ground Leakage Current ($1.556 \text{ mA}_{\text{peak}}$) using 8 kHz Switching Frequency

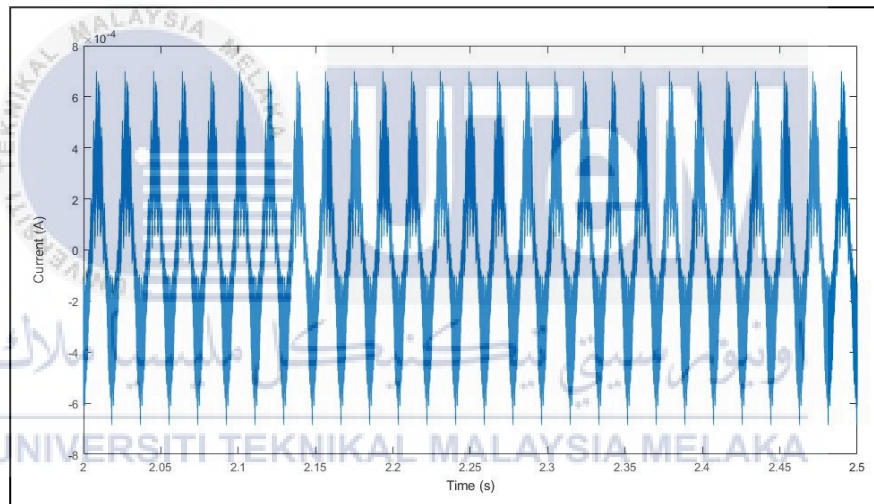


Figure 4.36: Ground Leakage Current ($1.1 \text{ mA}_{\text{peak}}$) using 16 kHz Switching Frequency

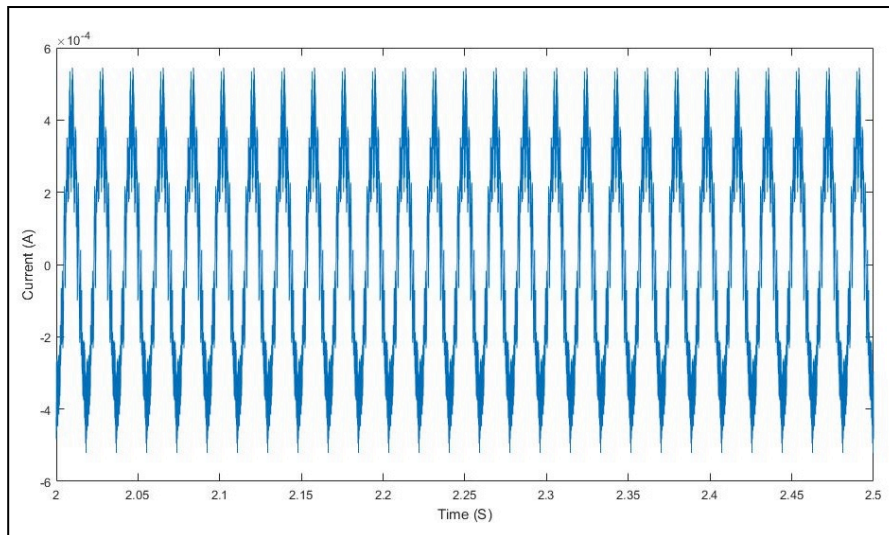


Figure 4.37: Ground Leakage Current ($529.4 \mu\text{A}_{\text{peak}}$) using 24 kHz Switching Frequency

4.3 Hardware Results

The result of the hardware will be presented in this section. The result was obtained from the hardware of the single-phase transformerless inverter that using unipolar and bipolar switching scheme. The single-phase transformerless inverter hardware is use to analyze the ground leakage current using a unipolar and bipolar switching technique, different parasitic capacitance value, and different filter design.

4.3.1 Pulse Width Modulation

Microcontroller XMC 4500 is use in this hardware to generate the pulse width modulation. XMS 4500 was generating bipolar and unipolar switching scheme. Figure 4.38 shows bipolar switching scheme generated by XMC 4500 and Figure 4.39 shows the unipolar switching scheme generated by XMC 4500.

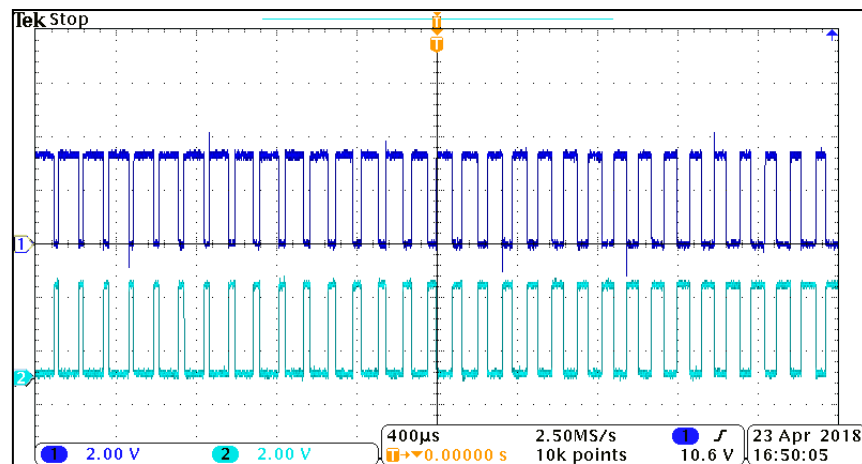


Figure 4.38: Bipolar Switching Scheme Using XMC 4500

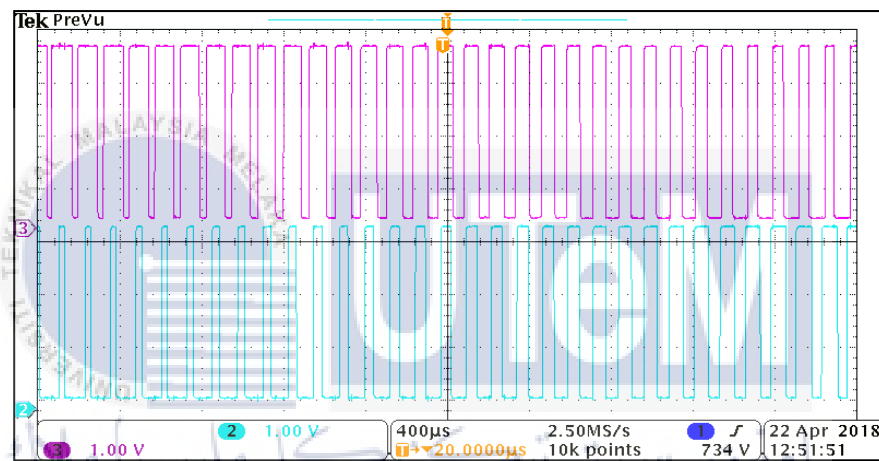


Figure 4.39: Unipolar Switching Scheme Using XMC 4500

4.3.2 Single Phase Transformerless Inverter

This section will represent the result of hardware development. The result was obtained from two switching techniques which are unipolar SPWM and bipolar SPWM. This stage of analysis was tested using 30 Vdc input voltage. Figure 4.40 (a) shows the output of V_{ao} and Figure 4.40 (b) shows the output of V_{bo} , which is when compared these two signals will produce fluctuating common mode voltage. Figure 4.41 shows the value of output voltage $30 V_{peak}$ using unipolar SPWM. Figure 4.42 shows the AC output voltage $24 V_{peak-to-peak}$ and AC output current $600 mA_{peak}$ of the inverter. Low THDv 0.5 % was produced in Figure 4.43. Due to fluctuating common mode voltage, a high ground leakage current ($100 mA_{peak}$) was produced as shown in Figure 4.44.

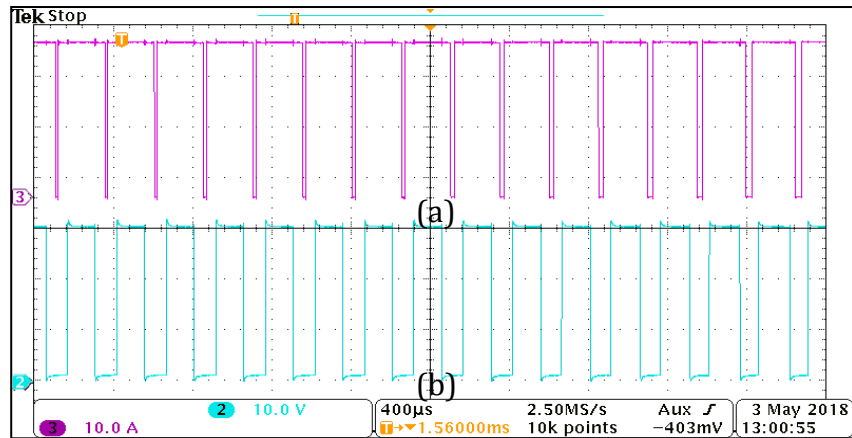


Figure 4.40: (a) V_{ao} Using Unipolar Switching Technique (b) V_{bo} Using Unipolar Switching Technique

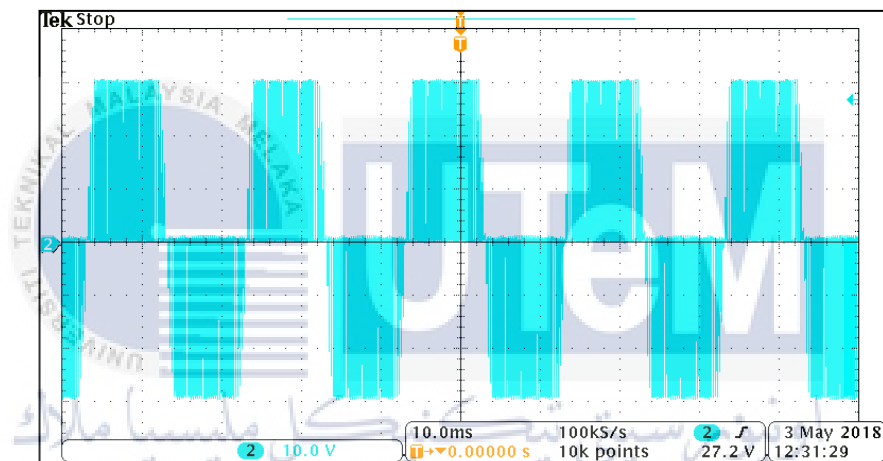


Figure 4.41: Output Inverter Voltage Using Unipolar Switching Technique $30 V_{peak}$ (10 V/div)

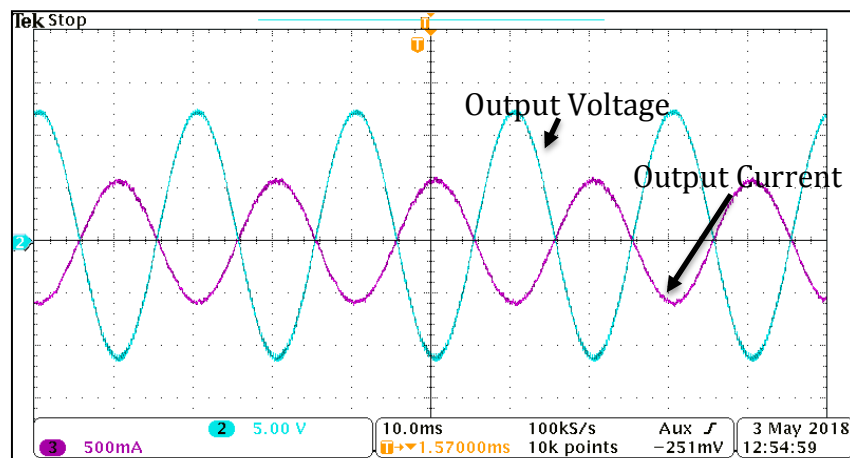


Figure 4.42: AC Waveform For Unipolar H-Bridge Inverter. Output Voltage $12 V_{peak}$ (Blue Trace 5 V/div) and Output Current $600 mA_{peak}$, (Purple Trace 500 mA/div)

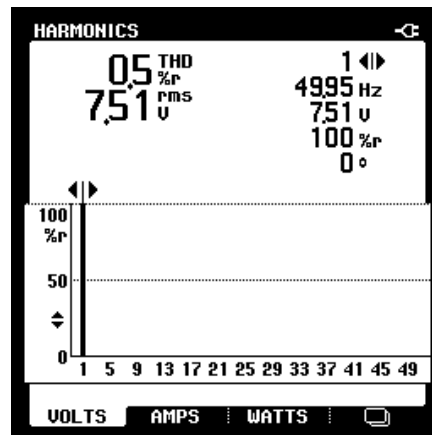


Figure 4.43: THD Output Voltage (0.5 %) for Unipolar H-Bridge Inverter Using Fluke 43B Power Quality Analyzer

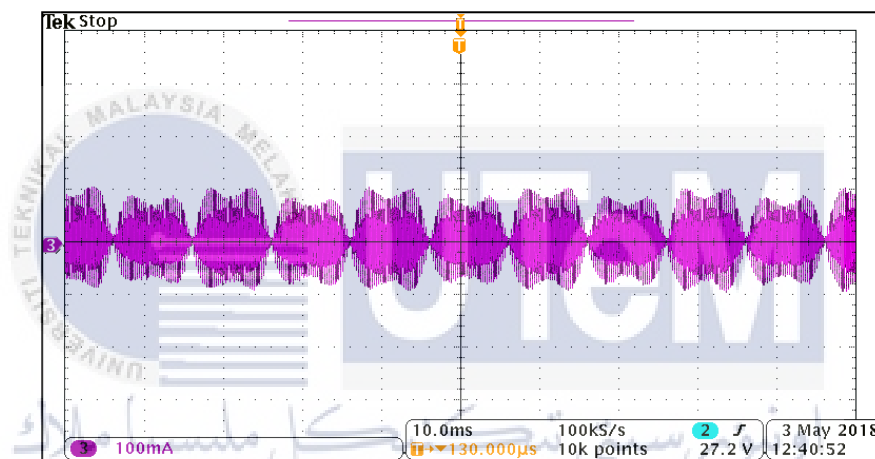


Figure 4.44: Ground Leakage Current Using Bipolar Switching Technique 100 mA_{peak} (100 mA/div)

Based on Figure 4.45, the constant common mode voltage can be calculated using Equation (3.1). Figure 4.45 (a) shows the output voltage from leg one IGBT while Figure 4.45 (b) shows the output voltage from another one leg, which the output is vice versa. Hence, the switching frequency was set to 8 kHz (double the frequency of unipolar SPWM) for the bipolar switching scheme to maintain the filter value as it used in unipolar H-Bridge inverter technique. Figure 4.46 shows the output voltage 30 V_{peak} of inverter (V_{ab}) using bipolar SPWM. The grid waveforms for bipolar SPWM H-Bridge inverter are shown at Figure 4.47 which the voltage output is 24 V_{peak} and current is 1.2 A_{peak}. Figure 4.48 shows the THD_v 1.7 % of bipolar H-Bridge inverter. Due to the bipolar SPWM, the low ground leakage current 1.8 mA_{peak} were produced and shown in Figure 4.49.

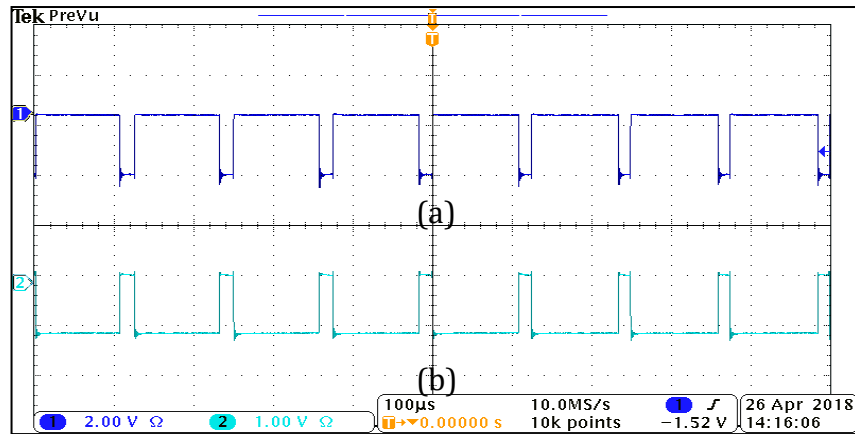


Figure 4.45: (a) V_{ao} Using Bipolar Switching Technique (b) V_{bo} Using Bipolar Switching Technique

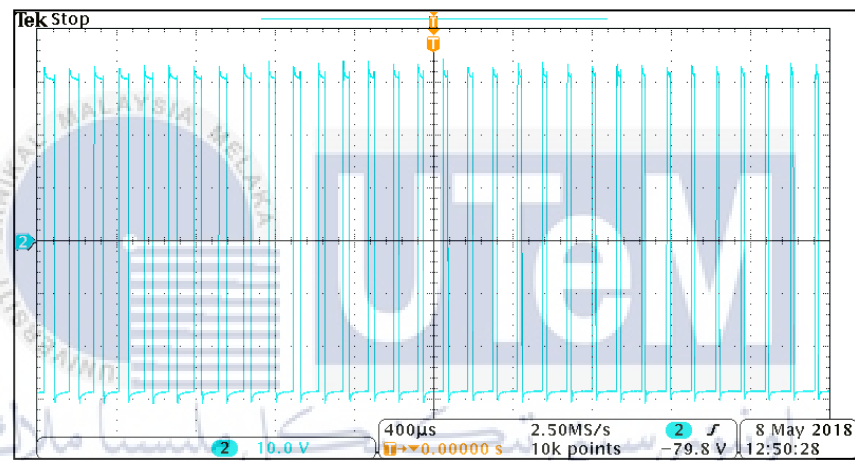


Figure 4.46: Output Inverter Voltage Using Bipolar Switching Technique 30 V_{ab} (10 V/div)

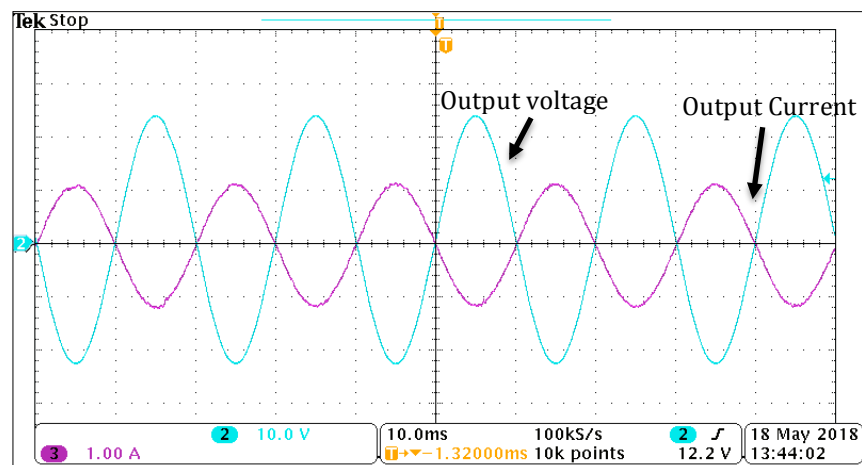


Figure 4.47: AC Waveform For Bipolar H-Bridge Inverter. Output Voltage 24 V_{peak} (Blue Trace 10.0 V/div) And Output Current 1.2 A_{peak} (Purple Trace 1 A/div)

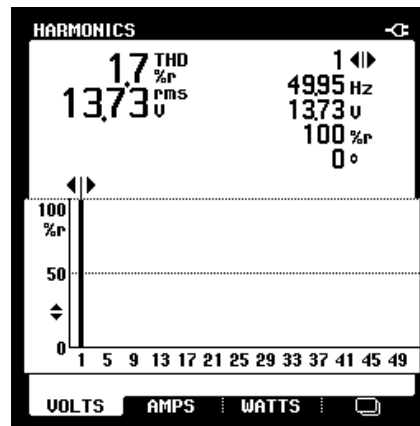


Figure 4.48: THD Output Voltage (1.7 %) For Bipolar H-Bridge Inverter Using Fluke 43B Power Quality Analyzer

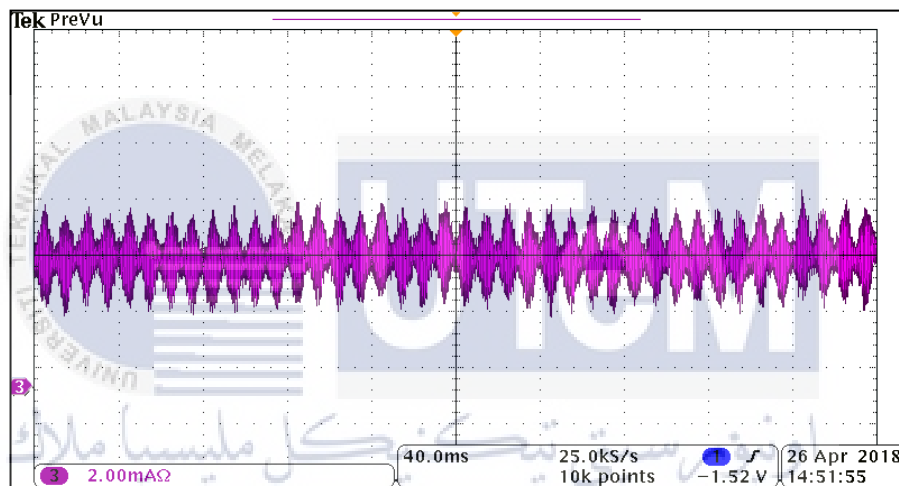


Figure 4.49: Ground Leakage Current Using Bipolar Switching Technique (1.8 mA_{peak})

4.3.3 Effect of Filter Design

Effect of filter design using hardware was analyzed. Same goes with simulation, the hardware also using two type of filter to be analyzed. The two type of LC filter are LC filter with one inductor and the other one is LC filter with split inductor. Value of inductor that used for the analysis is 5 mA. Figure 4.50 shows the effect of filter using one inductor on ground leakage current (2 A_{peak}). Figure 4.51 show the result of filler using split inductor and it shows the leakage current (1.8 mA_{peak}) is below 300 mA_{rms}.

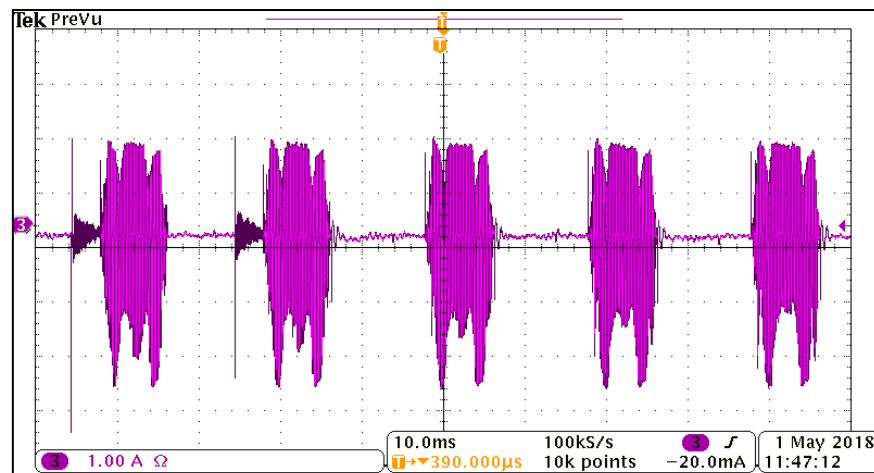


Figure 4.50: The Effect Of Filter With One Inductor On Ground Leakage Current 2
 A_{peak} (1 A/div)

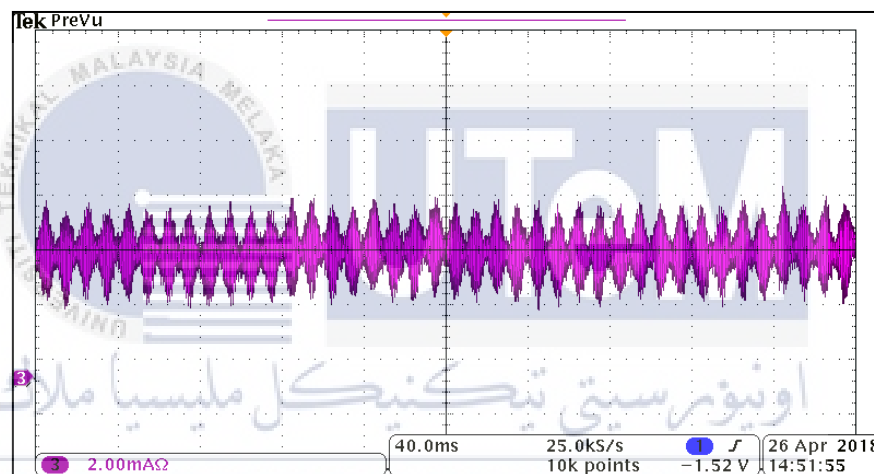


Figure 4.51: The Effect Of Filter With Split Inductor With Same Value On Ground
 Leakage Current $1.8 \text{ mA}_{\text{peak}}$ (2 mA/div)

4.3.4 Effect of Filter Impedance Matching

The effect of filter impedance matching using hardware was analyzed using value 1 mH, 2 mH, 5 mH, 6 mH and 7 mH of inductance. Figure 4.51 also shows the ground leakage current $1.8 \text{ mA}_{\text{peak}}$ using inductance ratio 1. Figure 4.52 (ground leakage current $40 \text{ mA}_{\text{peak}}$), 4.53 (ground leakage current $55 \text{ mA}_{\text{peak}}$), 4.54 (ground leakage current $160 \text{ mA}_{\text{peak}}$) and 4.55 (ground leakage current $500 \text{ mA}_{\text{peak}}$) shows the ground leakage current using inductance ratio 1.2, 1.4, 2 and 5. The leakage current that produced from mismatch impedance is higher compare with inductance using same value. The ground leakage current increases as increase the ratio.

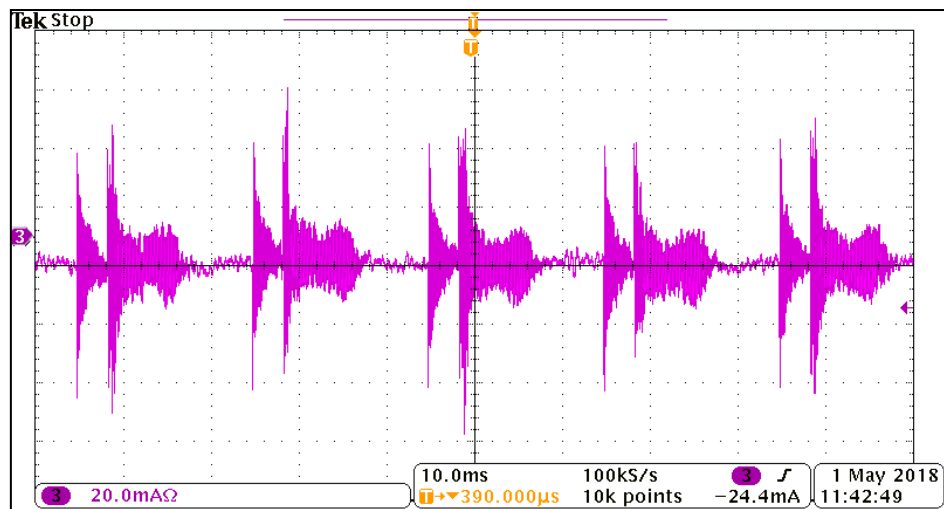


Figure 4.52: Ground Leakage Current $40 \text{ mA}_{\text{peak}}$ Using Filter Ratio 1.2 (20 mA/div)

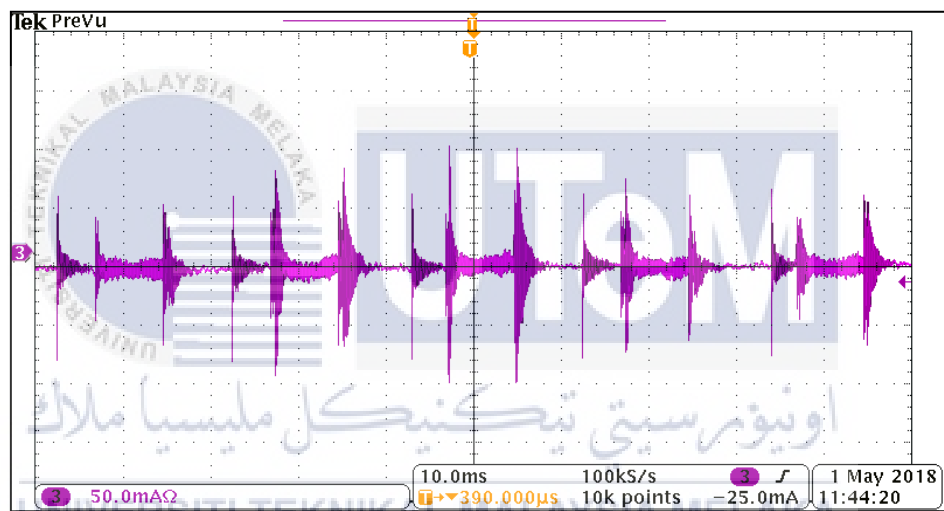


Figure 4.53: Ground Leakage Current $55 \text{ mA}_{\text{peak}}$ Using Filter Ratio 1.4 (50 mA/div)

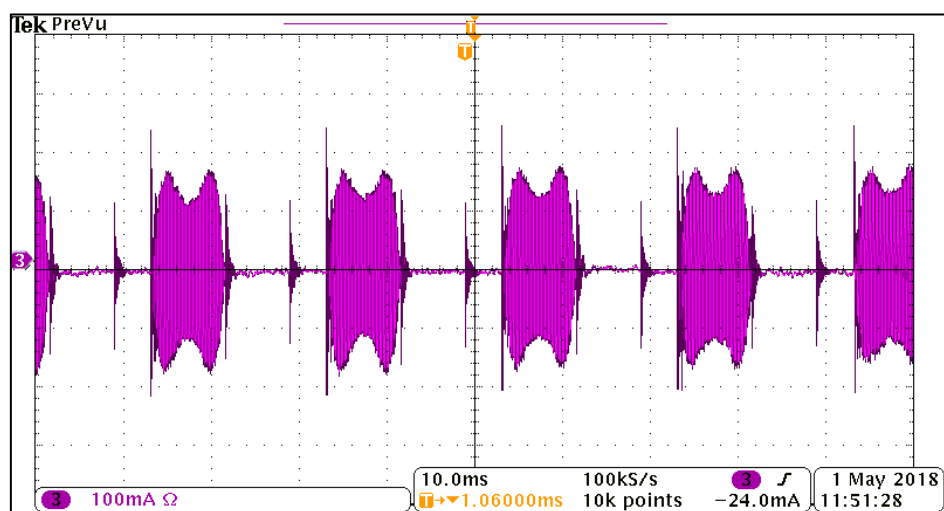


Figure 4.54: Ground Leakage Current $160 \text{ mA}_{\text{peak}}$ Using Filter Ratio 2 (100 mA/div)

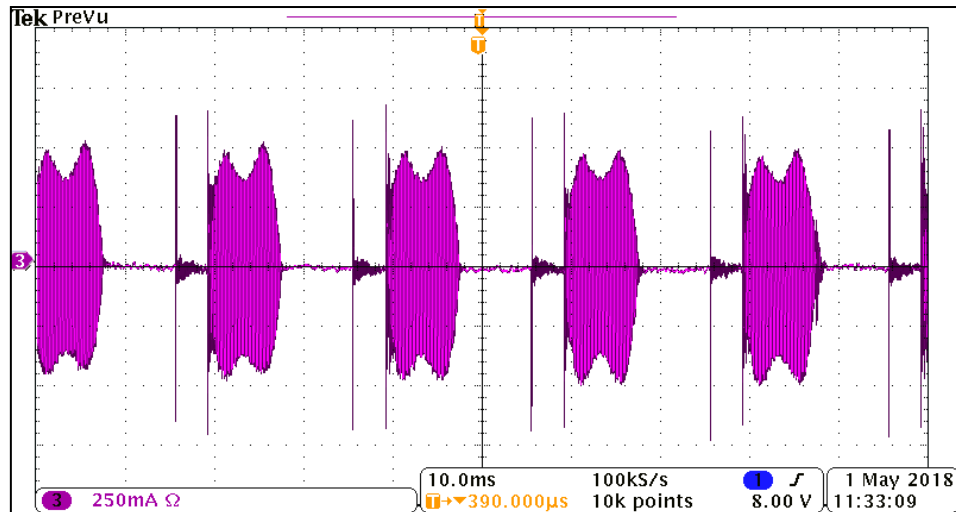


Figure 4.55: Ground Leakage Current 500 mA_{peak} Using Filter Ratio 5 (250 mA/div)

4.3.5 Effect of Parasitic Capacitance

There are 5 value of parasitic capacitance that has been used to analyze the ground leakage current. The values are varies from 10 nF to 50 nF. Based on the result, as increase value of parasitic capacitance it will increase the value of ground leakage current as shown in Figure 4.56 (ground leakage current 1.8 mA_{peak}), 4.57 (ground leakage current 2 mA_{peak}), 4.58 (ground leakage current 3 mA_{peak}) and 4.59 (ground leakage current 4.4 mA_{peak}).

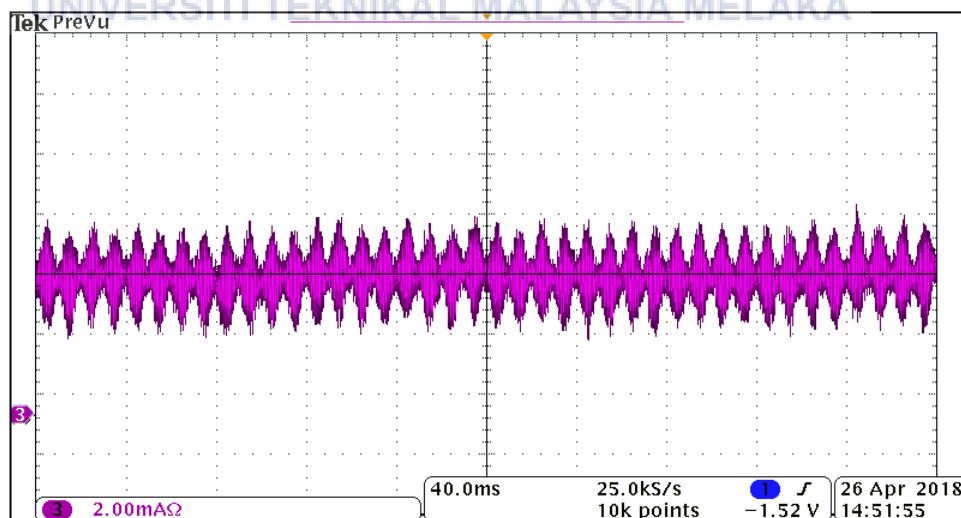


Figure 4.56: Ground Leakage Current 1.8 mA_{peak} With Parasitic Capacitor Value 10 nF (2 mA/div)

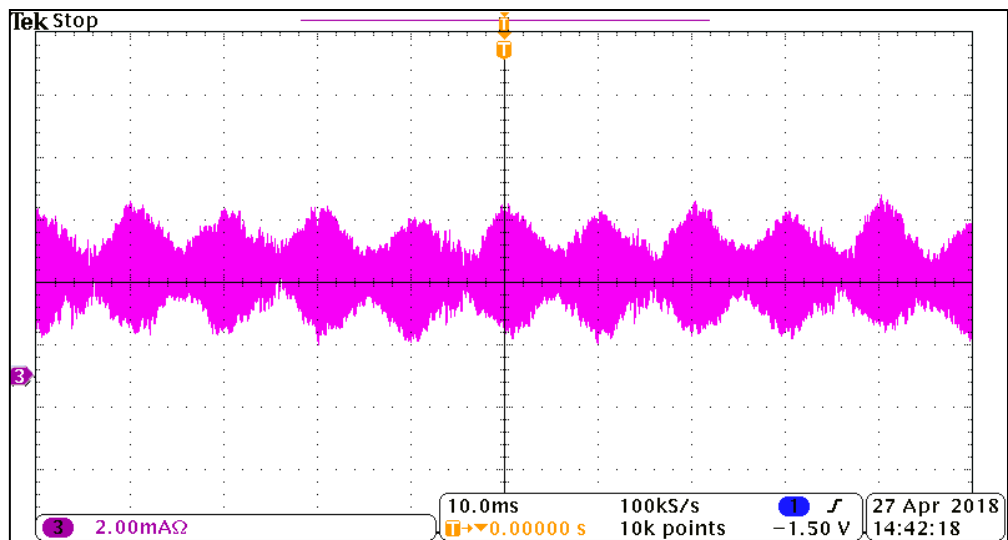


Figure 4.57: Ground Leakage Current $2 \text{ mA}_{\text{peak}}$ With Parasitic Capacitor Value 30 nF
(2 mA/div)

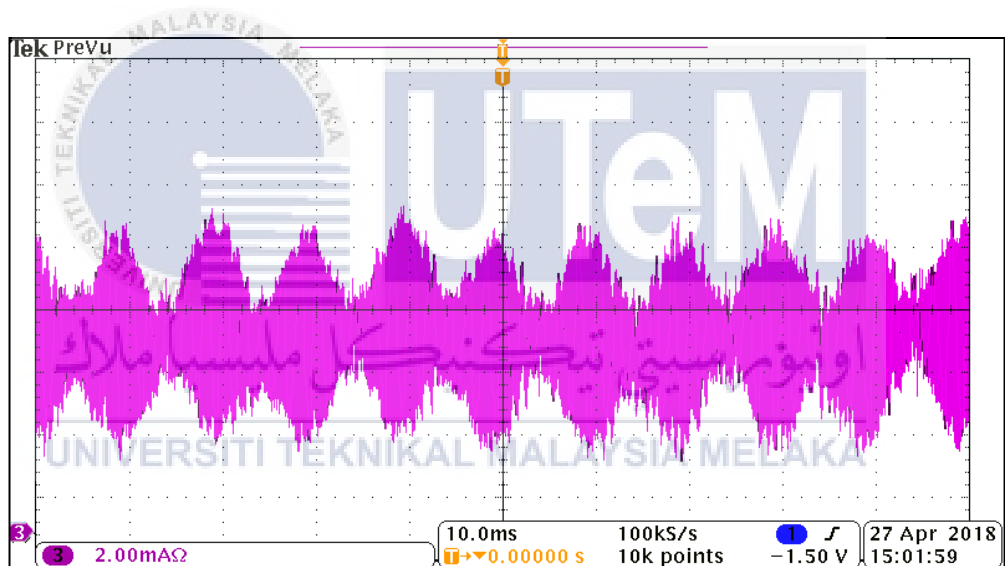


Figure 4.58: Ground Leakage Current $3 \text{ mA}_{\text{peak}}$ With Parasitic Capacitor Value 40 nF
(2 mA/div)

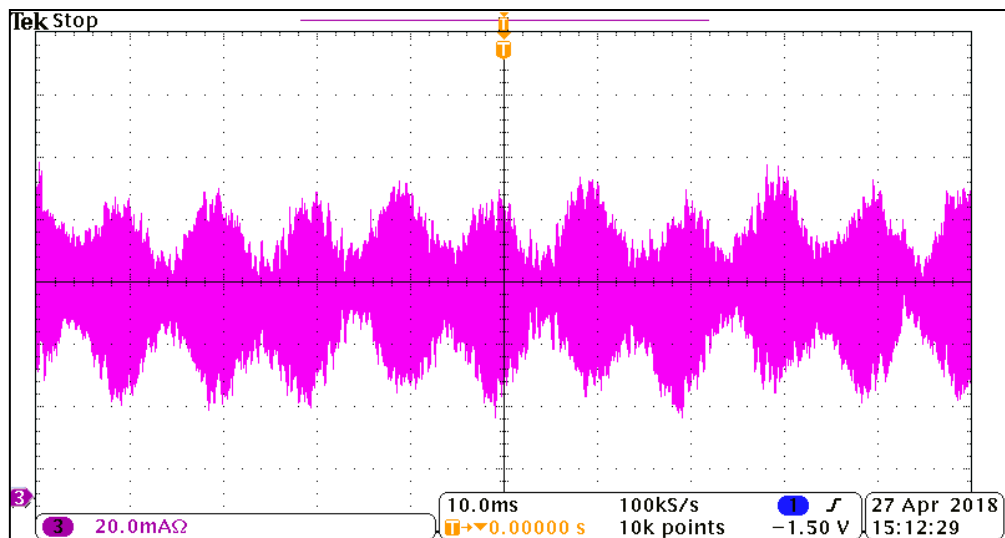


Figure 4.59: Ground Leakage Current $4.4 \text{ mA}_{\text{peak}}$ With Parasitic Capacitance Value 50 nF (20 mA/div)

4.3.6 Effect of Switching Frequency

Figure 4.60 (ground leakage current $1.556 \text{ mA}_{\text{peak}}$), 4.61 (ground leakage current $0.6 \text{ mA}_{\text{peak}}$) and 4.62 (ground leakage current $529.4 \mu \text{ A}$) shows the result experiment hardware of ground leakage current using switching frequency 8 kHz , 16 kHz and 24 kHz . The ground leakage current becomes decrease when the switching frequency increases.

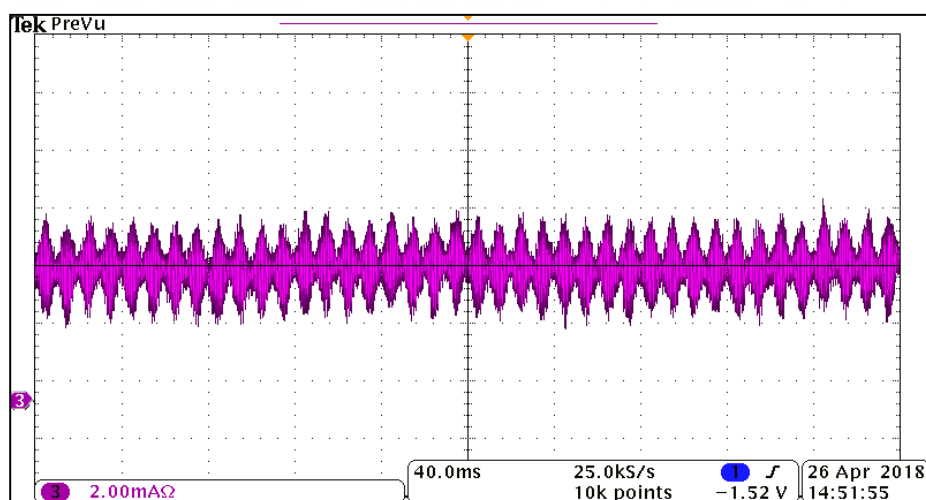


Figure 4.60: Ground Leakage Current $1.556 \text{ mA}_{\text{peak}}$ Using 8 kHz Switching Frequency (2 mA/div)

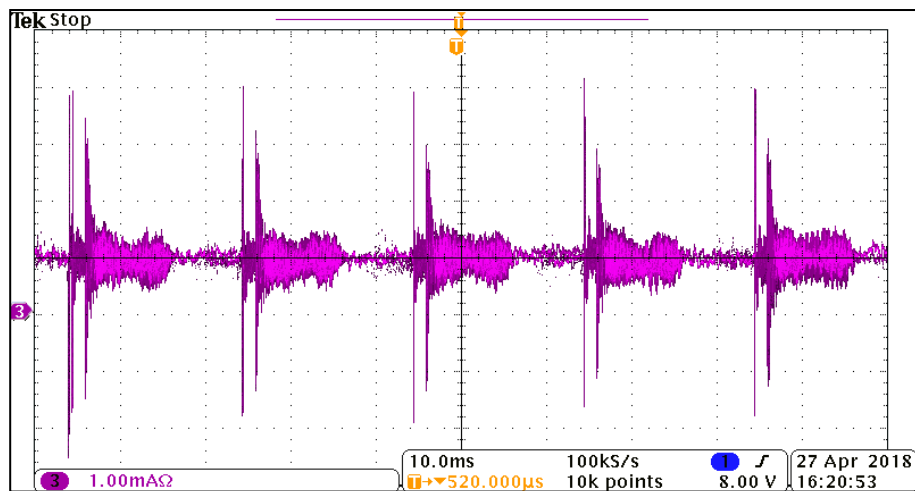


Figure 4.61: Ground Leakage Current $0.6 \text{ mA}_{\text{peak}}$ Using 16 kHz Switching Frequency (1 mA/div)

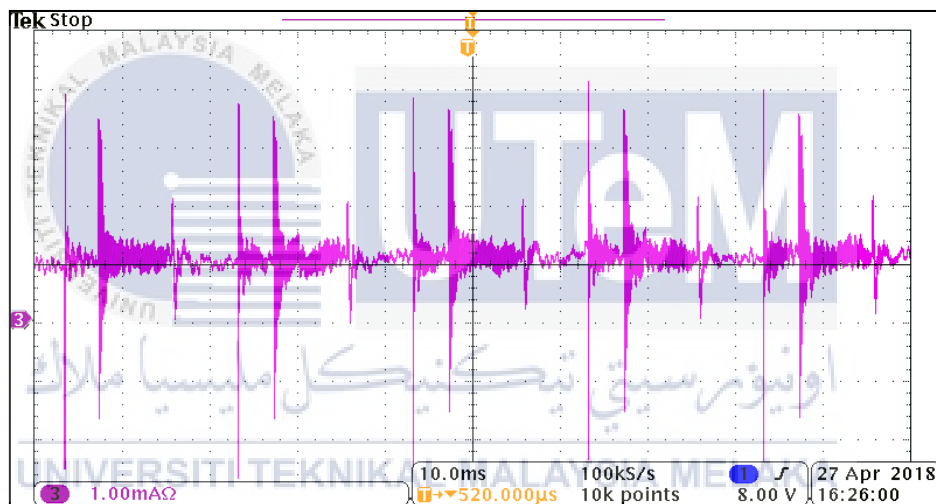


Figure 4.62: Ground Leakage Current $529.4 \mu\text{A}_{\text{peak}}$ Using 24 kHz Switching Frequency (1 mA/div)

4.4 Comparison between Simulation and Hardware Results

This section will discuss the comparison result between simulation and hardware. The single phase transformerless inverter were analyzed using simulation and experimental hardware. The comparison results were analyzed in term of ground leakage current. Firstly, the comparison of the simulation and experimental hardware was analyzing using two different switching techniques, which are bipolar SPWM and unipolar SPWM. The comparison results between simulation and hardware of

unipolar switching technique are shown in Table 4.2 and the bipolar switching technique shown in Table 4.3. Based on Table 4.2, the ground leakage currents produced are higher in both simulation ($155.2 \text{ mA}_{\text{peak}}$) and hardware ($100 \text{ mA}_{\text{peak}}$). This is because the unipolar switching techniques are having a fluctuated common-mode voltage. Table 4.3 showing the ground leakage current in simulation ($1.556 \text{ mA}_{\text{peak}}$) and hardware ($1.8 \text{ mA}_{\text{peak}}$) are lower due to constant common mode voltage. Result unipolar SPWM and bipolar SPWM are different between simulation and experiment hardware because have a conduction losses and switching losses. Furthermore, based on THD_v , the unipolar SPWM and bipolar SPWM are maintain below 5 % (IEEE Standard 519) for simulation and hardware.

Table 4.2: Unipolar switching technique comparison result between simulation and hardware using 4 kHz switching frequency

	Unipolar SPWM (Simulation)	Unipolar SPWM (Hardware)
Voltage Output (V_{peak})	30	30
Voltage Output (after insert filter) (V_{peak})	24.48	12
Current Output (mA_{peak})	24.48	600
THD_v (%)	0.75	0.5
Ground Leakage Current (mA_{peak})	155.2	100

Table 4.3: Bipolar switching technique comparison result between simulation and hardware using 8 kHz switching frequency

	Bipolar SPWM (Simulation)	Bipolar SPWM (Hardware)
Voltage Output (V_{peak})	30	30
Voltage Output (after insert filter) (V_{peak})	24.98	24
Current Output (A_{peak})	0.025	1.2
THD_v (%)	3.21	1.7
Ground Leakage Current (mA_{peak})	1.556	1.8

4.4.1 Analysis on LC Filter using One Inductance, LC Filter using Split Inductance, Parasitic Capacitance and Switching Frequency at Ground Leakage Current

Result of ground leakage current for bipolar SPWM that using LC filter with one inductance and LC filter with split inductance with same value are shown in Table 4.4. LC filter with one inductance produced high ground leakage current for simulation ($3 A_{\text{peak}}$) and experimental hardware ($2 A_{\text{peak}}$). It is because the LC filter with one inductance has a high inductance value and low attenuation. Besides, LC filter with one inductance required a high switching frequency to reduce harmonic. A lower ground leakage current ($1.556 \text{ mA}_{\text{peak}}$ for simulation and $1.8 \text{ mA}_{\text{peak}}$ for experimental hardware) was produced using LC filter with split inductance with same value due to better attenuation.

Due to low ground leakage current of LC filter split inductance with same value, the LC filter impedance matching was analyzed. The ground leakage current level changes based on filter ratio, L_r , shown in Figures 4.63, which are when L_{f1} and L_{f2} are match ($L_r = 1$) and its produces a low ground leakage current. The mismatching impedances are produces high ground leakage current. Based on the analysis, the ground leakage current is increase due to increase of filter ratio, L_r , for both analysis and experiment hardware. Therefore, filter design split inductor with same value is recommended to this system.

The parasitic capacitance was analyzed using value range from 10-50 nF. Figure 4.64 shows the ground leakage current was increase with increases of parasitic capacitance for simulation and experiment hardware.

Switching frequency also affecting the ground leakage current. Refer to Figure 4.65 the ground leakage current is reduced due to increasing of switching frequency for simulation and experiment hardware. Based on Equation (3.13), value of inductance is inversely proportional to switching frequency. Therefore, value of inductance is decrease due to higher switching frequency and the calculations are shown in Table 4.5.

Table 4.4: The comparison between simulation and experiment hardware by using LC filter with one inductance and split inductance with same value

LC Filter	Bipolar (Simulation)	Bipolar (Hardware)
One inductance	3 A	2 A
Split inductance with same value	1.556 mA	1.8 mA

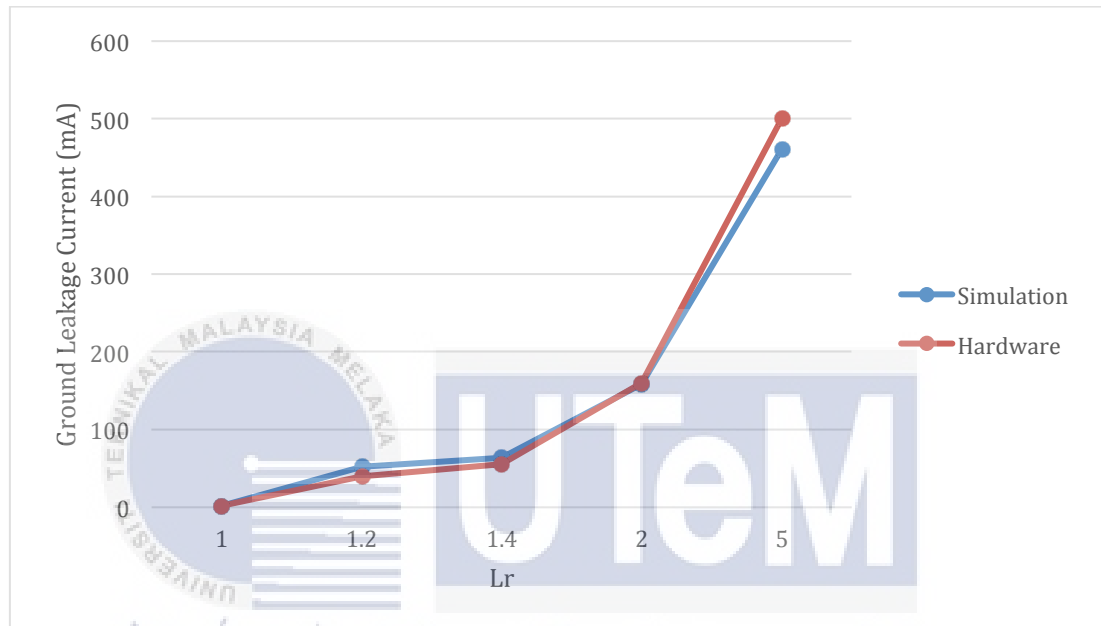


Figure 4.63: Ground Leakage Current Levels Against L_r (L_{f1}/L_{f2})

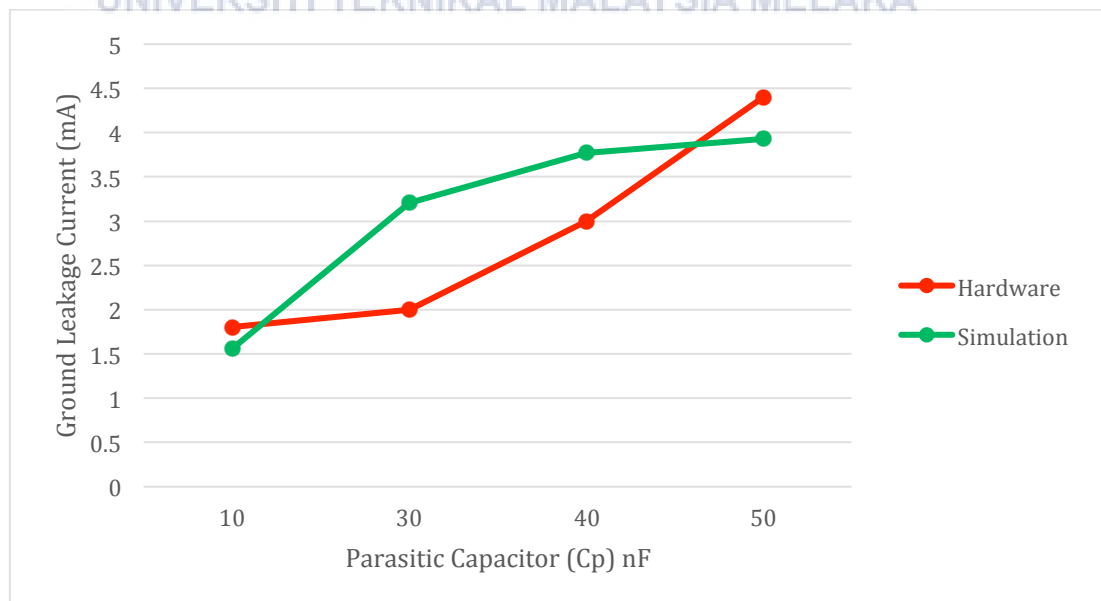


Figure 4.64: Parasitic Capacitance Vs. Ground Leakage Current

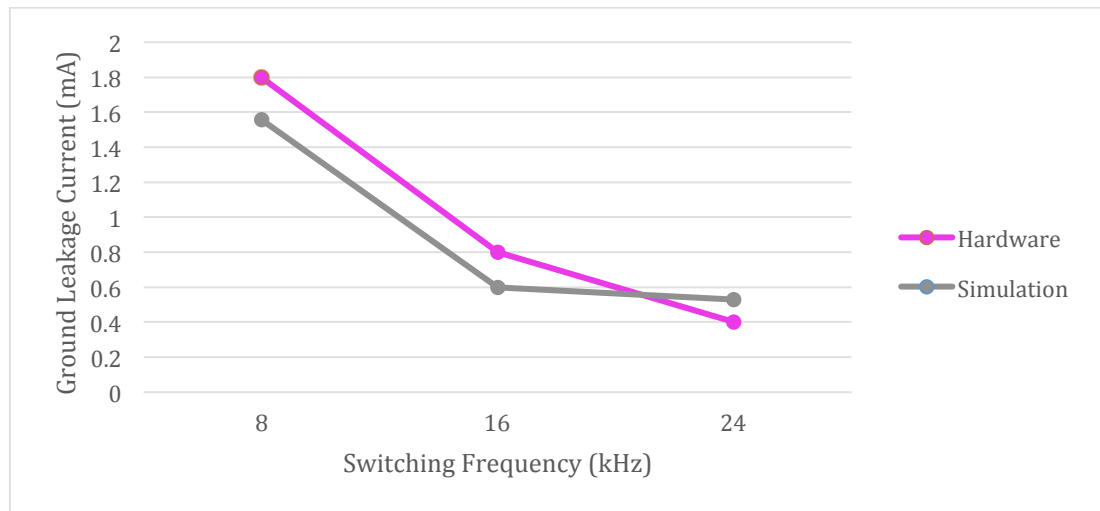


Figure 4.65: Comparison Effect Of Switching Frequency Between Simulation And Experimental Hardware

Table 4.5: Calculation of inductance value

Switching Frequency (kHz)	Inductance calculation
8	Assume $\% \Delta V_o = 0.313\%$ $\% \Delta V_o = \frac{0.313}{100} \times 30$ $\Delta V_o = 0.0939$ $L = \frac{30}{8 \times 0.0939 \times 8k}$ $= 5 \text{ mH}$
16	$L = \frac{30}{8 \times 0.0939 \times 16k}$ $= 2.5 \text{ mH}$
24	$L = \frac{30}{8 \times 0.0939 \times 24k}$ $= 1.7 \text{ mH}$

4.5 Summary

Simulation and experiment hardware on single-phase transformerless inverter is to identify the suitable switching technique. Based on the result, it shown that the bipolar switching technique give low ground leakage current. Therefore, a filter

design is analyzed to determine using one inductor or split inductor with same value. Filter that use split inductor with same value is giving a low ground leakage current. Then, a simulation and experiment hardware based on matching inductor was analyzed. Mismatched inductor produce a high ground leakage current based on the simulation. Thus, a match inductor value was used to achieve low ground leakage current. Parasitic capacitor also affects the ground leakage current. Value parasitic capacitance from 10 nF to 50 nF was analyzed. Lastly, the switching frequency was analyzed and the higher switching frequency will produce a low ground leakage current.



CHAPTER 5

CONCLUSION AND RECOMMENDATION

Single-phase transformerless inverter PV-grid connected generates high efficiency with a low-cost, small weight and high power density. In the performance of single-phase transformerless inverter was measured in term of ground leakage current ($\leq 300 \text{ mA}_{\text{rms}}$) and total harmonic distortion (THD). The main purpose of the single-phase transformerless inverter simulated and hardware development are to investigate the ground leakage currents effect. The simulation is using MATLAB/Simulink software. There are four factors that affect the ground leakage current, which are switching technique, filter design, parasitic capacitance and topology used.

Firstly, the unipolar and bipolar switching scheme was investigate but bipolar was selected due to low leakage current. Secondly, the design filter with one inductor and filter with split inductor was investigated. Thus, the filter with split inductor with same value is selected. Then, the matching inductor filter was analyzed. The various value of parasitic capacitance between 10 nF and 50 nF was analyzed. The higher value is selected due to worst condition. Lastly, the switching frequency was analyzed using value 8 kHz, 16 kHz and 24 kHz. Based on the result, the higher switching frequency produced the lower ground leakage current.

The performance of bipolar H-Bridge transformerless inverter was analyzed. The performance of bipolar H-Bridge transformerless inverter was verified using simulation and experiment hardware result. Bipolar SPWM technique produced low ground leakage current. Unfortunately that technique lack of power conversion efficiency due to two level of output voltage. Therefore, the unipolar SPWM with modified the H-Bridge circuit is recommendation for this project.

REFERENCES

- [1] Mohan, N. Undeland, T. M. (1995) Power Electronics, John Wiley & Sons, inc, United States of Amerika
- [2] Retrieved on 13 September, 2013 from
http://books.google.com.my/books?id=WwXi9LI5W1sC&pg=RA2-PA300&dq=Classification+of+Inverter&hl=en&sa=X&ei=Lx2CUuTdK8SVrgf_voG4AQ&redir_esc=y#v=onepage&q=Classification%20of%20Inverter&f=false
- [3] HART, D.W. (2011) Power electronic, Mcgraw-Hill Companies, Americas, NY
- [4] Garg, A., Rajasekar, S., & Gupta, R. (2013). A new modulation technique to eliminate leakage current in transformerless PV inverter. 2013 Students Conference on Engineering and Systems, SCES 2013.
- [5] Garg, A., Rajasekar, S., & Gupta, R. (2013). A new modulation technique to eliminate leakage current in transformerless PV inverter. 2013 Students Conference on Engineering and Systems, SCES 2013.
- [6] Surya Santoso, P. D., McGranaghan, M. F., Dugan, R. C., & Beaty, H. W. (2012). Fundamentals of Harmonics. Electrical Power Systems Quality, Third Edition. McGraw Hill Professional, Access Engineering.
- [7] Joshi, H. (2008). Harmonics. Residential, Commercial and Industrial Electrical Systems: Protection, Testing and Commissioning, Volume 3. McGraw Hill Professional, Access Engineering.
- [8] Akagi et al.2007
- [9] Emadi et al.,2005
- [10] Garg, A., Rajasekar, S., & Gupta, R. (2013). A new modulation technique to eliminate leakage current in transformerless PV inverter. 2013 Students Conference on Engineering and Systems, SCES 2013.
- [11] Taylor, P., System, P. G., Azri, M., Azri, M., Rahim, N. A., & Halim, W. A. (2015). Electric Power Components and Systems A Highly Efficient Single-phase Transformerless H- bridge Inverter for Reducing Leakage Ground Current A Highly

Efficient Single-phase Transformerless H-bridge Inverter for Reducing Leakage Ground Current in Photovoltaic Grid-connected System, (May), 37–41.

[12] Generation, G. P. V. P., Azri, M., Rahim, N. A., Fathi, M., & Elias, M. (n.d.). Transformerless DC/AC Converter for Grid-Connected PV Power Generation System.

[13] Jlljgz, G., Sjs, V. Y., Ft, Y., Ft, Y., Ft, Y., & Ft, T. (n.d.). >grlh0t.r:hg%, 3, 5–9.

[14] Somani, P. (2016). Design of HERIC Configuration Based Grid Connected Single Phase Transformer less Photovoltaic Inverter, 892–896.

[15] Beaty, H. W., & Fink, D. G. (2013). STATION DESIGN AND EQUIPMENT. Standard Handbook for Electrical Engineers, Sixteenth Edition. McGraw Hill Professional, Access Engineering.

[16] Ma, L., Tang, F., Zhou, F., Jin, X., & Tong, Y. (2008). Leakage current analysis of a single-phase transformer-less PV inverter connected to the grid. 2008 IEEE International Conference on Sustainable Energy Technologies, ICSET 2008, 285–289.

[17] Noman, A. M., Addoweesh, K. E., & Ai-haddad, K. (2016). Cascaded Multilevel Inverter Topology with High Frequency Galvanic Isolation for Grid Connected PV System, 3030–3037.

[18] No Title. (n.d.).

[19] Engineering, I. (2013). Hybrid System of Pv Solar / Wind &, 3666–3679.

[20] Cell, F., & Overview, S. (2012). Fuel Cell Power Systems.

[21] 4Sync-1. (n.d.).

[22] Azri, M., & Rahim, N. A. (2011). Design analysis of low-pass passive filter in single-phase grid-connected transformerless inverter. 2011 IEEE 1st Conference on Clean Energy and Technology, CET 2011, (August 2014), 348–353.

[23] Bo Yang, Wuhua Li, Yunjie Gu, Wenfeng Cui & Xiangning He (2012). Improved Transformerless Inverter With Common-Mode Leakage Current Elimination for a Photovoltaic Grid-Connected Power System”, IEEE Transactions on Power Electronics, 27, 752-762.

[24] Gate, I., Transistor, B., Soft, U., & Diode, R. (n.d.). IRG4PC50UD IRG4PC50UD, 1–10.

[25] Systems, D. S. P. D. (2007). eZdsp TM F28335 Technical.

[26] IEEE-519-1992.pdf. (n.d.).

[27] Kerekes, T. (2013). Analysis and Modeling of Transformerless Photovoltaic Inverter. Ijmer (Vol. 3).



APPENDICES

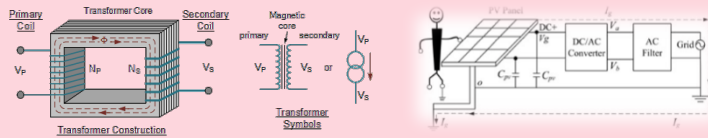


ABSTRACT

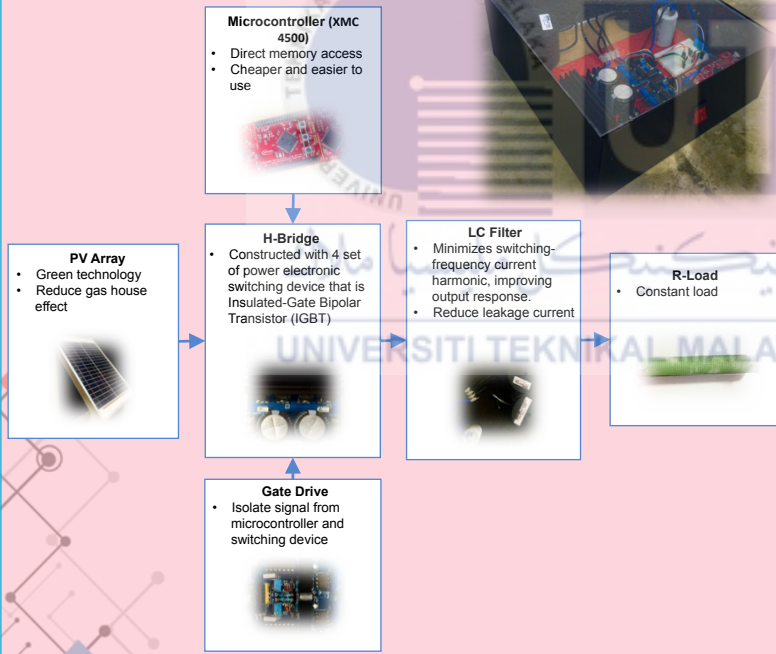
Grid-connected PV power generation systems have gained popularity due to the advent of green energy or renewable energy sources. Most existing PV grid-connected inverter systems incorporate a line transformer or high-frequency transformer in the systems to provide isolation between the utility grid and the PV module so that issues on electrical safety hazard can be avoided. This gain in electrical safety comes with a price of increased system size and cost, as transformers are known to be bulky and costly. Recently, to achieve higher efficiency, lower cost, lighter weight, and smaller size, the transformerless H-Bridge PV grid-connected system have been introduced. In transformerless systems, the PV panel connects directly to the grid neutral, introducing ground-leakage current (from the ground parasitic capacitance) to the system. By the German standard VDE0126-1-1, ground-leakage current must not exceed 300mA_{RMS} to avoid possible electrical hazard from touching the PV array. The leakage current is appearing because there is no galvanic isolation when using transformerless. Furthermore, factor effected ground leakage current is based on the topology used, switching strategy, parasitic capacitor and filter design. Appearing leakage current is causes the safety problem and increased system losses.

PROBLEM STATEMENT

- High ground leakage current (> 300 mA, standard VDE0126-1-1)
- Safety hazard problem
- High cost
- Low efficiency



METHODOLOGY



DISCUSSION

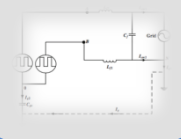
Switching strategy

- Bipolar SPWM
- Unipolar SPWM

Topology used for transformerless inverter circuit

- Single-phase transformerless inverter using bipolar SPWM

Factor effected ground leakage current (must not exceed 300mA)



AC Filter

$$I_{g1} = I_{cm1} + I_{cm2}$$

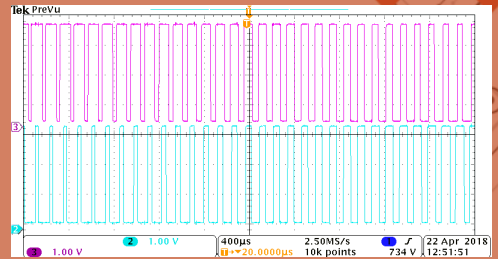
Parasitic Capacitance

$$I_{g2} = C_{PV} \frac{\Delta V_{C_{PV}}}{\Delta t}$$

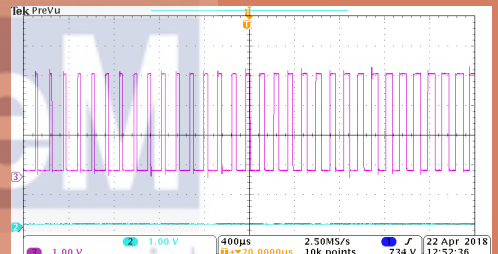
OBJECTIVE

- To model and analyze the single-phase transformerless inverter using Matlab/Simulink.
- To design and develop hardware of single-phase transformerless inverter.
- To verify the performance of single phase transformerless inverter between the simulation and hardware result.

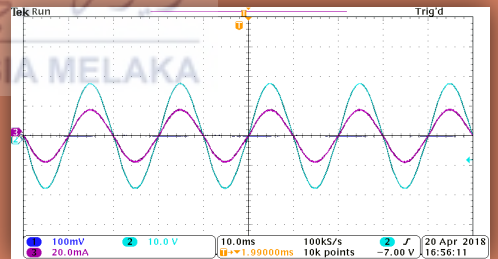
RESULT



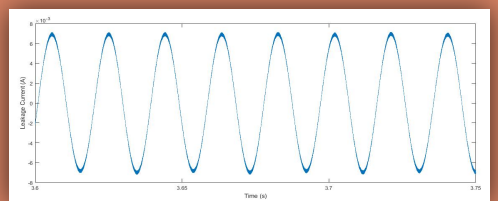
Unipolar signal using XMC 4500 microcontroller



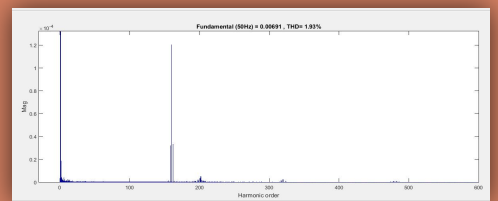
Bipolar signal using XMC 4500 microcontroller



Output Current and output voltage of inverter



Ground leakage current using bipolar switching technique (6.91mA)



THD ground leakage current for H-bridge inverter (1.93%)

ADVANTAGES

- ✓ No safety hazard problem
- ✓ Low leakage current
- ✓ Low cost

- ✓ High efficiency
- ✓ Easy to use

Name| NUR SYAMIMI BINI AHMAD FAUZI
 Supervisor1 | Dr MAASPALIZA BINI AZRI
 Supervisor2 | En ZULKIFLI BIN RAMLI